Effects of Magnesium on Wear Characteristics of SiC and Al_2O_3 Reinforced Aluminum Metal Matrix Composites

by

Md. Habibur Rahman
Student Number: 0412112005F

A thesis paper submitted to the Department of Materials and Metallurgical Engineering of Bangladesh University of Engineering and Technology, Dhaka in partial fulfillment of the requirements for the degree of

MASTER OF SCIENCE IN MATERIALS AND METALLURGICAL ENGINEERING

Department of Materials and Metallurgical Engineering

BANGLADESH UNIVERSITY OF ENGINEERING AND TECHNOLOGY

September, 2014

The thesis titled **"Effects of Magnesium on Wear Characteristics of SiC and Al_2O_3 Reinforced Aluminum Metal Matrix Composites"** Submitted by Md. Habibur Rahman, Student Number: 041211 2005F, Session: April 2012 has been accepted as satisfactory in partial fulfillment of the requirement for the degree of Master of Science in Materials and Metallurgical Engineering on September 17, 2014.

BOARD OF EXAMINERS

1. _____

Dr. Hossain Mohammad Mamun Al Rashed — Chairman
Assistant Professor — (Supervisor)
Department of Materials and Metallurgical Engineering
BUET, Dhaka-1000.

2. _____

Dr. Ahmed Sharif — Member
Professor and Head — (Ex-officio)
Department of Materials and Metallurgical Engineering
BUET, Dhaka-1000.

3. _____

Dr. Kazi Mohammad Shorowordi — Member
Assistant Professor
Department of Materials and Metallurgical Engineering
BUET, Dhaka-1000.

4. _____

Dr. A. K. M. Abdul Hakim — Member
Director (Retd.) — (External)
Planning and Development Division
Bangladesh Atomic Energy Commission, Dhaka.

DECLARATION

It is hereby declared that this thesis or any part of it has not been submitted elsewhere for the award of any degree or diploma.

Md. Habibur Rahman

ACKNOWLEDGEMENTS

The author is deeply indebted to his supervisor Dr. Hossain Mohammad Mamun Al Rashed, Assistant Professor, Department of Materials and Metallurgical Engineering (MME), Bangladesh university of Engineering and Technology (BUET) for his continuous guidance, help, suggestions and encouragement throughout the progress of the research work.

The author expresses his sincere gratitude and thanks to Dr. Ahmed Sharif, Professor and Head of Department of Materials and Metallurgical Engineering, BUET for providing him with the laboratory facilities to carry out this research work. The author also expresses his heartiest thanks to Dr. Md. Fakhrul Islam, Professor and Head of Department of Glass and Ceramics Engineering, BUET for giving permission to use Scanning Electron Microscope (SEM) and X-ray Fluorescence (XRF) laboratory facilities.

The author is highly thankful to Mr. Md. Wasim Uddin, Mr. Md. Faruk Hossain, Mr. Md. Shamsul Alam, Mr. Md. Harun Or Rashid, Mr. Ahammd Ullah and Mr. Md. Abdullah Al Maksud for their kind assistance with the laboratory works.

Finally, the author is deeply indebted to the authorities of BUET for providing financial support to carry out the research work.

ABSTRACT

The aim of this work is to investigate the effects of magnesium (Mg) on wear characteristics of silicon carbide (SiC) and alumina (Al_2O_3) reinforced aluminum metal matrix composites (Al-MMC). Al-MMC reinforced with varying wt. % of SiC and Al_2O_3 particles were fabricated using stir casting fabrication technique. Effects of Mg, heat treatment and amount of reinforcements on microstructure, tensile strength, hardness and wear characteristics of Al-MMC were investigated. Worn surfaces were also studied to reveal the mechanism involved in wear process.

Microstructural observation revealed random dispersion of reinforcing particles in Al matrix. Cluster of particles and porosities were observed in the microstructure. Many regions in the matrix were also observed without reinforcing particles indicating non-homogeneous distribution of reinforcing particles. In SEM observation, agglomerated particles, good adhesion between reinforcing particle and Al matrix and precipitation caused by heat treatment were observed. SiC reinforced Al-MMC showed superior tensile strength than unreinforced Al and increased with increasing SiC content. Non-homogeneous distribution of reinforcement adversely affected tensile strength of Al-MMC. Mg addition was found to be beneficial for hardness of both unreinforced Al and Al-MMC. Further increase of hardness occurred after heat treatment. Hardness values of Al-MMC was found higher than those of unreinforced Al and increased with increasing amount of SiC particles.

SiC Particles reinforced Al-MMC showed lower wear rate than unreinforced Al and wear rate decreased with increasing amount of SiC particles. Mg addition reduced the wear rate of both unreinforced Al and Al-MMC. Al-MMC containing higher amount of SiC than Al_2O_3 showed better wear resistance due to higher hardness value of SiC particles and wear rate decreased after heat treatment. From worn surfaces observation it was seemed that delamination wear mechanism was involved in wear process of Al-MMC where severe fracture and plastic deformation occurred.

TABLE OF CONTENTS

LIST OF FIGURES

Chapter 2

Chapter 3

Chapter 4

LIST OF TABLES

LIST OF ABBREVIATIONS

Al-MMC: Aluminum Metal Matrix Composites

SEM: Scanning Electron Microscope

EDX: Energy Dispersive X-Ray

XRF: X-ray Fluorescence

BHN: Brinell Hardness Number

VHN: Vickers Hardness Number

CHAPTER 1
INTRODUCTION

Aluminum metal matrix composites (Al-MMC) are considered as a group of new advanced materials due to its greater strength, improved stiffness, light weight, improved high temperature properties, controlled co-efficient of thermal expansion and heat management, excellent wear and abrasion resistance and improved damping capabilities [1-2]. Combination of these properties turned Al-MMC into useful engineering materials for structural, automobiles and space applications. As the level of using technology is being sophisticated day by day, so the materials used for different purposes have to be more efficient and effective [3].

In Al-MMC, Al or Al alloys form continuous phase termed as matrix in which hard ceramic particles known as reinforcement are embedded. Primary function of reinforcements in Al matrix is to carry most of the applied load. Ductile Al matrix binds the reinforcing particles together, transfers and distributes applied external loads to individual reinforcement. Good wetting of reinforcing particles in molten Al is necessary to form strong interfacial bond between reinforcing particles and Al matrix during casting. Strong interfacial bond between reinforcing particles and Al matrix allows transfer and distribution of applied external load from matrix to reinforcements [4]. Wetting of reinforcing particles is prerequisite for satisfactory interfacial bond formation during casting. These bonds are formed by mutual dissolution or chemical reactions of the particulates and matrix metal [5].

In general, the surface of hard ceramic particles is not wetted by the molten metal. Wetting of these particles can be achieved by coating with a wettable metal. Metal coating on ceramic particles increases the overall surface energy of the solid and improves wetting by enhancing the contacting interface to metal-metal instead of metal-ceramic. The addition of magnesium (Mg) as a reactive element can modify the wetting of reinforcing particles by producing a transient layer between the particles and the liquid matrix. This transient layer has a low wetting angle, decreases the surface tension of the liquid and surrounds the particles with a structure that is similar to both the particle and the matrix alloy [6]. The composites produced by liquid metallurgy technique show excellent bonding between the ceramic particles and the metal when a

reactive element is added to induce wettability. By generating strong interfacial bond, Mg addition to Al-MMC results in enhanced mechanical properties.

The present study includes the effects of Mg on wear characteristics of SiC and Al_2O_3 reinforced Al-MMC. Al-MMC reinforced with varying wt. % of SiC and Al_2O_3 particles were fabricated using stir casting technique. Stir casting is a cost effective liquid state fabrication technique in which preheated reinforcing materials are added in molten matrix metal followed by stirring and solidification. Prepared Al-MMC were heat treated by three steps- solution treatment at 500 °C for 4 hours followed by quenching and age hardening at 150 °C for 1.5 hours. Microstructures of as-cast and heat treated Al-MMC were observed to reveal particle distribution in Al matrix using both optical microscope and scanning electron microscope (SEM). Tensile strength of prepared Al-MMC was evaluated. Finally, the effects of Mg, heat treatment and amount of reinforcing particles on hardness and wear characteristics of Al-MMC were investigated. Worn surfaces were observed to find out the wear mechanism involved in wear process of Al and Al-MMC. Images of microstructure and worn surface were also analyzed.

From this work, it will be possible to manufacture Al-MMC reinforced with varying amount of SiC and Al_2O_3 particles. Information about distribution of reinforcing particles in Al matrix and different features of microstructure will be revealed by microstructural observation. It will also be possible to determine the effects of Mg, heat treatment and wt. % of reinforcing particles on hardness and wear characteristics of Al-MMC. An attempt will also be taken to reveal the mechanism involved in wear process of Al-MMC.

The reminder of the thesis is divided into several chapters. Chapter Two is a review of previous works relevant to this study. Initially it describes characteristics, properties and fabrication techniques of Al-MMC. It also describes about the effects of ceramic reinforcements on the behavior of Al matrix in Al-MMC, brief description about interface formation including role of Mg in improving interfacial bond strength, mechanical properties of Al-MMC, factors affecting the wear properties of Al-MMC and different types of wear mechanisms.

Chapter Three describes the materials and equipments used in the present work, Al-MMC preparation by stir casting fabrication technique, heat treatment of prepared Al-MMC and experimental procedure including microstructural observation and evaluation of tensile strength, hardness and wear properties of Al-MMC.

Chapter Four describes the results and discussion on microstructural observation, comparison of tensile strength between unreinforced Al and Al-MMC, effects of Mg addition, heat treatment and wt. % of reinforcements on hardness and wear properties of Al-MMC. Observation of worn surfaces, groove width measurement and finding out mechanism involved in wear process of Al-MMC are also included in this chapter.

Finally, chapter Five summarizes the major conclusions from the results of the present research.

CHAPTER 2
LITERATURE REVIEW

2.1 Aluminum Metal Matrix Composites (Al-MMC)

2.1.1 Aluminum metal matrix composites (Al-MMC)

A composite material is a material composed of two or more physically and chemically distinct phases. The composite generally has superior characteristics than those of each of the individual components. Usually the reinforcing component is distributed in the continuous or matrix component. Composite materials are generally classified on the basis of physical or chemical nature of matrix phase like polymer matrix, metal matrix, ceramic matrix etc. The properties of a composite are a function of the properties of the constituent phases, their relative amounts, and the geometry of the dispersed phases. The term "dispersed phase geometry" indicates the shape of the particles and the particle size, distribution and orientation [7].

In Al-MMC, one of the constituent is Al or Al alloy, which forms percolating network and is termed as matrix phase. The other constituent is embedded in this aluminum or aluminum alloy matrix and is termed as reinforcement, which is usually non-metallic and commonly ceramics such as SiC, B_4C, Al_2O_3 etc [1]. Al-MMC have been created to obtain combination of required mechanical properties such as stiffness, toughness, ambient and high temperature strength which is unavailable in unreinforced Al. Reinforcing particles like SiC, B_4C, Al_2O_3 etc. limit the amount of plastic deformation in the matrix and enhance the mechanical properties of the matrix [8]. Properties of Al-MMC can be tailored by varying the nature of constituents and their volume fraction.

2.1.2 Matrix and reinforcement

The matrix is the monolithic material into which reinforcement are embedded. Matrix is completely continuous and surrounds other phases. Reinforcements are distributed randomly in the matrix as shown in Fig. 2.1. Reinforcement is the part of the composite material that provides strength, stiffness and has the ability to carry load. In general, matrix is percolating soft phase with excellent ductility, formability and thermal conductivity in which hard reinforcements are embedded.

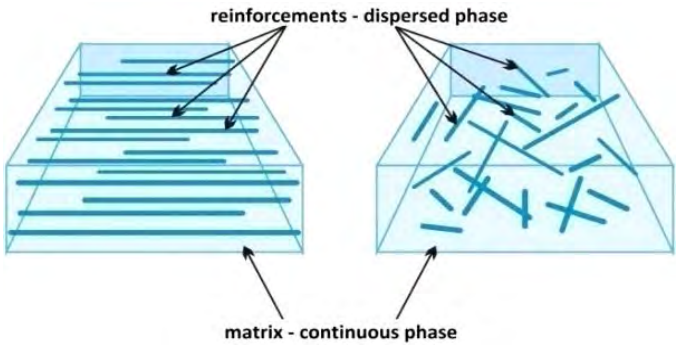

Fig. 2.1: Matrix and reinforcements in composite materials [9]

Depending on the type of material used as matrix, composite materials can be classified into three categories which are as follows:

a) Polymer matrix composites (PMC)
b) Ceramic matrix composites (CMC)
c) Metal matrix composites (MMC)

PMC can be used up to 180 °C but rarely beyond 350 °C. Limitation of using PMC at high temperature applications has widened the scope of using MMC over a wide range of temperatures. Besides, MMC allow tailoring of some useful properties that cannot be achieved in conventional metallic alloys. The MMC provide better transverse properties and higher toughness compared to polymer matrix composites [10].

Table 2.1 shows some of the metal matrix and associated reinforcing materials used to manufacture metal matrix composites. Reinforcements can be embedded in metallic matrix in the form of particulates, short fibers or continuous fibers.

Table 2.1: Metal matrix and reinforcements [10]

Matrix	**Reinforcements**
Aluminum and alloys	C, B_4C, SiO_2, SiC, W, Al_2O_3, Al_3Ni, ZrO_2
Titanium and alloys	B, SiC, Mo, SiO_2, Be, ZrO_2
Nickel and alloys	C, Be, Al_2O_3, SiC, Si_3N_4, W, Mo, B
Magnesium alloys	C, B, glass, Al_2O_3
Molybdenum and alloys	B, ZrO_2
Iron and steel	Fe, B, Al_2O_3, ZrO_2, W, SiO_2
Copper and alloys	C, B, Al_2O_3, E-glass

2.1.3 Advantages of Al-MMC

Aluminum is the most popular matrix for the metal matrix composites [11]. Introduction of reinforcements in Al matrix produces Al-MMC and it results in attractive combination of physical and mechanical properties which cannot be obtained with Al alloys. Increased quantities of Al-MMC are replacing conventional materials for their combination of properties [12]. There are certain advantages of using Al-MMC compared to unreinforced materials. These are as follows:

a) Light weight and high strength
b) High stiffness and toughness
c) Improved damping capabilities
d) Good wear and abrasion resistance
e) Low co-efficient of thermal expansion
f) Improved high temperature properties
g) Enhanced and tailored electrical properties

2.1.4 Classification of Al-MMC

Reinforcements in Al-MMC can be incorporated in the form of particle, short fiber, continuous fiber and mono filament. Depending on the type of reinforcement, Al-MMC can be classified into four categories as shown in Fig. 2.2.

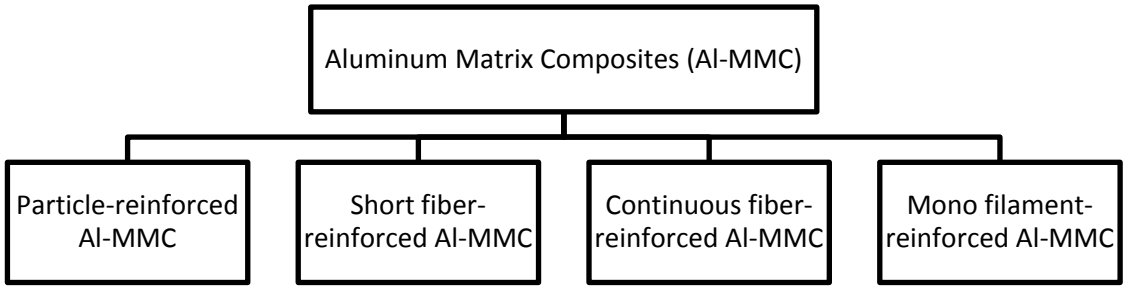

Fig. 2.2: Classification of Al-MMC

Fig. 2.3 shows a schematic presentation of different types of Al-MMC. Important features of above mentioned four types of Al-MMC are discussed below.

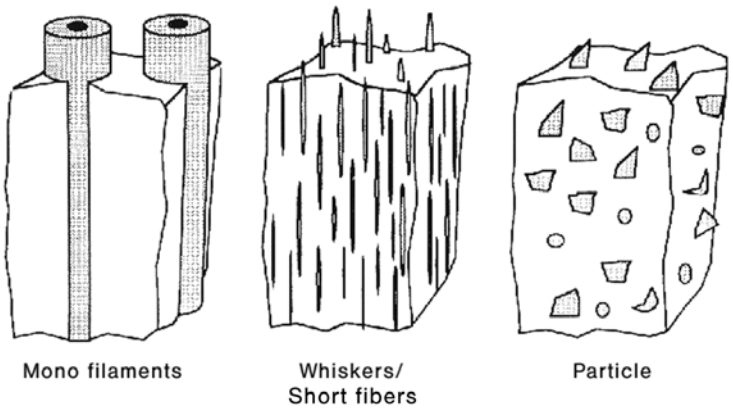

Fig. 2.3: Schematic presentation of different types of Al-MMC [13]

(a) Particle-reinforced Al-MMC

These types of Al-MMC contain equiaxed ceramic particles as reinforcement. Reinforcing ceramic particles are generally metallic oxides, carbides or borides like Al_2O_3, B_4C, SiC, TiB_2 etc. For structural and wear resistance applications, composites contain less than 30% reinforcing particles and for electronic packaging applications, composites contain more than 70% reinforcing particles by volume fraction. Particle reinforced Al-MMC can be prepared by both solid state (powder metallurgy process) and liquid state (stir casting, infiltration etc.) fabrication techniques. Mechanical properties of particle-reinforced Al-MMC are inferior compared to short fiber or continuous fiber or monofilament reinforced Al-MMC, but superior compared to unreinforced Al alloys. Particle-reinforced Al-MMC are isotropic in nature and different types of secondary forming operations like extrusion, rolling, forging can be applied to these composites [1].

(b) Short fiber and whisker-reinforced Al-MMC

These composites contain reinforcements with aspect ratio of greater than 5 and not in continuous form. Short alumina fibers reinforced Al-MMC are the first and most popular short fiber. These composites are extensively used in pistons and produced by squeeze infiltration process. Whisker reinforced Al-MMC can be produced by both powder metallurgy processing and infiltration route. Whisker reinforced Al-MMC showed superior mechanical properties compared to short fiber or particle reinforced Al-MMC. However, whisker reinforced Al-MMC are hazardous for health. Therefore, it has very limited commercial uses. Short fiber reinforced Al-MMC have properties between continuous and particle-reinforced Al-MMC [1].

(c) Continuous fiber-reinforced Al-MMC

In these composites, reinforcements are incorporated in the Al matrix in form of continuous fiber. Reinforced fiber can be parallel and pre-woven, braided before fabrication. Diameter of the fiber is usually less than 20 μm [1].

(d) Mono filament-reinforced Al-MMC

Mono filaments are fibers of large diameter (100-150μm).These Al-MMC are usually produced by chemical vapor deposition (CVD) process using SiC or B as core of carbon fiber or tungsten wire. Bending flexibility of mono filament is lower than multi filaments. Mono filament reinforced Al-MMC are manufactured using diffusion bonding techniques and use of these composites are limited to super plastic forming aluminum alloy matrices [1].

Moreover, hybrid Al-MMC have been developed which contain two or more types of reinforcements. Mixture of particle and whisker or mixture of fiber and particle or mixture of hard and soft reinforcements in aluminum matrix is examples of hybrid composites. Al-MMC containing carbon fibers and alumina particles is an example of hybrid composites which is used in cylindrical liner applications [1].

2.1.5 Processing of Al-MMC

Primary processes for manufacturing Al-MMC can be classified into two categories-

1. Solid state processes
2. Liquid state processes

Powder blending followed by consolidation, diffusion bonding and physical vapour deposition technique come under solid state processing. Liquid state processing includes stir casting, infiltration process, spray deposition and in-situ (reactive) processing. The selection of processing route depends on many factors including type and level of reinforcement loading and the degree of microstructural integrity desired.

Table 2.2 shows the feasibility of various primary processes for manufacturing different types on Al-MMC. It is clear from Table 2.2 that Al-MMC having same matrix and reinforcement combination can be manufactured by more than one route.

Table 2.2: Processing route for different types of Al-MMC [1]

Types of Al-MMC	**Blending and Consolidation**	**Diffusion bonding**	**Vapour deposition and consolidation**	**Infiltration process**
Continuous fiber-reinforced Al-MMC	Not in practice	Not in practice	In use	In use
Mono filament-reinforced Al-MMC	Not in practice	In use	In use	Generally not used
Particle-reinforced Al-MMC	In use	Not in practice	In use	In use
Short fiber and whisker-reinforced Al-MMC	In use	Not in practice	In use	Generally not used
Types of Al-MMC	**Stir casting / slurry casting**	**In-situ Process**	**Spray deposition and consolidation**	
Continuous fiber-reinforced Al-MMC	Not in practice	Information was not available	Not in practice	
Mono filament-reinforced Al-MMC	Not in practice	Not in practice	In use	
Particle-reinforced Al-MMC	In use	In use	In use	
Short fiber and whisker-reinforced Al-MMC	Not in practice	Not in practice	In use	

2.1.5.1 Solid state processing

(a) Powder blending and consolidation (PM processing): In this process, powdered metal and discontinuous reinforcement are mixed and then bonded through a process of compaction, de gassing, a nd t hermo-mechanical t reatment (possibly via hot i sostatic pressing or extrusion) .

Blending o f a luminum alloy p owder w ith c eramic s hort f iber/whisker p article i s a versatile technique for the production of Al-MMC. Blending can be carried out dry or in l iquid suspension. Blending is us ually f ollowed by cold c ompaction, c anning, degassing and high temperature consolidation stage such as hot isostatic pressing (HIP) or extrusion. PM processed Al-MMC, contain oxide particles in the form of plate-like particles of few t ens of nm t hick a nd i n vo lume fractions r anging from 0.05 t o 0.5 depending on pow der history a nd pr ocessing c onditions. T hese f ine oxi de p articles tends to act as a d ispersion-strengthening a gent and often has strong influence on t he matrix properties particularly during heat treatment [1].

(b) Diffusion bonding: Diffusion bonding is a solid state fabrication method, in which a matrix in form of foils and a dispersed phase in form of long fibers are stacked in a particular o rder a nd th en pressed at el evated t emperature T he f inished composite material has a multilayer structure. Diffusion bonding is used for fabrication of simple shaped pa rts (plates, t ubes) [14]. T he di ffusion bondi ng pr ocess i s illustrated i n F ig. 2.4.

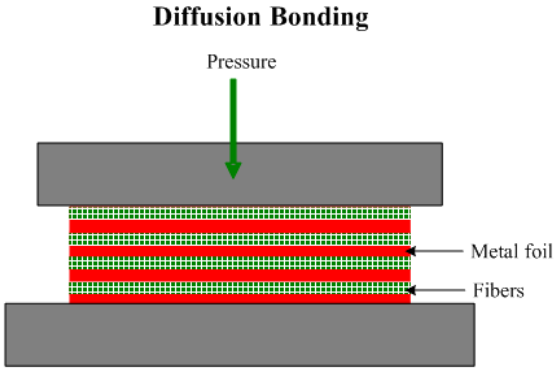

Fig. 2.4: Diffusion bonding [14]

Mono f ilament reinforced A l-MMC ar e m ainly pr oduced by t he d iffusion bond ing (foil-fiber-foil) route or by the evaporation of relatively thick layers of aluminum on the

surface of the fiber. Al-boron fiber composites have been produced by diffusion bonding via the foil-fiber-foil process. However, the process is more commonly used to produce Ti based fiber reinforced composites. The process is cumbersome and obtaining high fiber volume fraction and homogeneous fiber distribution is difficult. The process is not suitable to produce complex shapes and components [1].

(c) Physical vapour deposition: Physical vapour deposition is a thin film deposition process involving physical mechanisms such as evaporation or sputtering as distinct from one involving chemical reactions [15].

The process involves continuous passage of fiber through a region of high partial pressure of the metal to be deposited, where condensation takes place so as to produce a relatively thick coating on the fiber. The vapour is produced by directing a high power electron beam onto the end of a solid bar feed stock. Typical deposition rates are 5–10 μm per minute. Composite fabrication is usually completed by assembling the coated fibers into a bundle or a rray and consolidating in a hot pr ess or HIP operation. Composites with uniform distribution of fibers and volume fraction as high as 80% can be produced by this technique [1].

2.1.5.2 Liquid state processing

(a) Stir casting: Stir casting is a liquid state method of composite materials fabrication, in which a dispersed phase (ceramic particles, short fibers) is mixed with a molten matrix metal by means of mechanical stirring as shown Fig. 2.5. Stir Casting is the simplest and the most cost effective method of liquid state fabrication which offers wide selection of materials and processing conditions. The liquid composite material is then cast by conventional casting methods and may also be processed by conventional metal forming technologies.

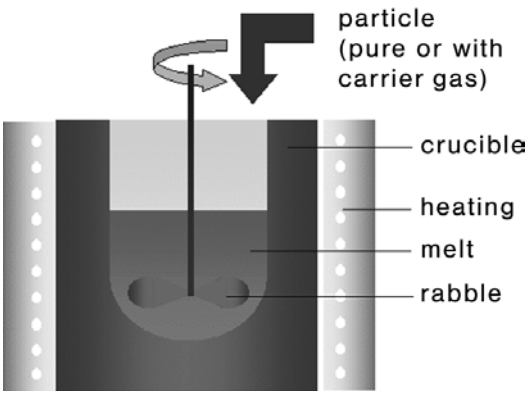

Fig. 2.5: Stir casting [16]

Stir casting process is characterized by the following features [17]:

a) Content of dispersed phase is limited (usually not more than 30 vol. %)
b) Distribution of dispersed phase throughout the matrix is not perfectly homogeneous
c) There are local clouds (clusters) of the dispersed particles (fibers)
d) There may be gravity segregation of the dispersed phase due to a difference in the densities of the dispersed and matrix phase.
e) The technology is relatively simple and of low cost
f) This process is not suitable for the incorporation of sub-micron size ceramics particles or whiskers.

(b) Infiltration process: Infiltration is a liquid state method of composite materials fabrication, in which a preformed dispersed phase (ceramic particles, fibers, woven) is soaked in a molten matrix metal, which fills the space between the dispersed phase inclusions. The motive force of an infiltration process may be either capillary force of the dispersed phase or an external pressure (gaseous, mechanical, electromagnetic, centrifugal or ultrasonic) applied to the liquid matrix phase (forced infiltration) [17].

In this process, liquid aluminum alloy is injected/infiltrated into the interstices of the porous pre-forms of continuous fiber/short fiber or whisker or particle to produce Al-MMC. Depending on the nature of reinforcement and its volume fraction preform can be infiltrated, with or without the application of pressure or vacuum. Al-MMC having reinforcement volume fraction ranging from 10 to 70% can be produced using a variety of infiltration techniques. In order for the preform to retain its integrity and shape, it is often necessary to use silica and alumina based mixtures as binder. Some level of porosity and local variations in the volume fractions of the reinforcement are often noticed in the Al-MMC processed by infiltration technique. The process is widely used to produce Al-MMC having particle/whisker/short fiber/continuous fiber as reinforcement [1].

Fig. 2.6 shows schematic diagram of different types of infiltration process such as pressure die in filtration, squeeze casting infiltration and gas pressure in filtration process.

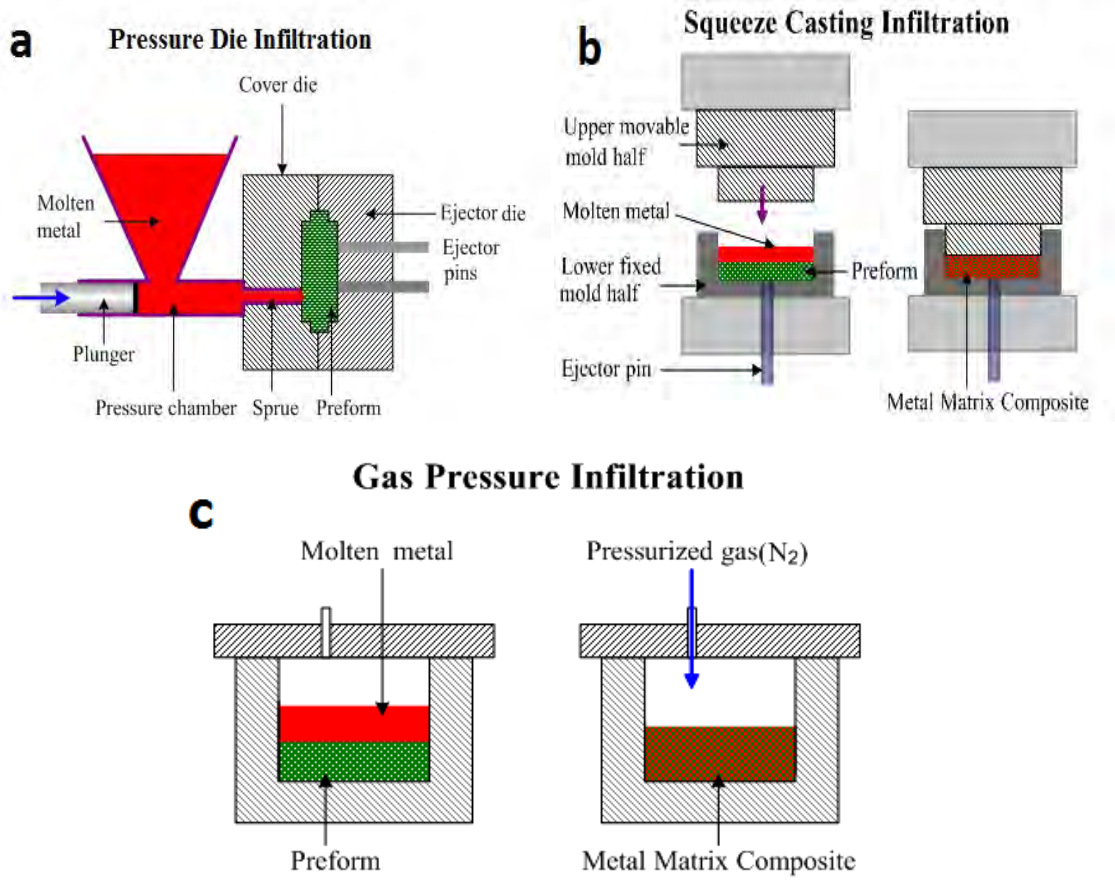

Fig. 2.6: Infiltration process (a) pressure die infiltration (b) squeeze casting infiltration (c) gas pressure infiltration [17]

(c) Spray deposition: Spray deposition is a method of casting near net shape metal components with homogeneous microstructures via the deposition of semi-solid sprayed droplets onto a shaped substrate. In spray forming an alloy is melted, normally in an induction furnace, and then the molten metal is slowly poured through a conical tundish into a small-bore ceramic nozzle [18]. The molten metal exits the furnace as a thin free-falling stream and is broken up into droplets by an annular array of gas jets, and these droplets then proceed downwards, accelerated by the gas jets to impact onto a substrate. The process is arranged such that the droplets strike the substrate whilst in the semi-solid condition, this provides sufficient liquid fraction to 'stick' the solid fraction together. Deposition continues, gradually building up a spray formed billet of metal on the substrate.

Spray deposition techniques fall into two distinct classes, depending whether the droplet stream is produced from a molten bath (Osprey process) or by continuous

feeding of cold metal into a zone of rapid heat injection (thermal spray process). Fig. 2.7 shows a schematic diagram of spray forming process.

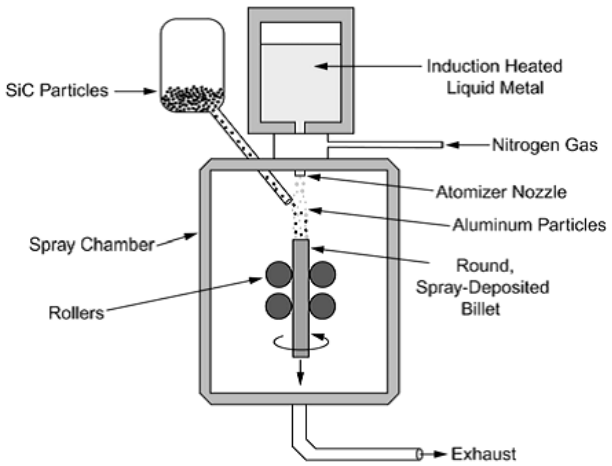

Fig. 2.7: The spray forming process [19]

The spray process has been extensively explored for the production of Al-MMC by injecting ceramic particle/whisker/short fiber into the spray. Al-MMC produced in this way often exhibit inhomogeneous distribution of ceramic particles. Porosity in the as sprayed state is typically about 5–10%. Depositions of this type are typically consolidated to full density by subsequent processing. Spray process also permit the production of continuous fiber reinforced aluminum matrix composites. For this, fibers are wrapped around a mandrel with controlled inter fiber spacing, and the matrix metal is sprayed onto the fibers. A composite monotype is thus formed; bulk composites are formed by hot pressing of composite monotypes. Fiber volume fraction and distribution is controlled by adjusting the fiber spacing and the number of fiber layers. Al-MMC processed by spray deposition technique is relatively in expensive with cost that is usually intermediate between stir cast and PM processes [1].

(d) In-situ processing (reactive processing): In-situ fabrication of MMC is a process in which dispersed reinforcing phase is formed in the matrix as a result of precipitation from the melt during its cooling and solidification [19]. There are several different processes that would fall under this category including liquid-gas, liquid-solid, liquid-liquid and mixed salt reactions. In these processes refractory reinforcement are created in a alloy matrix. A major limitation of in-situ technique is related to the thermodynamic restrictions on the composition and nature of the reinforcement phase that can form in a given system and the kinetic restrictions on the shape, size and

volume fraction of the reinforcement that can be achieved through chemical reactions under a given set of test conditions [1].

One of the examples is directional oxidation of aluminum also known as DIMOX process. In this process the alloy of Al–Mg is placed on the top of ceramic preform in a crucible. The entire assembly is heated to a suitable temperature in the atmosphere of free flowing nitrogen bearing gas mixture. Al–Mg alloy soon after melting infiltrates into the preform and composite is formed. Martin–Marietta's exothermic dispersion process or the XD^{Tm} process is another in-situ technique for composite processing. XD^{Tm} process is used to produce TiB_2 reinforced Al-MMC. The process is flexible and permits formation of both hard and soft phases of various sizes and morphologies [1].

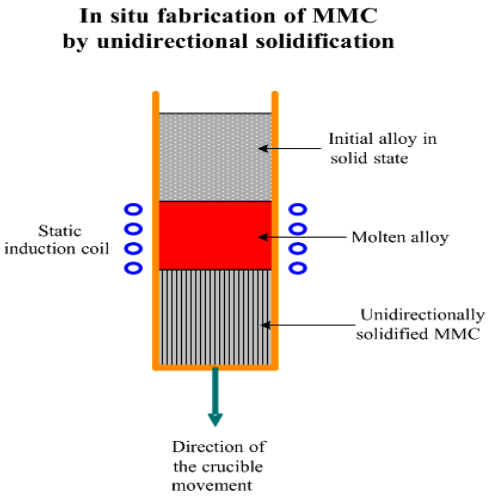

Fig. 2.8: In-situ fabrication technique [20]

A schematic diagram of in-situ fabrication technique of MMC by unidirectional solidification is shown in Fig. 2.8. Advantages of in-situ MMC are as follows [20]:

a) In situ synthesized particles and fibers are smaller than those in materials with separate fabrication of dispersed phase (ex-situ MMC). Fine particles provide better strengthening effect
b) In situ fabrication provides more homogeneous distribution of the dispersed phase particles
c) Bonding (adhesion) between the particles of in situ formed dispersed phase and the matrix is better than in ex-situ MMC

There are some disadvantages of in-situ MMC. These are as follows [20]:

a) Choice of the dispersed phases is limited by thermodynamic ability of their precipitation in particular matrix
b) The size of dispersed phase particles is determined by solidification conditions

2.1.6 Reinforcements used in Al-MMC

(a) Silicon carbide (SiC): Silicon carbide (SiC) is a compound of silicon and carbon with chemical formula SiC. SiC, as shown in Fig. 2.9 is exceedingly hard and synthetically produced crystalline compound.

Fig. 2.9: Silicon carbide [21]

Until the invention of boron carbide (B_4C) in 1929, SiC was the hardest synthetic material known. It has a Mohs hardness rating of 9, approaching that of diamond [22]. In addition to hardness, silicon carbide crystals have fracture characteristics that make them extremely useful in grinding wheels and in abrasive paper and cloth products. Its high thermal conductivity, high-temperature strength, low thermal expansion, and resistance to chemical reaction, makes SiC valuable in the manufacture of high-temperature bricks and other refractories. Table 2.3 shows the properties of SiC.

Table 2.3: Properties of SiC [23-25]

Properties	Values
Molecular mass	40.10 g mol^{-1}
Density	3.21 g cm^{-3}
Melting temperature	2730 °C
Application temperature	1400-1700 °C

Refractive index	2.55
Mohs hardness	9

Low density, high strength and hardness, low thermal expansion, high thermal conductivity and elastic modulus and excellent thermal shock resistance make SiC suitable to use in different applications. Silicon carbide is now widely used in abrasive cutting tools, structural materials, automobile parts, electric systems, electronic circuit elements, astronomy, thin filament pyrometer, heating elements, nuclear fuel particles and cladding, jewelry, steel production, catalyst support and graphene production [22].

(b) Alumina (Al_2O_3): Aluminum oxide (Al_2O_3) is a chemical compound of aluminum and oxygen with the chemical formula Al_2O_3. It is the most commonly occurring of several aluminum oxides and identified as aluminum (III) oxide. It is commonly called alumina. Besides, Al_2O_3 is also known as aloxide, aloxite, or alundum depending on particular forms or applications. It commonly occurs in its crystalline polymorphic phase α-Al_2O_3, in which it comprises the mineral corundum, varieties of which form the precious gems ruby and sapphire. Al_2O_3 is significant in its use to produce aluminum metal, as an abrasive owing to its hardness, and as a refractory material owing to its high melting point. Fig. 2.10 shows example of fine alumina powder.

Fig. 2.10: Aluminum oxide [26]

Al_2O_3 is an electrical insulator but has a relatively high thermal conductivity (30 $Wm^{-1}K^{-1}$) for a ceramic material [27]. Al_2O_3 is insoluble in water. In its most commonly occurring crystalline form, called corundum or α-aluminum oxide, its hardness makes it suitable for use as an abrasive and as a component in cutting tools. It

can resist attack of all gases except wet fluorine and it is resistant to all reagents except hydrofluoric acid and phosphoric acid. Table 2.4 shows the properties of Al_2O_3.

Table 2.4: Properties of Al_2O_3 [24, 27-28]

Properties	**Values**
Molecular mass	101.96 g mol^{-1}
Density	3.95-4.1 g cm^{-3}
Melting temperature	2072 °C
Boiling temperature	2977 °C
Thermal conductivity	30 W m^{-1} K^{-1}
Refractive index	1.76

Al_2O_3 is mostly used to produce aluminum metal. Aluminum metal is produced by electrolysis process from smelter-grade alumina. Calcined Al_2O_3 is used to produce different ceramics products like spark-plug insulators, integrated-circuit packages, bone and dental implants, laboratory ware, sandpaper grits and grinding wheels, and refractory linings for industrial furnaces. Activated alumina is a porous, granular substance that is used as a substrate for catalysts and as an adsorbent for removing water from gases and liquids. Now Al_2O_3 is also used as filler materials, catalyst, purifier, abrasive and composite reinforcements [29].

(c) Boron carbide (B_4C): Boron Carbide (B_4C) is one of the hardest materials known, ranking third behind diamond and cubic boron nitride. B_4C (Fig. 2.11) is an extremely hard material which is used in tank armor, bulletproof vests, nuclear shielding and in industrial applications.

Fig. 2.11: Boron carbide [30]

Boron carbide powder is mainly produced by reacting carbon with B_2O_3 in an electric arc furnace, through carbothermal reduction or by gas phase reactions. For commercial use B_4C powders usually need to be milled and purified to remove metallic impurities. B_4C is characterized by its good chemical resistance, low density, good nuclear properties and extreme hardness [31]. Table 2.5 shows the properties of B_4C.

Table 2.5: Properties of B_4C [31]

Properties	**Values**
Molecular mass	55.255 g mol^{-1}
Density	2.52 g cm^{-3}
Melting temperature	2763 °C
Boiling temperature	3500 °C
Electrical conductivity (at 25 °C)	140 S
Thermal conductivity	(30-42) W m^{-1} K^{-1}
Mohs hardness	9.497

Due to its high hardness, boron carbide powder is mainly used as an abrasive in polishing and lapping applications, and also as a loose abrasive in cutting applications such as water jet cutting. The extreme hardness of boron carbide gives it excellent wear and abrasion resistance and as a consequence it finds application as nozzles for slurry pumping, grit blasting and in water jet cutters.

Boron carbide can absorb neutrons without forming long lived radio-nuclides make the material attractive as an absorbent for neutron radiation arising in nuclear power plants. Nuclear applications of boron carbide include shielding, and control rod and shut down pellets [32].

Boron carbide, in conjunction with other materials also finds use as ballistic armor (including body or personal armor) where the combination of high hardness, high elastic modulus, and low density give the material an exceptionally high specific stopping power to defeat high velocity projectiles. Other applications of boron carbide include ceramic tooling dies, precision toll parts, evaporating boats for materials testing and mortars and pestles.

(d) Titanium carbide (TiC): Titanium carbide (TiC) is an extremely hard refractory ceramic material similar to tungsten carbide. It has the appearance of black powder with NaCl type face centered cubic crystal structure. TiC (Fig. 2.12) is mainly used in preparation of cermets, which are frequently used to machine steel materials at high cutting speed.

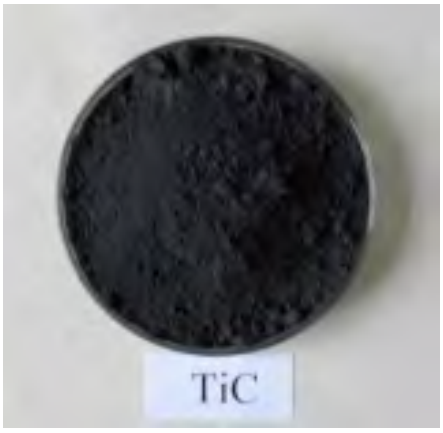

Fig. 2.12: Titanium carbide [33]

The resistance to wear, corrosion, and oxidation of a tungsten carbide-cobalt material can be increased by adding 6-30% of titanium carbide to tungsten carbide. This forms a solid solution that is more brittle and susceptible to breakage than the original material [34]. Table 2.6 shows the properties of TiC.

Table 2.6: Properties of TiC [35-36]

Properties	Values

Molecular mass	59.89 g mol^{-1}
Density	4.93g cm^{-3}
Melting temperature	3160 °C
Boiling temperature	4820 °C
Mohs hardness	9-9.5

TiC is used to manufacture wear-resistant tools and cutting tools, in the form of nano TiC ceramic in optics applications and to enhance the conductivity of materials and as a nucleating agent.

2.1.7 Applications of Al-MMC

Al-MMC are now used in wide range of applications as a successful "high-tech" engineering materials. The benefits of utilizing Al-MMC can be applied, economical and environmental. Al-MMC having different type of reinforcements (whiskers/particles/short fibers/continuous fibers) and produced both by solid state and liquid state processing have found their way to many practical applications. Some of the newer and visible applications of different types of Al-MMC are given below.

(a) Particle-reinforced Al-MMC

Amongst all Al-MMC, particle-reinforced Al-MMC cover largest quantity of composites produced and utilized on volume and weight basis. Particle-reinforced Al-MMC have been successfully used as components in automotive, aerospace, opto-mechanical assemblies and thermal management. These types of Al-MMC are also used as fan exit guide vene (FEGV) in the gas turbine engine, as ventral fins and fuel access cover doors in military aircraft. 40 vol. % SiC reinforced Al-MMC have been successfully used in flight control hydraulic manifolds [1].

(b) Whisker and short fiber-reinforced Al-MMC

The production of whisker-reinforced Al-MMC is very limited because handling of ceramic whiskers is health hazardous. However, SiC-whisker reinforced Al-MMC have been produced with appropriate safety measures and it is used as track shoes in advanced military tanks. Use of whisker-reinforced Al-MMC as track shoes helps in

reducing the weight of the tank. Short fiber-reinforced Al-MMC are also being used in piston and cylinder liner applications [1].

(c) Continuous fiber-reinforced Al-MMC

Continuous carbon fiber-reinforced Al-MMC have been used as antenna wave guides for the Hubble Space Telescope where composites provide high dimensional accuracy, high thermal and electrical conductivity with no outgassing oxidation resistance.

Continuous boron fiber-reinforced Al-MMC have been used as struts in main cargo bay of space shuttle. Recently, continuous alumina fiber-reinforced Al-MMC have been developed which offer equivalent strength at less than half the density and can retain its strength to 300 °C and beyond. Electrical conductivity of these composites is four times of the electrical conductivity of steel or half that of pure aluminum. These composites have been produced to use in several functional applications including [1]:

a) Core of an overhead electrical conductor
b) Automotive push rods
c) Flywheels for energy storage
d) Retainer rings for high-speed motors
e) Brake calipers

2.2 Effects of Ceramic Reinforcement on the Behavior of Aluminum Matrix in Al-MMC

If ceramic particles are present in Al-MMC of more than 10 % by volume fraction, it can affect the behavior of Al matrix during composite processing, heat treatment and in service. The effects can be both extrinsic and intrinsic.

2.2.1 Intrinsic effects

Intrinsic effects indicate microstructural changes, heat treatment characteristics and thermal stresses. These changes significantly alter and expand the physical, mechanical and tribological property limits of aluminum alloys. Properties of intrinsic effects that are caused by the presence of ceramic particles in Al-MMC are discussed below-

(a) Solidification structure of Al-MMC

Solidification behavior of Al-MMC is quite different from Al alloy due to the presence of ceramic particles in Al-MMC. Ceramic reinforcements act as a barrier to diffusion of heat and solute, catalyze the heterogeneous nucleation of phases crystallizing from the melt, restrict fluid convection, and induce morphological instabilities in the solid–liquid interface.

Heterogeneous nucleation of primary phase crystals on the surface of some ceramic reinforcement reduces the matrix grain size. In cast aluminum matrix composites, often grain sizes far in excess of the fiber or particle diameter. Matrix grain size larger than reinforcement size indicates that fibers do not nucleate the primary phase during solidification [1].

(b) Effect of ceramic reinforcements on age-hardening characteristics of Al alloys

The age hardening characteristics of Al alloys can be modified by introducing ceramic particles. Modifications depend on matrix composition, the size, morphology and volume fraction of reinforcements and composite fabrication techniques.

Some age-hardening modifications in Al-MMC are as follows [1]:

a) Composites based on Al–Cu–Mg alloy matrices exhibit accelerated ageing compared to the unreinforced alloys.
b) The peak temperature for precipitation was found to decrease with increasing volume fraction.
c) Room temperature ageing behavior of powder metallurgy processed Al–Cu–SiC composites is significantly different compared to that of cast and extruded composites.
d) The age hardening characteristics of the 6061 Al alloy are considerably altered by the presence of fibers. Fiber array inhibits natural ageing.
e) Presence of TiC particle retard ageing kinetics of 7075 Al alloys.

Modification of age-hardening characteristics of Al alloy is caused by the presence of ceramic particles in Al alloy matrix. When Al metal matrix is reinforced with ceramic particles, a large mismatch exists in co-efficient thermal expansion between reinforcements and Al alloy matrix resulted in increased dislocation density. This higher dislocation density in Al-MMC causes response to age-hardening [1].

(c) Thermal residual stresses

Al-MMC are often fabricated at above 500° C and upon cooling high thermal residual stresses are included in composites. The amount of thermal residual stresses that developed in Al-MMC depends on types of reinforcement, volume faction, diameter and aspect ratio. For example, more than 200 MPa thermal residual stresses are present in Al-30 vol. % SiC Al-MMC. Thermal residual stresses affect mechanical properties greatly. Thermal residual stresses caused by ceramic particles in Al-MMC result in symmetrical yielding and affect creep and fatigue behavior of prepared composites [1].

2.2.2 Extrinsic effects

When Al alloys are reinforced with ceramic particles, sliding wear resistance of Al-MMC is increased due to the intrinsic effect ceramic particles. In recent years, SiC reinforced Al-MMC are utilizing successfully in brake disc/ brake pad tribocouple. When Al-MMC brake disc slide against brake pad, an adherent tribolayer is formed on the drake disc surface at the contact region. This tribolayer increases the wear resistance of Al-MMC brake disc. Tribolayer contains mixed oxides which are transferred from brake pad to the brake disc during sliding. SiC particles present on brake disc surface cause material transfer from brake pad to contacting surface and a tribolayer is formed. Hence tribolayer formation is caused by the extrinsic effect of SiC reinforcements in Al-MMC [1].

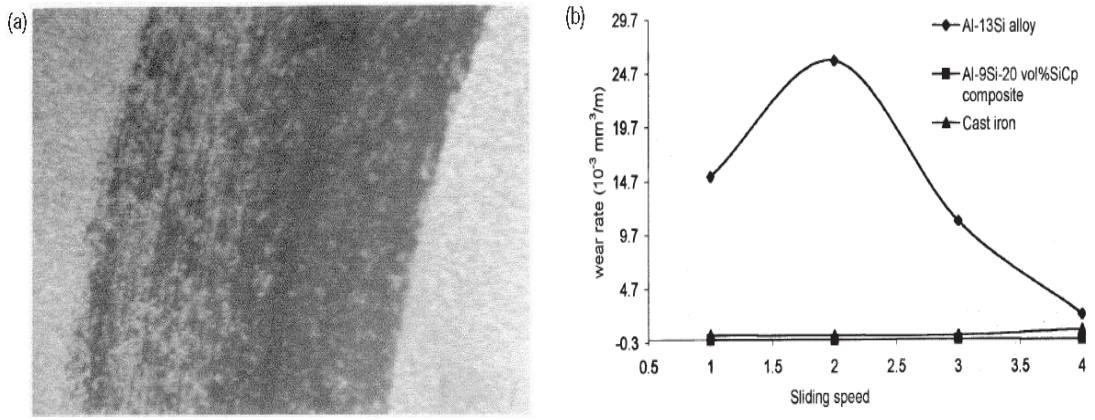

Fig. 2.13: (a) Formation of tribolayer on the worn surface of Al-MMC (disc) sliding against brake pad (b) Comparison of sliding wear rates of unreinforced Al alloy, SiC reinforced Al-MMC and grey cast iron (disc) against brake pad [1]

Fig. 2.13 (a) shows the formation of tribolayer on the worn surface of Al-MMC (disc) sliding against brake pad. Fig. 2.13 (b) shows the plots of wear rate of Al-MMC disc sliding against automobile brake pad. By comparing with unreinforced Al-Si alloy and cast iron, it is clear that Al-MMC have immense potential as lightweight brake discs in transportation industries. The extrinsic and intrinsic effects of SiC particles in Al-MMC have utilized advantageously [1].

2.3 Interface Formation in Al-MMC

2.3.1 Physical phenomena present at the interface

Considering physical and chemical properties of both the matrix and the reinforcement material, the actual strength and toughness desired for the final MMC, a compromise has to be achieved balancing often several conflicting requirements. For example, high strength can be achieved in continuous fiber-reinforced Al-MMC by preventing the reactions between the matrix and the inorganic fibers. A weak interface is desired to increase longitudinal strength and toughness while a strong interface is required to increase transverse strength in continuous fiber-reinforced Al-MMC. Al-MMC with strong interface, a crack has to propagate across both interface and reinforcing particles while for Al-MMC with weak interface, a crack has to propagate following the interface. If however the matrix is weak in comparison with both the interface and the particle strength, the failure will propagate through the matrix itself [37].

The wettability of the reinforcement material by the liquid metallic matrix plays a major role in the bonding formation. It mainly depends on heat of formation, electronic structure of the reinforcement and the molten metal, temperature, time, atmosphere, roughness and crystallography of the reinforcements. Surface roughness of the reinforcing material improves the mechanical interlocking at the interface, though the contribution of the resulting interfacial shear strength is secondary compared to chemical bonding. Large differences in thermal expansion coefficient between the matrix and the reinforcement should be avoided as they can induce internal matrix stresses and ultimately give rise to interfacial failures [37].

2.3.2 Role of magnesium

Wetting of ceramic particles in molten metal is an important requirement to create bonding between reinforcements and matrix metal during Al-MMC processing by

liquid metallurgy fabrication techniques. Bonding is formed by mutual dissolution or chemical reactions between reinforcements and matrix metal. Hereafter, wetting of ceramic particles in liquid metal is necessary. Wetting can be improved by following ways [38]:

a) increasing the surface energies of the reinforcements
b) decreasing the surface tension of the liquid matrix alloy
c) decreasing the solid/liquid interfacial energy at the reinforcement- matrix interface

If Mg is added in molten matrix metal during casting, it performs above three requirements as a powerful surfactant as well as a reactive element. Mg scavenges oxygen from the surface of reinforcing particle, thus thinning the gas layer improves wetting and causes reactions to form strong bond at reinforcement-matrix metal interface [38]. The bonding force between the liquid and solid phases can be expressed in terms of contact angle referred to in the Young-Dupre equation-

$$\gamma_{sg} = \gamma_{sl} + \gamma_{lg}\cos\theta$$

where "s", "l" and "g" stand for solid, liquid and gaseous phases respectively [6]. The magnitude of the contact angle (θ) in this equation, as shown in Fig. 2.14, describes the wettability [6], .i.e.

a) $\theta = 0°$, perfect wettability
b) $\theta = 180°$, no wetting
c) $0° < \theta < 180°$, partial wetting

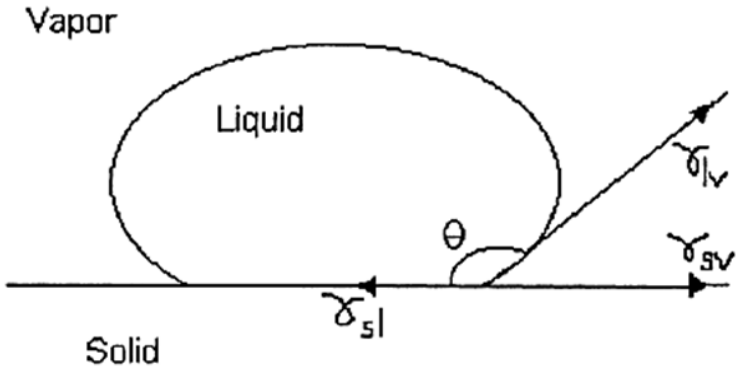

Fig. 2.14: Schematic diagram showing the contact angle that describes wettability [6]

In general, the surface of non-metallic particles is not wetted by the metallic metal, regardless of the cleaning techniques carried out. Wetting has been achieved by coating with a wettable metal. Metal coating on ceramic particles increases the overall surface energy of the solid, and improves wetting by enhancing the contacting interface to metal-metal instead of metal-ceramic. The addition of certain alloying elements can modify the matrix metal alloy by producing a transient layer between the particles and the liquid matrix. This transient layer has a low wetting angle, decreases the surface tension of the liquid, and surrounds the particles with a structure that is similar to both the particle and the matrix alloy. The composites produced by liquid metallurgy techniques show excellent bonding between the ceramic and the metal when reactive elements, such as Mg, Ca, Ti, or Zr are added to induce wettability. The addition of Mg to molten Al to promote the wetting of alumina is particularly successful [6].

2.3.3 Reactions at interface

Al-SiC system is a reactive system that produces Al_4SiC_4 or Al_4C_3 compound at the interface of particles and metal. It is detrimental for composite properties and should be minimized by the following ways [37]:

a) using suitable coatings on reinforcing particles
b) using high silicon (Si) content Al alloys as matrix metal
c) using pre oxidized SiC particulates

In Al-Al_2O_3 composites, Al_2O_3 particles dissolve in Al. Addition of Mg promotes the formation of $MgAl_2O_4$ spinal with Al_2O_3.Some studies found that different compounds are formed at different temperatures in Al-B_4C interface. Normally Al_3BC is formed, but AlB_{10}, $Al_3B_{48}C_2$, $AlB_{24}C_4$ can also be formed.

Interfacial reactions that occur between SiC, Al_2O_3, B_4C, SiO_2 etc. reinforcing particles and (Al + Mg) matrix metal are summarized in Table 2.7.

Table 2.7: Interfacial reactions of selected reinforcing particles with Al and (Al + Mg) [37]

Reinforcing	**Interfacial reactions with Al**	**Interfacial reactions with (Al +**

particles		Mg)
SiC	$4\ Al + 3\ SiC \rightarrow Al_4C_3 + 3\ Si$	$4\ Al + 3\ SiC \rightarrow Al_4C_3 + 3\ Si$ $Al + SiC \rightarrow Al_4SiC_4$
TiC	$4\ Al + 3\ TiC \rightarrow Al_4C_3 + 3\ Ti$ $13\ Al + 3TiC \rightarrow Al_4C_3 + 3\ Al_3Ti$	Information were not available
Al_2O_3	No reaction	$3\ Mg + 4\ Al_2O_3 \rightarrow 3\ MgAl_2O_4 + 2\ Al$ $3\ Mg + Al_2O_3 \rightarrow 3\ MgO + 2\ Al$
B_4C	$27\ Al + 6\ B_4C \rightarrow 6\ Al_3BC + 9AlB_2$ AlB_{10}, $Al_3B_{48}C_2$, $AlB_{24}C_4$ also form	$27\ Al + 6\ B_4C \rightarrow 6\ Al_3BC + 9\ AlB_2$
SiO_2	No reaction	$Mg + 2\ SiO_2 + 2\ Al \rightarrow MgAl_2O_4 + 2\ Si$ $2\ MgAl_2O_4 + 3\ Si \rightarrow 2\ MgO + 3\ SiO_2 + 4Al$

2.3.4 Metallurgy of interfacial area

A very short solidification time is required for Al-MMC to avoid excess chemical reactions at interface. Differences in thermal capacity and conductivity between the reinforcing particles and the matrix induce localized temperature gradients during the cooling process. It is believed that solidification of the metallic matrix is generally a directional outward process which starts from the inside of the metallic matrix and ends at the reinforcing material surface. Whereas this problem is mostly limited to few insoluble impurities (Fe, Si etc.) been carried to the interface for single metal systems, heterogeneities such as insoluble precipitates or en riched phases are often found concentrated at the interface and grain boundaries when working with alloys (Cu, Si containing Al alloys). Depending on the alloy undesired phases can be dissolved by a subsequent heat treatment. Commercial alloys containing Ti, Zr, and Mn as " grain refiner" cannot be used as matrix for the preparation of MMC [37].

There are several ways through which the interfacial reactions can be triggered. By acting on the matrix composition, its reactivity toward the reinforcing material can be altered. For example the high reactivity of Al toward SiC can be minimized by saturating the Al matrix with Si, preventing most of the deleterious Al_4C_3 formation.

By acting on reinforcements, the reactivity towards the matrix can be altered. A surface treatment can be used to passivate the surface of the reinforcing material which is effective in the system of Al-SiC. Here a prior high temperature surface oxidation of SiC to SiO_2 prevents Al_4C_3 formation and increases the bonding [37]. Poor wettability of reinforcements can be enhanced by liquid metals. Introduction of a reactive gas in the mixing chamber can lead to wetting improvement. Alternatively raising the temperature at which the mixing is achieved enhances the wetting but also the risks of creation of deleterious thermodynamically favored but kinetically slow to form phases. In addition, the surface tension of the molten metal can be reduced by traces of alloying elements. Such effects has been reported for Al using Pb, Sn, Mg, and Sr. Finally the processing type and parameters have to be selected and adjusted to a particular MMC system. Metals are generally more reactive in the liquid rather than in the solid state. Consequently short processing times, *i.e.* short contact times between the liquid metal and the reinforcement can limit the extent of interfacial reactions. For example, SiC reinforced Al-MMC which is free of interfacial aluminum carbide can be processed in few seconds by squeeze casting without the need of saturating the matrix with Si [37].

2.4 Mechanical Properties of Al-MMC

2.4.1 Hardness

The resistance to indentation or scratch is termed as hardness. Among various instruments for measurement of hardness, Brinell, Rockwell and Vickers hardness testers are significant. Theoretically, the rule of mixture for composites helps in approximating the hardness values.

$$Hc = Vr\,Hr + Vm\,Hm$$

Where ‘c’, ‘r’, and ‘m’ stand for composite, reinforcement and matrix respectively and V and H stand for volume fraction and hardness respectively. Among the variants of reinforcements, the low aspect ratio particle reinforcements are of much significant in imparting the hardness of the material in which they are dispersed (the hardness of fiber reinforced MMC < whisker reinforced MMC < particle dispersed MMC) [39].

The hardness of the composites containing hard ceramic particles depends on the size of reinforcement, the structure of the composite and good interface bonding. The micro-hardness is a direct, simple and easy method of measuring the interface bonding

strength between the matrix and reinforcement. Particle reinforced MMC possess better plastic forming capability than that of whisker or fiber reinforced MMC. Moreover, these composites exhibit excellent heat and wear resistances due to the superior hardness and heat resistance characteristics of the particles that are dispersed in the matrix.

2.4.2 Tensile strength

Tensile strength of Al-MMC is important depending on its applications. The modified rules of mixture can be effective in predicting upper and lower bound values of the modulus and strength properties of the composites. An optimized combination of surface and bulk mechanical properties may be achieved, if Al-MMC are processed with a controlled gradient of reinforcing particles and also by adopting a better method of manufacturing. Although there is no clear relation between mechanical properties of the composites, volume fraction, type of reinforcement and surface nature of reinforcements, the reduced size of the reinforcement particles is believed to be effective in improving the strength of the composites.

The structure and properties of the reinforcements control the mechanical properties of the composites. Increase in elastic modulus and strength of the composites are reasoned to the strong interface that transfers and distributes the load from the matrix to the reinforcement. Further, the improved interface strength and better dispersion of the particles in the matrix can also be achieved by preheating the reinforcements.

2.4.3 Impact toughness

Toughness can be regarded as a measure of energy absorbed in the process of fracture or more specifically as the resistance to crack propagation, which is normally designated by K_{IC}. The toughness of MMC depends on matrix alloy composition and microstructure; reinforcement type, size, and orientation; and processing insofar as it affects microstructural variables, e.g., distribution of reinforcement, porosity, segregation, etc.

For a given volume fraction (V_f) of reinforcements, the larger the diameter of the fiber, the tougher the composite. This is because the larger the fiber diameter for a given fiber volume fraction, the larger the amount of tough, metallic matrix in the inter-fiber region that can undergo plastic deformation and thus contribute to the toughness [19].

Unidirectional fiber reinforcement can lead to easy crack initiation and propagation compared to the unreinforced alloy matrix. Braiding of fibers can make the crack propagation toughness increase tremendously because of extensive matrix deformation, fiber bundle debonding, and pullout. The fracture energy is the maximum for a composite consisting of three-dimensionally arranged alumina fibers in an aluminum matrix. The general range of K_{IC} values for particle-reinforced Al-MMC is between15−30 $MPa \cdot m^{1/2}$ when short fiber or whisker-reinforced MMC have 5−10 $MPa.m^{1/2}$ [19].

2.4.4 Thermal stresses

In general, ceramic reinforcements (fibers, whiskers, or particles) have a coefficient of thermal expansion lower than that of most metallic matrices. This means that when the composite is subjected to a temperature change, thermal stresses are generated in both components.

Thermal expansion mismatch between the reinforcement and the matrix is an important consideration. It should also be recognized that it is something that is difficult to avoid in any composite, however, the overall thermal expansion characteristics of a composite can be controlled by controlling the proportion of reinforcement and matrix and the distribution of the reinforcement in the matrix [19].

2.4.5 Fatigue

The fatigue behavior of MMC is very important for many engineering applications involving cyclic or dynamic loading. When the composite materials are subjected to cyclic stress amplitude, the resulting strain amplitude may change with continued cycling. Cyclic strain produces a number of damaging process which affects the microstructure and the resulting cyclic strain resistance and low-cycle fatigue. The cyclic strain amplitude reversals to the failure can be viewed as an indication of the resistance of the composites microstructure to microscopic crack formation, potential propagation and coalescence of the cracks culminating in fracture. The strains are much lower in the composite materials than they would be in the unreinforced material. This is because of the higher elastic modulus and higher proportional limit of the composite material. The presence of particulate reinforcements results in the development of localized stresses from constraints in matrix deformation around the reinforcing particles. The highly localized stresses contribute to the observed work-hardening

behavior of the composites. The concentration of the localized stresses results from constraints in matrix deformation that occur because of the significant difference in elastic modulus of the constituents of the composite, i.e. the discontinuous particulate-reinforcement and continuous phases and the continuous aluminum alloy metal matrix.

2.4.6 Creep

The phenomenon creep refers to time-dependent deformation. Creep is defined as the progressive deformation of a material under the action of a constant applied load. Creep does not become significant until temperatures of the order of 0.3 T_m for metals and 0.4 T_m for alloys is reached. Creep behavior in particle-reinforced MMC is characterized by a progressively increasing creep rate (tertiary creep) over most of the creep life.

Clauer & Henson [40] have reported the enhancement of creep resistance in dispersion-strengthened materials, due to precipitation hardening. In these systems, the enhanced strength is due to the effective blocking of dislocation movement by insoluble particles on the slip plane, rather than the particles actually carrying any proportion of the load. Hence power-law creep rates are significantly curtailed, even at low volume fractions (1%).

Barai & Wang [41] have developed a composite model to examine the creep resistance of nanocrystalline solids. This model divides the material into two regions, one the plastically harder grain interior and the other the plastically softer grain-boundary affected zone. The creep rate of each phase is described by a unified constitutive equation that can account for the effect of stress, strain-hardening, and temperature. The increase of creep resistance is attributed to the decrease of grain size through the Hall–Petch effect, but a continuous decrease of grain size would increase the presence of the softer grain boundary affected zone and this in turn could result in the softening effect for the nanocrystalline solid.

2.4.7 Elongation

Ductility is one of the important aspects in the mechanical properties of composites. The tensile elongation decreases rapidly with the addition of reinforcing particles and with increased aging time in the heat treatable alloys. Matrix deformation between closely spaced elastic particles would be highly constrained, resulting in local stress levels. It has also been reported that the reaction products (Al_4C_3) which were formed

at the interface between SiC and Al alloy matrix as a result of reactions between reinforcing particles and Al matrix has significant effect on the ductility rather than strength [42].

2.5 Wear properties of Al-MMC

Wear is the surface damage or removal of material from one or both of two surfaces in a sliding, rolling or impact motion relative to one another. In most cases, wear occurs through surface interactions at asperities. During relative motion, first material on the contacting surface may be displaced so that properties of the solid body, at least at or near the surface, are altered, but little or no material is actually lost. Later, material may be removed from a surface and may result in the transfer to the mating surface or mat break loose as wear particle. In the case of transfer from one surface to another, net volume or mass loss of the interface is zero, although one of the surfaces is worn (with a net volume or mass loss). Wear damage precedes actual loss of material, and it may also occur independently. Definition of wear is generally based on loss of material, but it should be emphasized that damage due to material displacement on a given body (observed using microscopy), with no net change in weight or volume, also constitutes wear.

Wear is a complex phenomenon in which real contact area between two solid surfaces compared with the apparent area of contact is invariably very small being limiting to the points of contact between surface and asperities. The load applied to the surfaces will be transferred through these points of contact and the localized forces can be very large. Wear, as friction is not material property, it is a system response. Operating conditions affect interface wear. Erroneously it is sometimes assumed that high-friction interfaces exhibit high wear rates. This is necessarily not true. For example, interfaces with solid lubricants and polymers exhibit relatively low friction and high wear, whereas ceramics exhibit moderate friction but very low wear.

2.5.1 Factors affecting the wear of Al based composite materials

The principal tribological parameters that control the friction and wear performance of reinforced Al-MMC are mechanical and physical factors extrinsic to the material undergoing surface interaction such as the effect of load normal to the tribo-contact, the sliding velocity, the sliding distance, the reinforcement orientation, the environment,

temperature, the surface finish and the counterpart and material factors intrinsic to the material undergoing surface interaction such as the reinforcement type, size, shape and distribution of the reinforcement, the matrix microstructure and the reinforcement volume fraction.

With regard to the material factors, the volume fraction of reinforcement (V_r) has the strongest effect on the wear resistance. However, the variations of the wear rates of MMC as functions of V_r are affected by the shape and size of the whiskers, fibers and particles used for reinforcement. Additionally, the effective V_r, at which the wear rate reaches its minimum value, are considerably different depending on the kind of reinforcement and matrix material as well as on the sliding conditions. Therefore, it is difficult to select the type of reinforcement and volume fraction that would give optimum wear properties. Based on experimental results on wear behavior of MMC conducted under different test conditions, the effect of different parameter on the wear of MMC are discussed below.

2.5.1.1 Effect of extrinsic (mechanical and physical) factors

(a) Applied normal load

Applied load affects the wear rate of alloy and composites significantly and is the most dominating factor controlling the wear behavior. The wear rate varies with normal load, which is an indicative of Archard's law and is significantly lower in case of composites. The cumulative volume loss increases with increasing applied normal load. Further, with increased applied load the contact surface temperature increases. By measuring the wear rate as a function of applied load, it has been reported that a critical load exists below this load, where the wear rate is mild and steady; above this load a severe wear rate occurs and the critical load decreases with temperature. If the load is further increased, then the unreinforced and reinforced composites eventually seize. The seizure event is accompanied by a sudden increase in wear rate, heavy noise and vibration. This type of seizure is referred to as galling seizure [39].

The specific wear rate of Al-alloy has been reported to decrease with increase in the applied load. Al-alloy easily undergoes thermal softening and re-crystallization at higher temperature compared with the composites because the strength of the composites at higher temperature is greater. As a result, the wear rate of the Al-alloy is

increased drastically at higher loads. At low loads, as particles act as load bearing constituents, the direct involvement of Al-alloy in the wear process is prevented. Metallographic observations at low loads indicate that there is less chemical interaction of the composite with the counter-face due to smaller true contact area. The wear debris size is of the order of millimeters at higher load while at the lower load, it is of the order of a few hundred micrometers. As the load is increased, the proportion of metallic wear debris increases and the size of the delamination is increased for the composite. At the highest load, the worn surface of the materials can be described as classical rachetting wear.

The transition in wear rate is observed for many MMC is faster and test temperature dependent and is believed to be the result of voiding/cracking between reinforcement and the matrix, both of which lead to fragmentation and delamination of the surface. Thus, the maximum load a composite can support during sliding without excessive wear can be obtained by the fracture toughness values of the reinforcement [39].

(b) Sliding speed/velocity

With the increase of sliding speed/velocity/distance, the wear rate and cumulative wear loss increases for all the materials. The sliding speed influences the wear mechanism strongly and at low sliding speed, the wear rate of the composites is lower. This may happen because at high speed, the micro thermal softening of matrix material may take place, which further, lowers the bonding effect of the reinforced particles with that of matrix material. At higher sliding velocity, wear rate is lower for MMC and is due to the formation of a compact transfer layer at the region of the worn surfaces. The amount of the constituents of the counter-body in the transfer layer is seen to increase as sliding velocity increases thus forming a protective cover which tends to reduce wear rate. It has been reported that massive wear occurs if the particles are smaller than a threshold value at higher speeds [39].

(c) Effect of temperature

The wear volume increases substantially above a characteristic temperature that exists between the mild and severe wear transition. Mild to severe wear occurs when friction-induced heating raises the contact surface temperature above a critical value (at about 0.4 times the absolute melting temperature of the matrix). The composite transition

temperature is higher than that of the unreinforced alloy thus the composite suffers lower wear volume. The higher the normal pressure, the lower is the transition temperature. The higher thermal conductivity of the reinforcement contributes in improving wear resistance [39].

(d) Surface finish and hardness of counterpart

Surface roughness affects the wear rate. The higher the roughness, the higher will be the wear rate. The counter-face hardness is inversely proportional to the wear rate thus the counter material with a lower hardness reduces the wear resistance due to the mutual abrasion between the counter material and the wear surface of the specimen. Wear of the counter-face depends on the mechanism of wear of the composite. An increase in load generally results in an increased wear rate of both the composite pin and counter-face. Increasing the volume fraction of particles in the composite reduces its wear rate but increases the wear rate of the counter-face, thus when both counter-face and composite wear are considered, an optimum volume fraction of particles exists at which wear is lowest [39].

(e) Nominal contact area

Wear coefficient and wear rate depends on the nominal specimen contact area. A smaller nominal specimen contact area yields a smaller wear coefficient value, as the wear asperity volume available is smaller. It is also observed that, generally, an increase in load or sliding speed also increases the volume loss and consequently the wear coefficient. From the literature, it can be concluded that the wear coefficient values obtained from the pins with a smaller nominal contact area were indeed lower by an average of about 12% than the larger ones, due to the availability of smaller asperity wear volumes. Hence extreme care should exercise in the interpretation of wear coefficient data obtained from different testing methods or the use of different nominal specimen contact areas [39].

2.5.1.2 Effect of intrinsic (material) factors

(a) Reinforcement size and shape

The wear resistance of a material depends on its hardness, strength, ductility, toughness, the kind of reinforcement, its volume fraction (V_f) and the particle size. The

particle reinforcements are the most effective in improving the wear resistance of MMC provided that good interfacial bonding between the reinforcement and the matrix exists.

The wear resistance of the composites is improved by preventing direct metallic contacts that induce subsurface deformation. The addition of hard ceramic particles improves the resistance to seizure at elevated temperatures. The particulate allow considerable thermal softening effects without having adverse effects on the wear behavior. The reinforcement also causes higher hardness, superior elastic modulus, greater dynamic modulus, better damping capacity and less coefficient of thermal expansion of the matrix alloy. The presence of the ceramic particles provides a higher thermal stability, increased abrasion and sliding wear resistance at high temperature and delays the transition from mild to severe wear.

It is found that the wear rate decreases with decrease in the grain size. This can be attributed to the grain boundary strengthening of Al leading to strain hardening. Such behavior may be attributed to the change in the grain shape from equiaxed to columnar ones. The reinforcement particles with size of several micrometers have higher bonding strength with the matrix, which support the applied load effectively and prevent the crack to initiate and propagate in the subsurface wear region. Therefore, the wear resistance of the composites is improved significantly. The predominant friction mechanism at particulate sizes below 13 μm involves adhesion and micro ploughing, these being augmented by hard third body SiC abrasion with increasing particulate size. Adhesion and micro cutting are the predominant wear mechanisms for smaller reinforcements, the higher wear rates is observed in the larger particulate reinforced composite tribo-system being associated with increased particulate cracking-induced subsurface delamination.

It is required to emphasize the role of second phase particles in providing localized areas of high stress concentrations that influenced flow stress and wear rate. The highest wear resistance was obtained in microstructures associated with fine, well-dispersed semi-coherent particles. For materials characterized by carbides, dispersed in a soft matrix, a decrease in the particle mean free path by reducing the carbide size resulted in improved wear resistance. The wear resistance of composites, compared to the alloys, was attributed to their favorable distribution of particles of a relatively small size.

The main concern about Al-MMC is that, larger the volume fraction and finer the size of the reinforcement, expensive are the Al-MMC. Hence, there is a need to reduce the cost component by optimizing its volume fraction and avoiding/minimizing the use of finer particles. The reinforcement of fine Al_2O_3 particles strengthens the Al-matrix and enhances the wear resistance. The residual alloy phase and the presence of a rigid ceramic skeleton enable the blunting or lubricating properties of the alloy in producing good tribological properties [39].

(b) Effect of different types of reinforcements

The SiC reinforcement in the Al-MMC is more fracture resistant compared to Al_2O_3 and SiC. The SiC particles are harder than other reinforcements and will provide a more effective barrier to subsurface shear by the motion of the adjacent steel counter-face and this result is likely due to differences in particles shape. An additional drawback of Al-MMC with reinforcing phases, such as SiC and Al_2O_3 is the tendency of the reinforcement to act as a second-body abrasive against the counter-face increasing its wear rates. In addition, reinforcement liberated as wear debris acts as a third-body abrasive to both surfaces. The two effects result in a higher wear rate for the system as a whole when MMC is used compared to the monolithic, while the extent of this problem depends on the mechanical properties of the counterface material.

The presence of iron oxide debris in the wear track plays an important role as it has been reported to be beneficial in reducing the resistance to friction for MMC reinforced with Al_2O_3 or SiC particles sliding against steel. The debris for mild wear mainly consists of ferric oxide (Fe_2O_3), while the debris for severe wear was composed of Al_2O_3, Al, α-Fe phases. Moreover, the addition of Si-Fe eutectic alloy and Al_2O_3 particles increases the transition load from mild to severe wear of Al 2024 alloy by more than three times and decreases the coefficient of friction.

Incorporation of TiO_2 particles results in the wear of disc. The TiO_2 particles appear to reduce both plastic flow in the matrix and the metal transfer to the pin. The TiC reinforced Al 356 alloy is the hardest and exhibits the lowest wear rate and an increase in the load at which the transition from low wear rate to high wear rate occurs. An addition of granite particulate to Al 6061 has found that it not only delays the transition wear but also reduces the wear rate and coefficient of friction. The experimental results have shown a significant enhancement in the wear resistance of B_4C particles

reinforced Al 5083 MMC. Cryogenically treated composites may show considerable reduction in the wear rate with an increase in hardness and strength at higher applied loads. The $MoSi_2$ and Cr_3Si reinforced alloys (2124, 5056) exhibits the lowest specific wear rates. The wear resistance of the composites can be improved by incorporating TiB_2 particle reinforcement and the refinement of the matrix grains greatly improves the mechanical properties of the composites. Further, the TiB_2 particles markedly improve the wear performance of the Al–4Cu alloy. It can be said that TiB_2 particles not only protect the matrix by virtue of their high hardness but also by generating the fine iron rich debris which acts as an effective lubricating medium [39].

(c) Effect of reinforcements volume fraction

It has been reported that the wear resistance of composite increases with increase in volume fraction of the reinforcement. The wear resistance of MMC can be improved by increasing the volume fraction of the reinforcing ceramic phase by as much as 70%. Also the dry sliding wear resistance increases with increase in particle volume fraction. At higher volume fraction, the friction coefficient has been found higher and there is almost no effect of load on friction coefficient.

The wear rates of the counter-face material increases with increase of volume fraction of the ceramic particles. This is mainly due to the fact that the hardness and strength of composites are higher and they increase with increase in filler content. The volumetric wear rate increases with increasing applied load while it decreases with increasing volume fraction of the filler material. This may be due to the reason that addition of ceramic content results in a pronounced drop in ductility accompanied by an increase in hardness which may further increase the wear resistance of the MMC. At any constant load, wear rate decreases with increase in addition of SiC and improves the load bearing properties of Al-alloy during sliding. Increase in the addition of SiC restricts the flow or deformation of the matrix material with respect to load.

The cumulative volume loss and the wear rate decreases linearly with increasing volume fraction of Titanium Carbide (TiC) in pure Al. Average coefficient of friction also decreases linearly due to a protective cover provided by transfer layer with increasing volume fraction of TiC. Increase in volume fraction of TiC increases the wear rate of the counter-face. Hence it is suggested that when both counter-face and

composite wear are considered, an optimum volume fraction of particles exists at which wear is lowest [39].

(d) Effect of interfacial bonding

The wear behavior of hard particle reinforced composite depends primarily on the type of interfacial bonding between the Al-matrix and the reinforcement. This is because of the strong interfacial bond which plays a critical role in transferring loads from the matrix to the hard particles, resulting in less wear of the material. In case of poor interfacial bonding, the interface offers site for crack nucleation and tends to pull out the particle from the wear surface tending to higher wear loss. For example, the Ni and Cu coated SiC dispersed Al-SiC composites generally lead to good quality interface characteristics and exhibit the improved wear properties [39].

(e) Effect of porosity

The wear rate of in-situ composites containing relatively lower reinforcing particle increases gradually with increasing volume fraction of porosity up to critical porosity value of about 4 vol.%, but beyond that level, wear rate increases more rapidly. This could be attributed to its combined effect on real area of contact and subsurface crack propagation. Also, the wear coefficient increases considerably with increasing porosity content in this group of cast in situ composite. Sometimes, the contributions of the reinforcing particles in enhancing the wear resistance have been obliterated by increased porosity content and therefore, it should be controlled in cast in-situ composites. However, a limited amount of porosity could be tolerated in cast in-situ composites without impairing its wear resistance significantly. The wear rate of the cast in-situ composites containing relatively lower porosity decreases continuously with increasing particle content, more than expected on the basis of decreasing real area of contact. It is, therefore, expected that blunting of subsurface cracks at porosity could decrease wear debris generation as indicated by decreasing wear coefficient with increasing particle content at lower level of porosity [39].

(f) Effect of wettability

Wettability of the reinforcement in the matrix and interfacial strength are related to one another. Micro-hardness value, coefficient of friction and wear property of metal matrix composite are generally affected by wettability of reinforcements. The decrease in the coefficient of friction value and increase in the wear resistance are due to better distribution of the particle in the matrix, which is due to the improvement in the wettability of the reinforcing phase with the matrix. For example, to improve surface wetting during casting, the graphite particles were coated with a nickel [39].

2.5.1.3 Effect of lubrication

Concerning wear mechanisms under lubricated conditions, the degree of direct contact between the surfaces is minimal and the wear progresses via layers of debris. For all materials, wear loss in lubricated tests at constant load decreases as hardness increases. However, for lubricated conditions, Al-MMC with higher hardness show higher wear resistance.

Scuffing and seizure problems may be addressed by incorporating solid lubricants, namely, Graphite in Al–Si alloys reinforced with SiC or Al_2O_3 particles. It has been found that the addition of graphite flakes or particles in Al-alloys increases the loads and velocities at which seizure took place under the boundary lubricated and dry sliding conditions.

The high seizure resistance of graphitic Al-matrix composites has been attributed to the formation of graphite layers on the contact surfaces that act as solid lubricants, which reduce metal to metal contact between the sliding pairs. One more important factor is that the lubricant used will act as a coolant between the two sliding surfaces avoiding the consequences of increasing temperature of the metals in contact [39].

2.5.1.4 Effect of load and work hardening

In case of alloy, rate of work hardening may be higher and also there is every possibility of entrapment of loose abrasives in the matrix, resulting in relatively reduced wear rate in alloy as compared to the composite with increasing load. In case of abrasive wear, the overall effect of abrasive size on wear rate becomes significantly less as compared to the contribution of load when the matrix of the composite is already subjected to a certain amount of strain hardening effect before being subjected to wear.

Decreasing wear rate with sliding distance is a definite indication of more effectiveness of work hardening of the subsurface regions due to increasing wear induced plastic deformation. Subsurface hardening is evidenced by increased hardness in the subsurface region as compared to the unaffected bulk.

With the repeated dry sliding test, a working hard layer occurs on the wear surface and this promotes wear resistance of the composites. At the same time, the wear surface temperature increases subsequently. As a result, re-crystallization takes place in the worn surface during the dry sliding, which results in the decrease of the wear surface hardness and this considerably counteracts the promoting effect of the wear resistance by work hardening. Moreover, the oxidization layer formed on wear surface of the sample is beneficial in enhancing the wear resistance [39].

2.5.1.5 Effect of mechanical mixed layer (MML)

During sliding at higher wear-rates, high temperature is developed at the sliding surface due to which the specimen softens and becomes plastic. It reacts with the available oxygen and forms their respective oxides. The hard brittle oxide formed on the surface of the specimen becomes thicker and continuous, covering the entire surface. The Aluminum oxide film acts partly as an insulator for thermal conduction. This MML is responsible for the decrease in the wear-rate and friction of the MMC. The transfer of steel inclusions from counter-face surfaces to the composite wear surfaces is another mechanism which contributes to the increase in wear resistance of the composites. This indicates that the inclusions act as additional reinforcements at the wear surface of composite and are load supporting and the specific wear rate decreases with increasing MML thickness. The MML forms on the worn surface of matrix and composite and it serves as a protective layer and a solid lubricant. In composites having low volume fraction, the MML is stable under low loads and unstable under higher loads. In the composite having higher volume fraction of reinforcement, the MML is stable under high loads. The MML are formed in the worn surfaces at a variety of sliding loads. The mixed layers have micro-structural features comprising of a mixture of ultrafine-grained structures in which the constituent variations depend on the sliding loads.

Some characteristics of the MML, which can be used to distinguish it from the normal composite material, are: (a) a darker color than the normal composite material when observed under optical microscope (b) The presence of chemical elements coming from the counter-face (c) A higher micro-hardness value in the MML and abrupt change to too much lower values outside the MML. The hardness of the MML is found to be much harder than that of the matrix hardness in the composite. Actually, the hardness of the MML is independent of the composite and the value is comparable to the hardness of the steel counter-face. It is noted that the MML is not formed in the non-reinforced material, mainly because no trace of iron is found on the worn surface. Micro-hardness studies along the vertically sectioned surface starting from the worn surface show that the magnitude of the hardness of the specimen decreases with the distance from the worn surface, which indicates that the sub-surface nearer to the worn surface is hardened due to strain hardening effect than the region away from the worn surface [39].

2.5.1.6 Effect of heat treatment

The alloy and composites exhibit minimum wear rate after heat treatment due to improved hardness. In case of cast alloy, the value of wear constant is higher than that of the heat treated alloy and composites. During the wear process, the cracks are mainly nucleated at the matrix and reinforcement interfaces. Heat-treated alloy and composite showed better strength and hardness that resulted in fewer propensities for crack nucleation and showed enhancement in wear resistance. In case of heat-treated alloy, the effective stress applied on the composite surface during wear process is less due to higher strength and ductility of the Al matrix. This results in less cracking tendency of the composite surface as compared to the cast alloy. The heat treatment does not radically change the morphology, but hardening of the matrix by precipitation hardening took place, which led to higher hardness and strength [39].

The highest wear resistance can be obtained for T6 thermal treatment condition. The studies determined that the maximum hardening of the matrix is obtained when the composite material is solubilied at a temperature of 560 °C for 3 hours, quenched in ice water at 0 °C and ageing done at a temperature of 175 °C for 7 hours. It was found that the heat treatment T6 for 7 hours was the one that provided the matrix greater hardness and therefore it was the one, which gave the MMC the higher wear resistance. The

higher hardness and yield strength of the composite by T6 heat treatment would have the advantage of preventing the formation of aluminum debris and decreasing its transfer to the surface of steel.

When aged at the lowest temperatures (between 50-1500C), the hardness and abrasive wear resistance of under-aged composites were found to be relatively low. Raising the ageing temperature to 200 °C increased the hardness and abrasion resistance of the composites to the peak-aged condition. At 250 °C the composites were over-aged and this resulted in a reduction in hardness and wear resistance due to the coarsening of the inter-metallic precipitates.

Decreasing the discontinuously reinforced aluminum (DRA) matrix strength through under-aging and over-aging heat treatments decreases the DRA wear rate under abrasion conditions by enhancing the formation of a protective solid film [39].

2.5.2 Wear mechanisms

2.5.2.1 Abrasive wear

Abrasive wear occurs when asperities of a rough, hard surface or hard particles slide on a softer surface and damage the interface by plastic deformation or fracture. In the case of ductile materials with high fracture toughness (e.g. metals and alloys), hard asperities or hard particles result in the plastic flow of the softer material. Most metallic and ceramic surfaces during sliding show clear evidence of plastic flow, even some for ceramic brittle materials. Contacting asperities of metals deform plastically even at the higher loads. In the case of brittle materials with low fracture toughness, wear occurs by brittle fracture. In these cases, the worn zone consists of significant cracking [43].

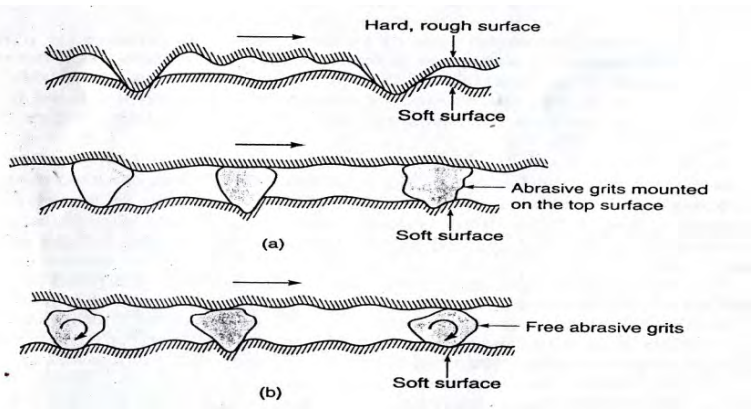

Fig 2.15: Schematics of (a) a rough, hard surface or a surface mounted with abrasive grits sliding on a softer surface and (b) free abrasive grits caught between the surfaces with at least one of the surfaces softer than abrasive grits [43]

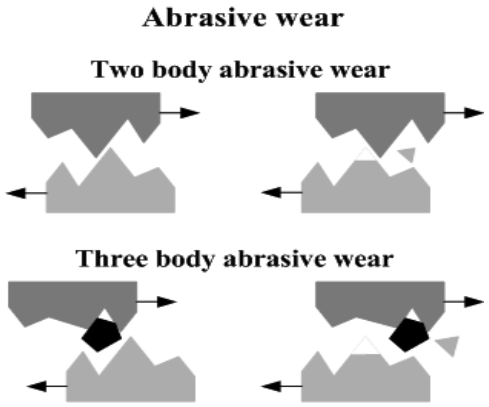

Fig. 2.16: Two body and three body abrasive wear [44]

There are two general situations for abrasive wear as shown in Fig. 2.15 and Fig. 2.16. In the first case, the hard surface is the harder of two rubbing surfaces (two-body abrasion), for example, in mechanical operations, such as grinding, cutting and machining; and in the second case, the hard surface is the third body, generally a small particle of abrasive, caught between the two other surfaces and sufficiently harder that it is able to abrade either one or both of the mating surfaces (three-body abrasion), for example, in free abrasive lapping and polishing. In most abrasive wear situations, scratching (of mostly the softer surface) is observed as a series of grooves parallel to the direction of sliding [43].

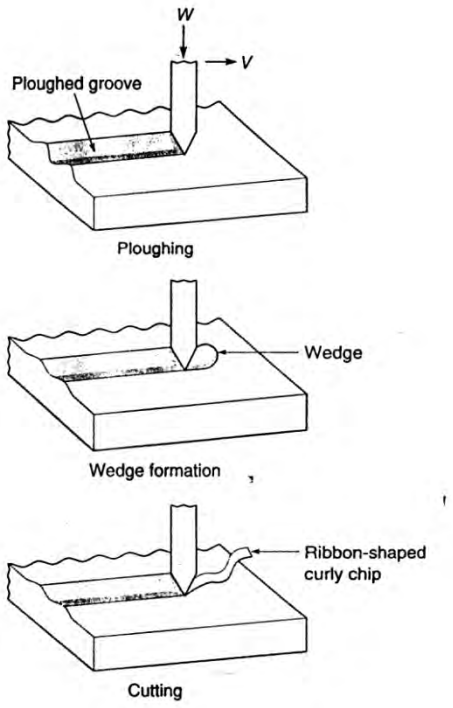

Fig. 2.17: Schematic of abrasive wear processes as a result of plastic deformation by three deformation modes [43]

Material removal from a surface via plastic deformation during abrasion can occur by several deformation modes which include ploughing, wedge formation and cutting as shown in Fig. 2.17. Ploughing results in a series of grooves as a result of the plastic flow of the softer material. In the ploughing process, material is displaced from a groove to the sides without removal of material. However, after surface has been ploughed several times, material removal can occur by a low cycle fatigue mechanism. When ploughing occurs, ridges form along the side of the ploughed grooves regardless of whether or not wear particles are formed. These ridges become flattened, which eventually fracture after repeated loading and unloading cycles. The ploughing process also causes subsurface plastic deformation and may contribute to the nucleation of surface and subsurface cracks. Further loading and unloading (low-cycle, high stress fatigue) cause these cracks and preexisting voids and cracks to propagate and join neighboring cracks, which eventually shear to the surface leading to thin wear platelets.

In wedge formation of abrasive wear, an abrasive tip ploughs a groove and develops a wedge on its front. It generally occurs when the ratio of shear strength of the interface relative to the shear strength of the bulk is high (about 0.5-1). In this situation, only

some of the material displaced from the groove is displaced to the sides and remaining material show up as a wedge.

In the cutting form of abrasive wear, an abrasive tip with large attack angle ploughs a groove a removes the material in the form of discontinuous or ribbon-shaped debris particles similar to that produced in a metal cutting operation. This process results in generally significant removal of material and the displaced material relative to the size of the groove is very little [43].

2.5.2.2 Adhesive wear

Adhesive wear occurs when two nominally flat solid bodies are in sliding contact, whether lubricated or not. Adhesion or bonding occurs at the asperity contacts at the interface and these contacts are sheared by sliding, which may result in detachment of a fragment from one surface and attachment to the other surface. As the sliding continues, the transferred fragments may come of f the surface on which they are transferred and be transferred back to the original surface, or else form loose wear particles. Some are fractured by a fatigue process during repeated loading and unloading action resulting in formation of loose particles [43].

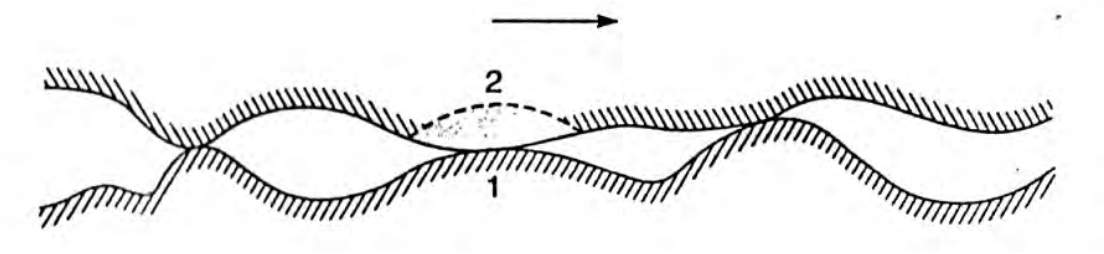

Fig. 2.18: Schematic showing two possibilities of break (1 & 2) during shearing of an interface [43]

Several mechanisms have been proposed for the detachment of a fragment of a material. In an early theory of sliding wear it was suggested that shearing can occur at the original interface or in the weakest region in one of the two bodies as shown in Fig. 2.18. In most cases interfacial adhesion strength is expected to be small as compared to the breaking strength of the surrounding local regions; thus the break during shearing occurs at the interface (path 1)in most of the contacts and no wear occurs in that sliding cycle. In a small fraction of contacts, break may occur in one of the two bodies (path 2)

and a small fragment may attach to the other surface. These transfer fragments are irregular and occur in blocks.

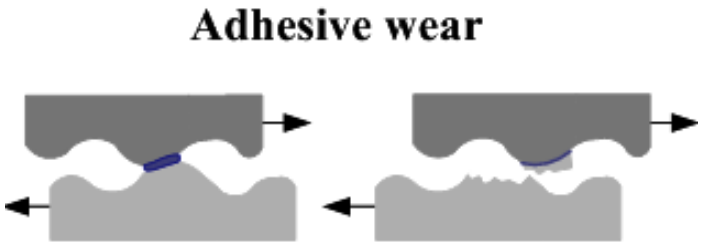

Fig. 2.19: Adhesive wear [44]

Fig. 2.19 shows a schematic diagram of adhesive wear. Adhesive wear is a result of micro-junctions caused by welding between the opposing asperities on the rubbing surfaces of the counter bodies. The load applied to the contacting asperities is so high that they deform and adhere to each other forming micro-joints.

2.5.2.3 Fatigue wear

Subsurface and surface fatigues are observed during repeated rolling and sliding, respectively. The repeated loading and unloading cycles to which the materials are exposed may induce the formation of subsurface or surface cracks, which eventually, after a critical number of cycles, will result in the breakup of the surface with the formation of large fragments, leaving large pits in the surface, also known as pitting. Prior to this critical point, negligible wear takes place, which is in marked contrast to the wear caused by an adhesive or abrasive mechanism, where wear causes a gradual deterioration from the start of running. Therefore the amount of material removed by fatigue wear is not a useful parameter. Much more relevant is the useful life in terms of the number of revolutions or time before fatigue failure occurs [43].

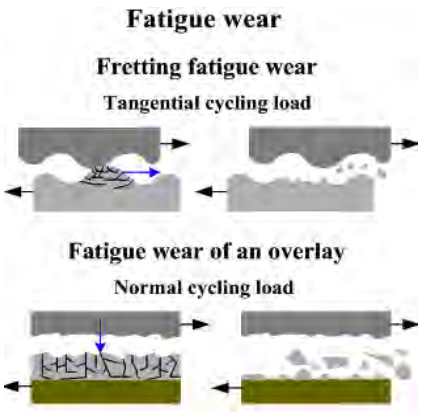

Fig. 2.20: Fatigue wear [44]

Fig. 2.20 illustrates fatigue wear caused by tangential cyclic load and normal cyclic load.

Chemically enhanced crack growth (most common in ceramics) is commonly referred to as static fatigue. In the presence of tensile stresses and water vapor at the crack tip in many ceramics, a chemically induced rupture of the crack-tip bonds occurs rapidly, which increases the crack velocity. Chemically enhanced deformation and fracture result in an increased wear of surface layers in static and dynamic (rolling and sliding) conditions.

2.5.2.4 Impact by erosion and percussion

Two broad types of wear phenomena belong under this heading- erosive and percussive wear. Erosion can occur by jets and streams of solid particles, liquid droplets, and implosion of bubbles formed in the liquid. Percussion occurs from repetitive solid body impacts. Repeated impacts result in progressive loss of solid material.

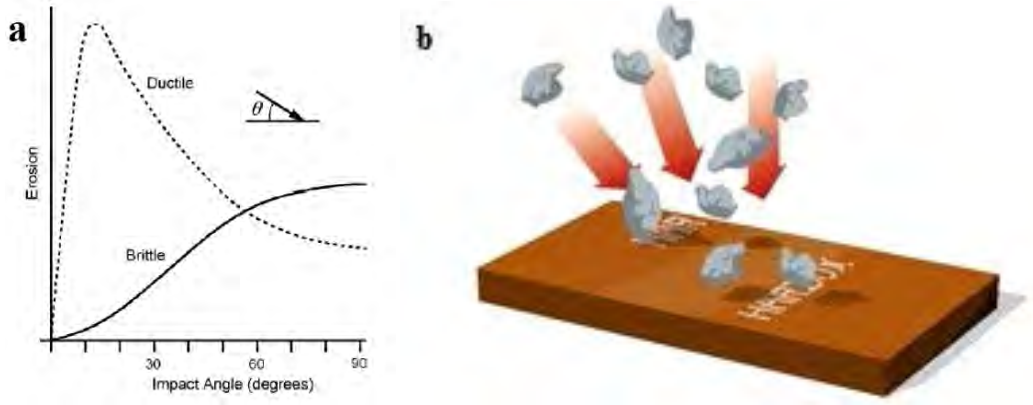

Fig 2.21: (a) Erosion rate as a function of attack angle (b) Impact by percussion [45-46]

Solid particle erosion occurs by impingement of solid particles. It is a form of abrasion that is generally treated rather differently because the contact stress arises from the kinetic energy of particles flowing in an air or liquid stream as it encounters a surface. The particle velocity and impact angle combined with the size of the abrasive give a measure of the kinetic energy of the impinging particles, that is, of the square of the velocity. Wear debris formed in erosion occurs as result of repeated impacts.

As in the case of abrasive wear, erosive wear occurs by plastic deformation and/or brittle fracture, dependent upon material being eroded away and upon operating parameters. Wear rate dependence on the impact angle for ductile and brittle materials is different as shown in Fig. 2.21(a). Ductile materials will undergo wear by a process of plastic deformation in which the material is removed by displacing or cutting action of the eroded particle. In a brittle material, on the other hand material will be removed by the formation and intersection of cracks that radiate out from the point of impact of the eroded particle. The shape of the abrasive particles affects that pattern of plastic deformation around each indentation, consequently the proportion of the material displaced from each impact. In the case of brittle materials, the degree and severity of cracking will be affected by the shape of abrasive particles. Sharper particles would lead to more localized deformation and consequently wear, as compared to the more rounded particles.

Cavitation erosion is a special type of erosion. Cavitation is defined as the repeated nucleation, growth, violent collapse of cavities or bubbles in a liquid. Cavitation erosion arises when a solid and fluid are in relative motion, and bubbles formed in the fluid become unstable and implode against the surface of the solid. When bubbles collapse that are in contact with or very close to solid surface, it will collapse asymmetrically, forming a microjet of liquid directed toward the solid. The solid material will absorb the impact energy as elastic deformation, plastic deformation or fracture. The latter two processes may cause localized deformation and/or erosion of the solid surface [43].

Percussion is a repetitive solid body impact as shown in Fig. 2.21 (b) such as experienced by print hammers in high speed electromechanical applications and high asperities of the surfaces in a gas bearing. In most practical machine applications, the impact is associated with sliding that is the relative approach of the contacting surfaces has both normal and tangential components known as compound impact. Percussive wear occurs by hybrid wear mechanisms which combine several of the following mechanisms: adhesive, abrasive, surface fatigue, fracture and tribochemical wear [43].

2.5.2.5 Chemical or corrosion

Chemical or corrosive wear occurs when sliding takes place in a corrosive environment. In air the most dominant corrosive medium is oxygen and chemical wear

in air is generally called oxidative wear. In the absence of sliding, the chemical products of the corrosion would form a film typically less than a micrometer thick on the surfaces, which would tend to slow down or even arrest the corrosion, but the sliding action wears the chemical film away, so that the chemical attack can continue. Thus chemical wear requires both chemical reactions and rubbing. Fig. 2.22 shows a schematic diagram of corrosion wear [43].

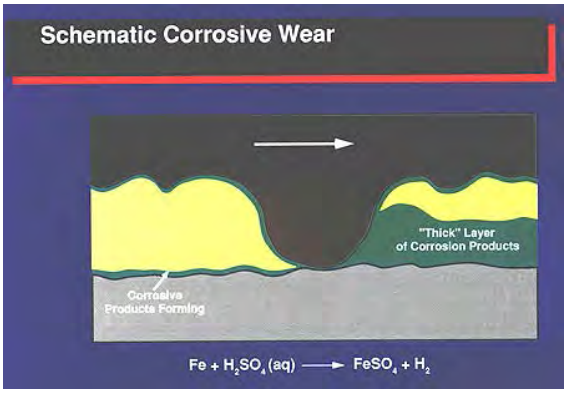

Fig. 2.22: Corrosion wear [47]

Corrosion can occur because of chemical or electrochemical interaction of the interface with the environment. Chemical corrosion occurs in a highly corrosive environment and in high temperature and in high humidity environments. Electrochemical corrosion is a chemical reaction accompanied by the passage of electric current, and for this to occur a potential difference must exists between two regions. The region at low potential is known as an anode and the region at high potential is known as a cathode. If there is a current flow between anode and cathode through an electrolyte, at the anode the metal dissolves in the form of ions and liberates electrons. The electrons migrate through the metal to the cathode and reduce either ions or oxygen. Thus, electrochemical corrosion is equivalent to a short connected battery with partial anodic and partial cathodic reactions occurring on the two sliding members or in a sliding member on two regions atomic distances away. These regions may shift to different locations. Electrochemical corrosion is influenced by the relative electropotential. Electrochemical corrosion may accelerate in a corrosive environment because corrosive fluids may provide a conductive medium necessary for electrochemical corrosion to occur on the rubbing surfaces. The most common liquid environments are aqueous and here small amount of dissolved gases commonly oxygen or carbon dioxide, influence corrosion [43].

2.5.2.6 Fretting wear

Fretting occurs where low-amplitude oscillatory motion in the tangential direction takes place between contacting surfaces, which are nominally at rest. This is a common occurrence, since most machinery is subjected to vibration, both in transit and in operation.

Fig. 2.23: Fretting corrosion wear [47]

Basically, fretting is a form of adhesive and abrasive wear where the normal load causes adhesion between asperities and oscillatory movement causes ruptures resulting in wear debris. Most commonly, fretting is combined with corrosion, in which case the wear mode is known as fretting corrosion. Fig. 2.23 illustrates fretting corrosion wear mechanism. For example, in the case of steel particles, the freshly worn nascent surfaces oxidize to Fe_2O_3 and the characteristic fine reddish-brown powder is produced known as cocoa. These oxide particles are abrasive. Because of the close fit of the surfaces and the oscillatory small amplitude motion, the surfaces are never brought out of contact, and therefore, there is little opportunity for the products of the action to escape. Further oscillatory motion causes abrasive wear and oscillation and so on. Therefore, the amount of wear per unit sliding distance due to fretting may be larger than that from adhesive and abrasive wear. The oscillatory movement is usually result from external vibration, but in many cases it is the consequence of one of the members of the contact being subjected to a cyclic stress, which results in early initiation of fatigue cracks and results in a usually more damaging aspect of fretting, known as fretting fatigue. Surfaces subjected to fretting wear have a characteristic appearance with red-brown patches on ferrous metals and adjacent areas that are highly polished because of the lapping quality of the hard iron oxide debris [43].

2.5.2.7 Delamination wear

Suh [48] proposed that at low sliding speeds, wear debris formation could be described by a delamination wear theory. Wear processes such as adhesive wear, fretting and fatigue were all related to this same mechanism. Suh stated that wear occurred by the following sequential steps:

a) Cyclic plastic deformation of surface layers by normal and tangential loads
b) Crack or void nucleation in the deformed layers at inclusions or second-phase particles
c) Crack growth nearly parallel to the surface
d) Formation of thin, long wear debris particles and their removal by extension of cracks to the surface

The rate-determining mechanism of wear showed dependence on the metallurgical structure. When sub-surface deformation controlled the wear rate, hardness and fracture toughness were both considered to be major influencing factors.

Jahanmir and Suh [49] showed that for microstructures containing hard second phase particles, if sufficient plastic deformation occurred during sliding wear, crack nucleation was favored at these particles. In this situation, where inter-particle spacing is an important variable, crack propagation controlled the wear rate. Void formation was primarily attributed to the plastic flow of the matrix around these hard particles. Void formation occurred very readily around hard particles but crack propagation occurred vary slowly. The depth at which the void nucleation was initiated and the void size tended to increase with increased friction coefficient and applied load.

Suh's delamination theory proposed that voids only nucleated at a defined depth below the sliding wear surface, void formation was related to hydrostatic pressure which existed directly under a contact region. Voids therefore nucleated below a level where hydrostatic pressure was not large enough to suppress there formation and above a depth where plastic deformation was sufficient to nucleated voids around these hard particles. The existence of this critical depth dictated the resultant dimensions of the wear particle debris, especially the thickness of plate-like debris [50].

In delamination wear mechanism, hardness and friction coefficient plays a major role in the overall wear process. Crack propagation is considered the wear-rate controlling

factor. Cracks are initiated at the particle/matrix interface or by the fracture of the particles. For crack nucleation at particle/matrix interfaces the following conditions are necessary [50]:

a) Tensile stress across the interface should exceed the interfacial bond strength
b) Elastic strain energy released upon decohesion of the interface should be sufficient to account for the surface energy of the crack created

2.6 Recent Works on Al-MMC

C. Neelima Devi et al. [3] studied the microstructural aspects of aluminum silicon carbide metal matrix composites. Aluminum metal matrix composites reinforced with silicon carbide particles were prepared by casting process varying the mass percentage of reinforcing particles. The microstructures revealed that lower stirring speed with lower stirring time during composite casting resulted in higher amount of particles clustering. Uniform stirring speed and stirring time resulted in better distribution of reinforcing particles in aluminum matrix. Clustering of particles and some places without SiC inclusions were also observed in the microstructures. That was due to the varying the contact time between the SiC particles and molten aluminum during composite processing, high surface tension and poor wetting behavior of silicon carbide particles in molten aluminum. To overcome the problem of high surface tension and low wetting behavior of silicon carbide in molten aluminum, the paper also suggested applying mechanical force uniformly during reinforcing particles distribution in metal matrix composites.

Madhu Kumar YC et al. [12] investigated mechanical properties of glass particulates reinforced aluminum alloy 6061 metal matrix composites. Aluminum based metal matrix composites containing 3, 6, 9 and 12 wt. % of glass particulates were prepared using stir casting fabrication technique. Microstructures, tensile strength and hardness of the fabricated composites were evaluated. The experimental results showed that tensile strength and hardness of composites increased with increasing wt. % of glass particulates upto 9 wt. % and then decreased with increasing wt. % of glass particulates. 9 wt. % glass particulates reinforced aluminum matrix composites showed maximum tensile strength and hardness. Microstructural observation revealed that glass particulates were dispersed uniformly in the aluminum matrix at all weight percentages

Madeva Nagaral et al. [51] studied the effect of Al_2O_3 particles on mechanical and wear properties of 6061 Al alloy metal matrix composites. Al metal matrix composites containing 3, 6, 9 and 12 wt. % of Al_2O_3 particles were prepared using stir casting route. Mechanical properties, microstructural observation and wear characteristics of the prepared composites were evaluated. Tensile strength and hardness of composites increased while percentage of elongation decreased with increasing the wt. % of Al_2O_3 particulates. The authors indicated that increasing wt. % of harder and stiffer Al_2O_3 particles that restricted the plastic deformation of Al matrix was responsible for high hardness and tensile strength. Wear test results showed that wear rate decreased with increasing sliding distance. Reinforcing aluminum matrix with Al_2O_3 particles increased wear resistance and 12 wt. % Al_2O_3 reinforced composite showed maximum wear resistance. The authors indicated that incorporation of hard Al_2O_3 particles in Al alloy matrix restricted the ploughing action of hard steel counterpart and improved wear resistance.

Vinayak Janiwarad et al. [52] studied the effect of heat treatment on microstructure, mechanical properties and mechanical behavior of Al-Si-Mg alloy reinforced with Al_2O_3 and graphite. Composites with varied percentage of Al_2O_3 and graphite were manufactured by stir casting process. Fabricated composites were subjected to T6 heat treatment. Microstructural observation revealed uniform distribution of reinforcing particles in the metallic matrix. A strong interfacial bond between reinforcing particles and metal matrix was formed resulted in increase of strength and hardness in composites compared to unreinforced alloy. Experimental results showed that heat treatment operation increased both UTS and elongation. Particulates reinforced composites showed better damping properties than un reinforced alloy. It was also suggested that graphite particles were better reinforcement than alumina.

V.C. Uvaraja et al. [53] investigated the influence of operating parameters such as applied load, sliding speed, percentage of reinforcement content and sliding distance on the dry sliding wear of aluminum 6061 hybrid composite reinforced with SiC and B_4C. Hybrid composites were prepared using stir casting process containing varying volume fraction of SiC (5, 10 and 15%) and keeping the volume fraction of B_4C fixed (3%). All wear tests were performed under dry sliding conditions using pin-on-disc method. Hardness test indicated that hardness of the prepared composites increased with increasing the total volume fraction of reinforcements. The test results showed that as

the sliding distance increased, both co-efficient of friction and wear rate decreased at three different loads (10, 20 and 40 N). As the load increases, both co-efficient of friction and wear rate increased. (15 % SiC + 3 % B_4C) particulates reinforced Al matrix composites showed lowest co-efficient of friction wear rate in all cases. Highest volume fraction of SiC (15%) with fixed volume fraction of B_4C (3%) showed lowest wear rate at fixed load. The authors concluded that hybrid composites showed better hardness and tribological properties compared to unreinforced alloy due to the presence of hard phase SiC and B_4C particulates embedded uniformly in aluminum 6061 based matrix.

GENG Lin et al. [54] investigated the effects of Mg content on the microstructures and mechanical properties of SiC_p/Al-Mg composites. Composites containing 10 % SiC_p by volume fraction with varying Mg content of 2.5 %, 4.2 % and 6.8 % by mass fraction were prepared using semi-solid stirring techniques. Microstructural observation revealed that SiC_p were distributed homogeneously in matrix. Composites with high Mg content showed more homogeneous distribution of SiC_p particles in matrix. TEM micrographs indicated that Mg addition improved wettability and a good interfacial bond formation during solidification. Tensile test results showed that SiC_p/Al-Mg composites had better tensile strength compared to Al-Mg alloys. It was found that tensile strength of composites increased with increasing Mg content.

K.M. Shorowordi et al. [2] studied microstructure and interface characteristics of B_4C, SiC and Al_2O_3 reinforced Al matrix composites. Al matrix composites containing varying volume fractions of reinforcing particles were prepared using stir casting manufacturing technique. In microstructural observation, Al-B_4C composites showed better particles distribution compared to Al-SiC and Al -Al_2O_3 composites. An interfacial reaction product was found at Al-SiC interface while no reaction product was found at Al-B_4C and Al-Al_2O_3 interface. From fracture surface analysis, it was thought that Al-B_4C composites had better interfacial bonding than other two composites.

R. S. Rana et al. [55] investigated the effect of Mg enhancement on mechanical property and wear behavior of LM6 aluminum alloy. Aluminum alloy containing Mg was prepared by die casting process. Mechanical and tribological properties of prepared alloy were evaluated. The results showed that addition of Mg content in LM6 aluminum alloy reduced ultimate tensile strength, young's modulus and yield strength

and increased hardness. Mg addition also increased the hardness and reduced wear rate of LM6 alloy.

Israa. A.K. [56] studied the effect of SiC content on the dry sliding wear behavior and mechanical properties of Al- 4% Cu matrix alloy. Al-SiC composites with varying wt. % of SiC particles were prepared by liquid metallurgy method. 8 wt. % SiC reinforced composite showed higher wear resistance compared to other composites and base alloy. It was observed that wear resistance increased with increasing wt. % of SiC and applied normal load but decreased with increasing sliding speed. With the increase of wt. % of SiC, ultimate tensile strength, yield strength and hardness increased but ductility decreased.

Sujit Das et al. [57] studied the mechanical properties and forgeability of heat treated SiC reinforced aluminum metal matrix composites. Aluminum-silicon metal matrix composites reinforced with 0, 5, 10, 15 and 20 wt. % SiC of size 400 meshes were produced by powder metallurgy method. The effect of process conditions on the consolidation was investigated in terms of the relative density changes concurrent with microstructural evolutions. The mechanical properties like hardness and forgeability of the different composites were also investigated. Microstructural study indicated uniform distribution of SiC particles in metal matrix composites. Hardness increased and density decreased with increasing the wt. % of SiC particles in aluminum metal matrix composites. Forgeability of metal matrix composite was remarkably decreased with the increase of weight % of SiC in metal matrix composite as well as when it wass water quenched after heat treatment but in case of air cooling after heat treatment forgeability little bit increased than that of without heat treatment.

Sourav Kayal et al. [58] studied the mechanical properties of as cast silicon carbide particulate reinforced aluminum alloy metal matrix composites. LM6 alloy matrix composites reinforced with varying wt. % of SiC were fabricated using green sand molding process. Microstructural study revealed uniform distribution of SiC particles throughout metal matrix composite castings. Brinnel hardness of the composites was found to increase with increasing the wt. % of SiC. Tensile strength and Young's modulus values of prepared composites were increased with increasing the wt. % of SiC in composites.

Reddappa H.N et al. [59] studied about dry sliding friction and wear behavior of aluminum/beryl composites. Al6061-beryl composites containing four different wt. % (2, 6, 10 and 15) of beryl were fabricated using a vortex method (stir casting method). It was observed from the experimentation that the specific wear rate and average coefficient of friction decreased linearly with increasing weight fraction of beryl for the former while the latter with increasing normal load and weight fraction of beryl. The best result of minimum wear was obtained at 10% weight fraction of beryl (size of particles: 53-75μm).

2.7 Scope of Current Work

The current research work emphasizes to investigate the effect of Mg on wear characteristics of SiC and Al_2O_3 reinforced Al-MMC. The specific objectives includes microstructural analysis of stir cast Al-MMC, quantitative analysis of reinforcing particles distribution in Al matrix using image analysis technique, evaluation of the effect of Mg, heat treatment and amount of reinforcing particles on hardness and wear characteristics of Al-MMC and to observe worn surfaces and finding out the wear mechanism that involved in material removal during wear.

From this work, it will be possible to fabricate SiC and Al_2O_3 reinforced Al-MMC using stir casting fabrication technique. Based on experimental results, it will also be possible to evaluate effects of Mg on wear characteristics of Al-MMC. This may provide important information regarding wear characteristics of Al-MMC.

CHAPTER 3
EXPERIMENTAL PROCEDURE

Al was used as matrix and SiC and Al_2O_3 particles were used as reinforcing particles. Al-MMC reinforced with varying amount of SiC and Al_2O_3 were prepared using stir casting fabrication technique. Stir casting is a cost effective liquid state fabrication technique in which preheated reinforcing materials are added in molten matrix metal followed by stirring and casting. Stir casting fabrication technique was followed because it is an inexpensive process and it offers wide selection of materials and processing conditions. Prepared Al-MMC were heat treated to evaluate the effect of heat treatment. Experimental designs of present work are as follows:

a) Preparing SiC and Al_2O_3 reinforced Al-MMC using stir casting fabrication technique
b) Observing microstructures of prepared composites using both optical microscope and scanning electron microscope (SEM) to reveal particle distribution in Al matrix
c) Comparison of tensile strength of unreinforced Al and Al-MMC
d) Evaluating the effect of Mg, heat treatment and amount of reinforcing particles on hardness and wear characteristics of prepared Al-MMC
e) Determination of wear mechanism which is involved in wear test

3.1 Materials

(a) Matrix material

Al was used as matrix base metal. The composition of Al used in this work is shown in Table 3.1, determined using Optical Emission Spectroscopy (OES). Ribbon shaped Mg was added to increase the wetting between matrix and reinforcement.

Table 3.1: Composition of Al used as matrix base metal (wt. %)

Elements	Fe	Si	Mn	Cu	Mg	Al
Wt. %	0.16	0.19	0.01	0.01	0.01	Balance

(b) Reinforcement material

SiC a nd Al $_2O_3$ particles w ere u sed as r einforcement material. P articles w ere mesh analyzed a nd mesh nu mber of -200/+270 was u sed as r einforcements. P article si ze distribution of SiC and Al_2O_3 is shown in Fig. 3.1 and 3.2 respectively.

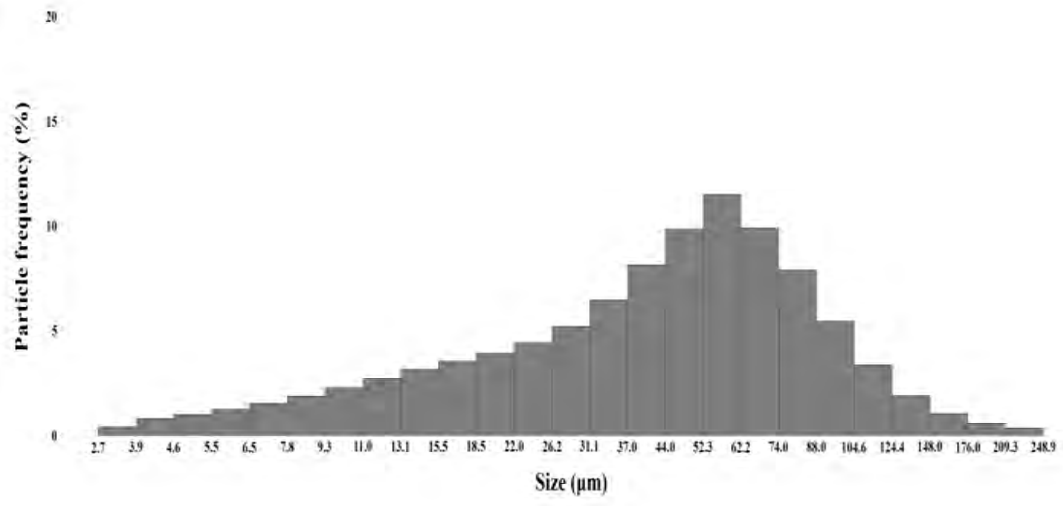

Fig. 3.1: Particle size distribution of SiC

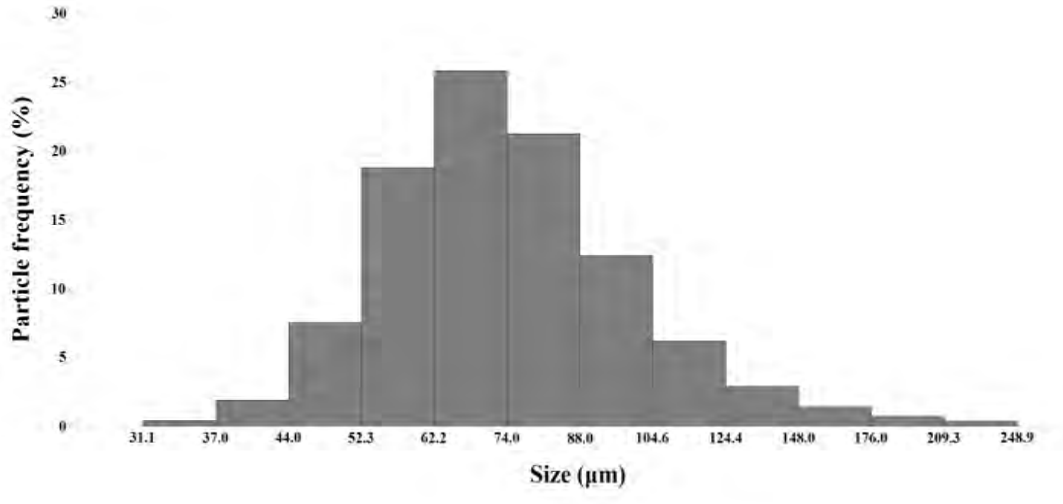

Fig. 3.2: Particle size distribution of Al_2O_3

3.2 Preparation of Composites

SiC and Al_2O_3 reinforced Al-MMC were prepared in this study by stir casting process. In this experiment, Al used as matrix base metal and SiC and Al_2O_3 particles were used as reinforcements. SiC and Al_2O_3 particles were sieve analyzed and particles of mesh number -200/+270 were used.

Al was cleaned and melted in a natural gas fired pit furnace. When the temperature of the liquid Al reached at 750 °C, Mg wrapped with Al foil paper was added in the melt. Molten liquid metal was then shifted to electrical resistance heating stirring furnace. Heat treated SiC and Al_2O_3 were added in the molten Al through a sheet metal funnel at 730 °C. To increase the surface reactivity and reduce the temperature difference between reinforcing particles and liquid Al, SiC and Al_2O_3 particles were preheated in an electric furnace (BLUE M furnace) at 800 °C for about two hours. After SiC and Al_2O_3 addition, the liquid metal-reinforcing particles mixture was stirred for 5 minutes with a graphite stirrer in stirring furnace at rpm of 500. Finally composites were poured in preheated metal moulds at 670 °C. The melt was allowed to solidify in the moulds. Steps followed for Al-MMC fabrication are shown in Fig. 3.3. The dimension of as-cast Al-MMC was (19.5 cm × 7 cm × 2 cm). The designations of prepared Al-MMC are shown in Table 3.2.

To evaluate the effect of heat treatment, as-cast Al-MMC were heat treated by three steps – solution treatment, quenching and age hardening. As-cast Al-MMC were heated at 500 °C for 4 hours followed by quenching in water. Then fabricated Al-MMC were age hardened at 150 °C for 1.5 hours and finally air cooled. Heat treatment cycle of Al-MMC is shown in Fig. 3.4.

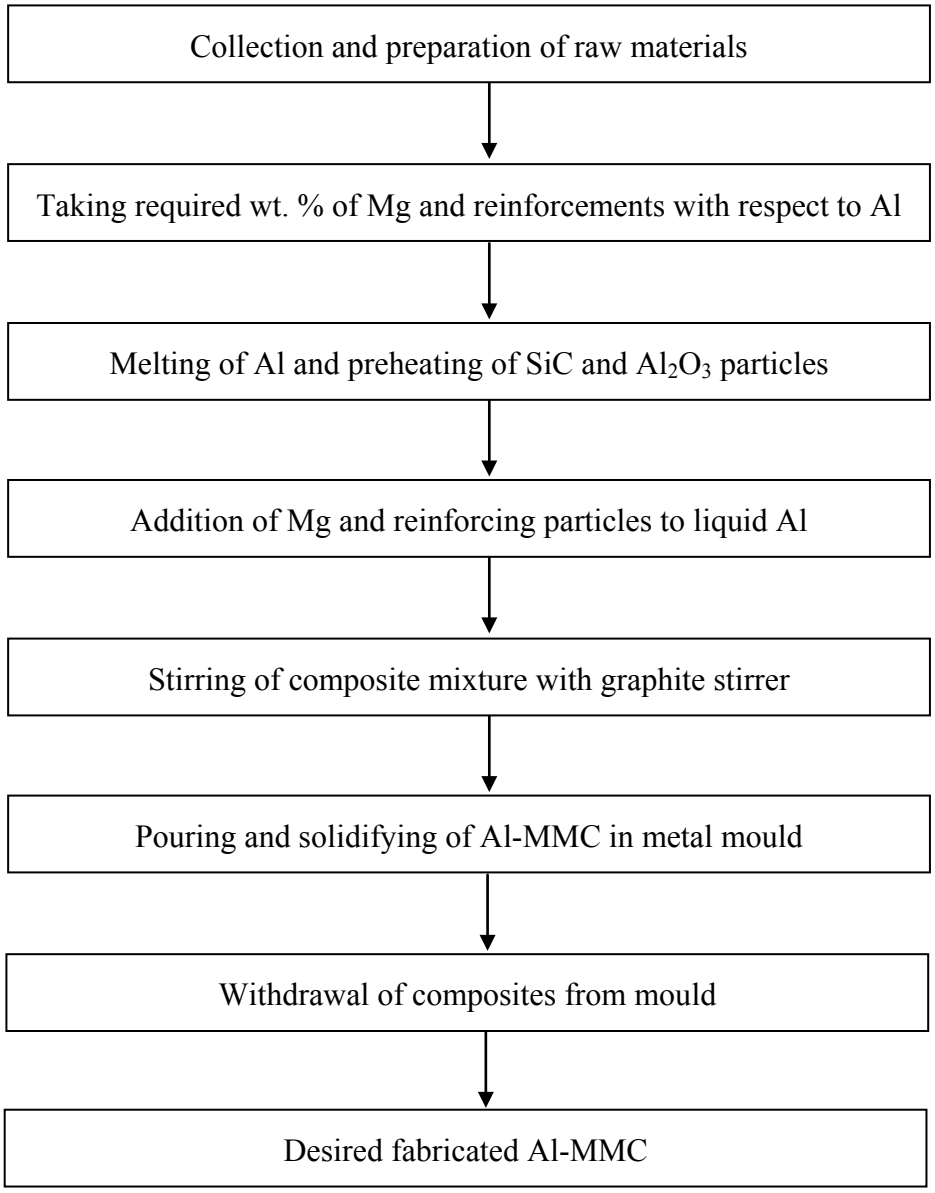

Fig. 3.3: Steps followed for fabricating Al-MMC

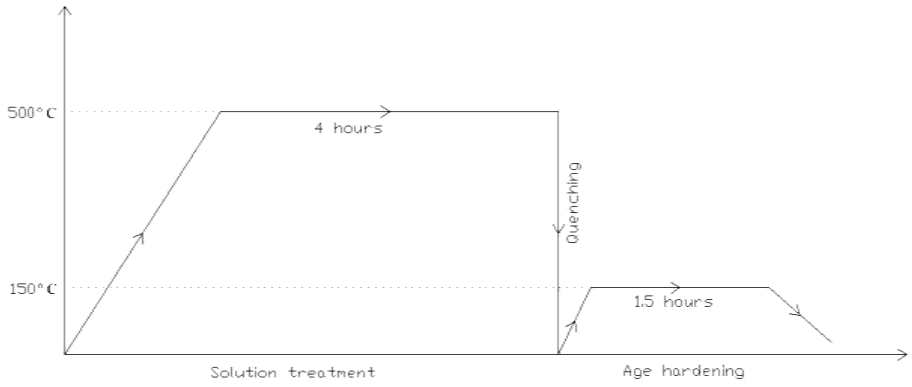

Fig. 3.4: Heat treatment cycle of Al-MMC

Table 3.2: Designation of prepared Al-MMC

Base metal	Mg (wt. %)	Reinforcements (wt. %)	Designation
Al	1	5 % SiC	Al-1M-5S
		10 % SiC	Al-1M-10S
		20 % SiC	Al-1M-20S
	0	No reinforcements	Al
		5 % Al_2O_3 + 10 % SiC	Al-5A-10S
		10 % Al_2O_3 + 5 % SiC	Al-10A-5S
	2	No reinforcements	Al-2M
		5 % Al_2O_3 + 10 % SiC	Al-2M-5A-10S
		10 % Al_2O_3 + 5 % SiC	Al-2M-10A-5S

Composition of as-cast Al-MMC was determined by X-ray fluorescence (XRF) test. It showed the amount of Mg present in the fabricated Al-MMC. XRF test result is shown in Table. 3.3.

Table 3.3: Composition of as-cast Al-MMC obtained from XRF test

Al-MMC	Al	Mg	Fe	Si	Ni	Zn
Al-2M	95.06	2.92	0.32	1.06	0.01	0.09
Al-2M-10S-5A	88.14	3.25	0.49	2.06	0.02	0.18
Al-2M-5S-10A	91.54	2.03	0.22	1.22	0.01	0.02

From test results as shown in Table 3.3, it is seen that some anomalous results were found in XRF test. For example, Si content was found 0.19 % in base Al metal as shown in table 3.1. Although no Si content was added to Al-2M, but Si content was found 1.06 % in XRF test.

In XRF test, accurate result is obtained by using calibration curve produced by Certified Reference Materials (CRM). But CRM was not available for Al-2M and Al-MMC as mentioned in Table 3.3. Hence, composition was determined in XRF test using Fundamental Parameters Method (FPM) which showed less accurate results. Pick overlapping of elements might be another reason for anomalous results.

3.3 Microstructural Observation

Microstructures of prepared Al-MMC were observed to reveal the distribution of reinforcing particles in Al matrix. Samples of dimensions (10 mm × 10 mm) were taken from prepared Al-MMC and they were grinded with revolving grinding wheel. Then they were metallographically polished different grades of emery papers. Finally, samples were subjected to cloth polished with fine alumina powder. Microstructures were observed in both unetched and etched conditions using OPTICA software assisted optical microscope. Etching solution contained 75% water, 15% HF and 10% HCl.

3.4 Scanning Electron Microscopy

Scanning electron microscopy (SEM) was conducted to reveal particles distribution in Al matrix. Samples of dimension (10 mm × 10 mm) were cut and prepared by following procedure as discussed in section 3.3. Microstructures were observed in unetched condition using JEOL JSM-7600F field emission SEM.

3.5 Hardness Observation

To measure hardness values of prepared Al-MMC, samples were taken from castings and mounted with bakelite so that they could not move when the load was applied.

Vickers hardness of prepared Al-MMC was measured using Vickers hardness tester (Future Tech FV-800). A diamond indenter was impressed on material at a load of 5 kg for 10 seconds. Considering the segregation effect of the reinforcements in the matrix, five readings were taken for each sample and average value was accepted.

To determine Brinell hardness values of Al-MMC, a load of 3KN was applied with 10 mm steel ball for 10 seconds using SHIMADZU Universal Testing Machine (UH-500 kN A). The diameter of the resulting indentation on sample surface was measured and Brinell Hardness Number (BHN) was calculated from following expression-

$$\text{BHN} = \frac{2P}{\pi D\left[D-\sqrt{D^2-d^2}\right]}$$

Where, P = load (kg), D = diameter of steel ball (mm), d = diameter of indentation on sample surface (mm).

3.6 Tensile Test

Tensile test was carried out using Instron tensile testing machine. The test was conducted at a strain rate of 2mm/min at room temperature. Tensile test samples were prepared using lathe machine and shaper machine. Dimension of the tensile test samples is shown in Fig. 3.5.

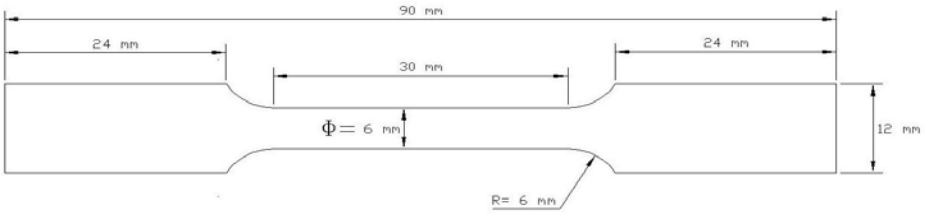

Fig. 3.5: Dimension of tensile test sample

3.7 Wear Test

Wear tests were conducted by using the pin-on-disc method. All the tests were conducted in air and dry sliding condition. The disc was of cast iron with hardness HRC 47 and diameter 9 cm. An arm which could move freely in both vertical and horizontal direction was used to hold and load the pin specimen vertically on the cast iron disk. Fig. 3.6 shows a schematic diagram of pin on disc wear test method.

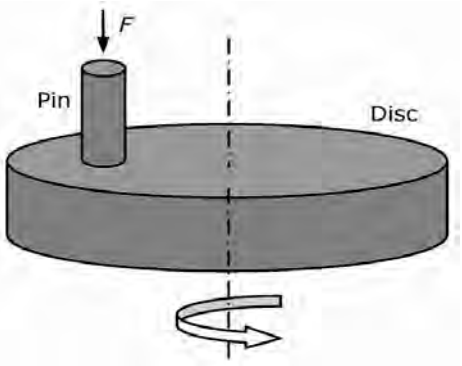

Fig. 3.6: Schematic diagram of pin on disc method of wear test [60]

Wear tests as discussed in sections 4.4.1, 4.4.2 and 4.4.3 were conducted applying 0.4 MPa load at sliding velocity of 1.19 m/s using cylindrical samples of diameter 8 mm and height 10 mm. Wear tests of section 4.4.4 were conducted applying 0.51 MPa load at sliding velocity of 1.26 m/s using pin shaped samples. The diameter of head and tail was 8mm and 5 mm respectively and the length of head and tail was 4 mm and 8 mm respectively of wear test sample.

Before starting the wear test, cast iron counter discs were washed with detergent to remove oil and grease followed by cleaning with acetone. For a fixed sliding distance, weight loss was determined by the mass difference of initial mass and final mass of wear samples. Worn surface of wear samples were observed with OPTICA software assisted optical microscope and stereoscope using Canon PowerShot A75.

3.8 Image Analysis

For image analysis, ImageJ software package was used. Area percentages of reinforcing particles in Al matrix as well as groove width on worn surfaces were measured using image analysis method**.**

Microstructures of SiC and Al_2O_3 reinforced Al-MMC were examined with ImageJ software to calculate the area fractions of reinforcements in Al matrix. To use ImageJ software effectively, three SEM photographs were taken in the same magnification. The color difference was used to separate particulate and matrix. The steps followed to measure area percentage of reinforcing particles in Al matrix and groove width on worn surface are shown in Fig. 3.7 and 3.8 respectively.

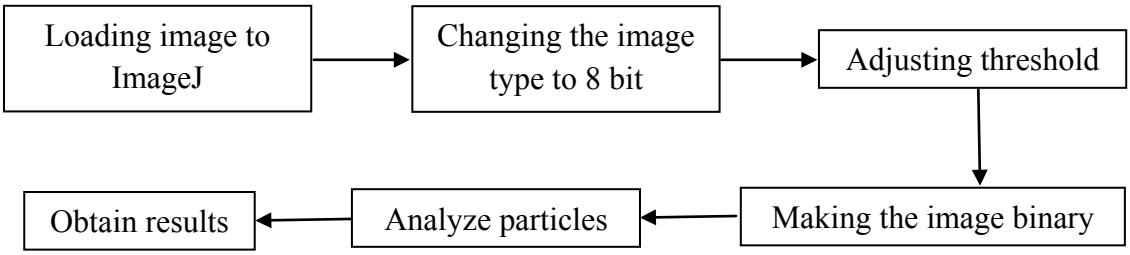

Fig. 3.7: Flow chart to obtain particle distribution

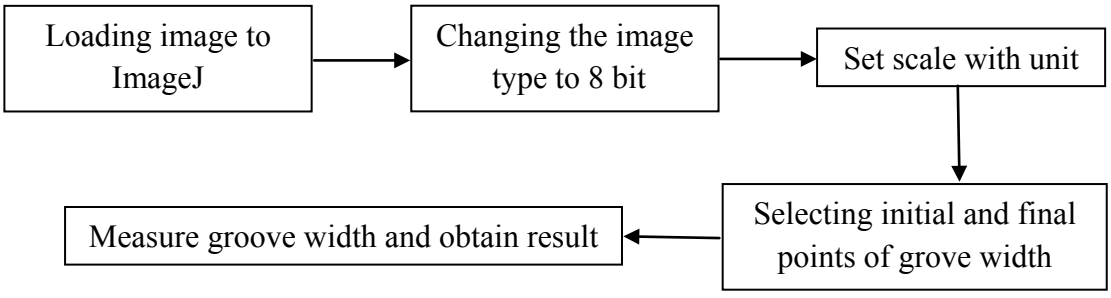

Fig. 3.8: Flow chart to measure groove width

CHAPTER 4
RESULTS AND DISCUSSION

4.1 Microstructural Observation

4.1.1 Optical microstructure

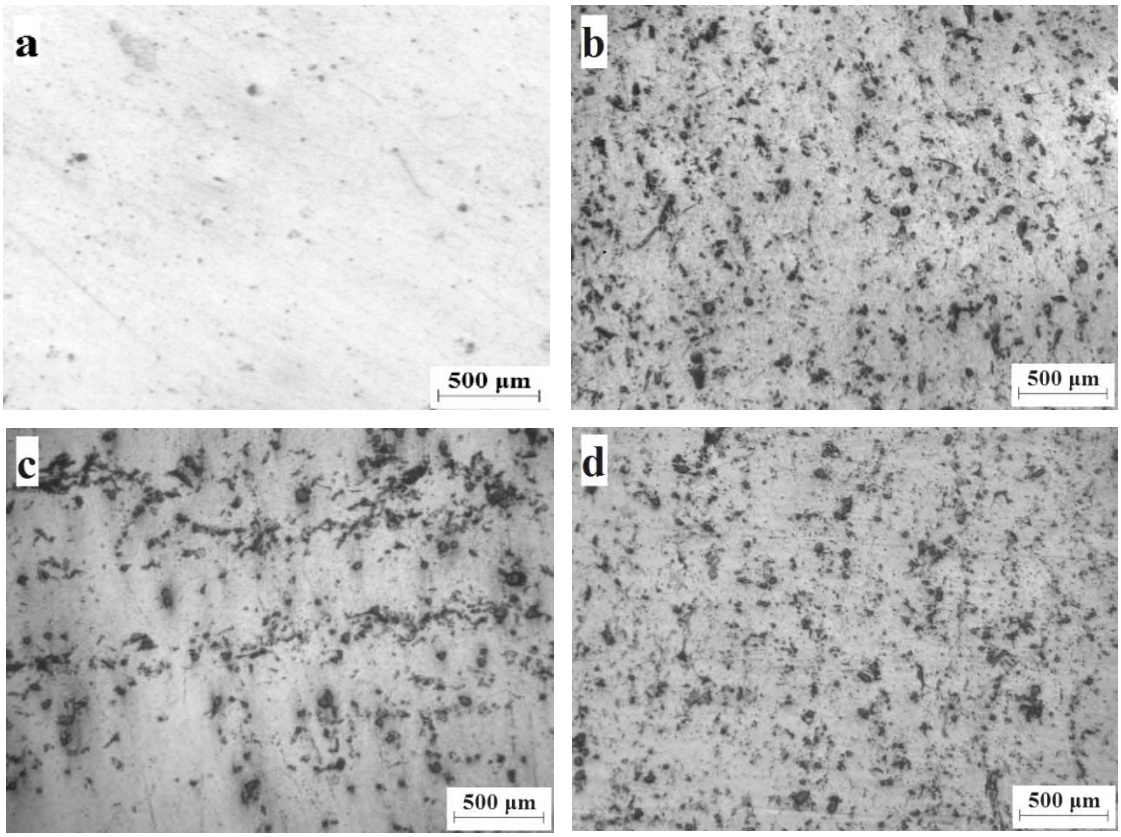

Fig. 4.1: Optical microstructure of as-cast (a) Al (b) Al-1M-5S (c) Al-1M-10S (d) Al-1M-20S

Fig. 4.1 (a) shows optical microstructure of unreinforced Al. Fig. 4.1 (b), 4.1 (c) and 4.1 (d) show optical microstructures of SiC reinforced Al-MMC where SiC particles were dispersed randomly in Al matrix. Uniform distribution of reinforcing particles was observed in the microstructures of Al-1M-5S and Al-1M-20S as shown in Fig. 4.1 (b) and 4.1 (d) respectively. In case of Al-1M-10S, non-homogeneous dispersion of SiC particles in Al matrix was observed as shown in Fig 4.1 (c). Many areas in Al matrix were identified without SiC particles.

Porosities were present in all microstructures. Porosities are detrimental to the mechanical properties of Al-MMC. Porosities in Al-MMC might be formed due to following reasons [6, 42]:

a) entrapped air between reinforcing particles during casting
b) hydrogen evolution caused by chemical reaction between water vapour absorbed on the surface of reinforcing particles and Al melt
c) shrinkage during solidification

It has been reported that holding time for mixing, stirring speed as well as size and position of the impeller also significantly affect the porosity formation [42].

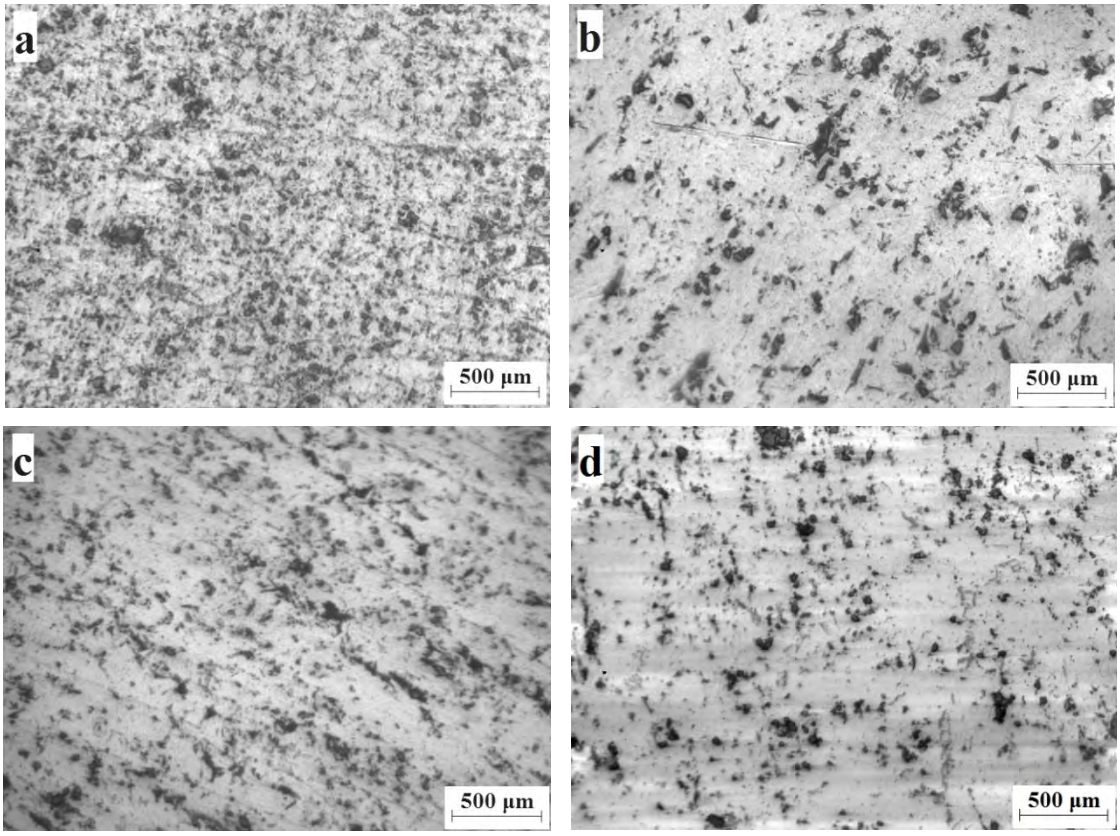

Fig. 4.2: Optical microstructure of as-cast (a) Al-5A-10S (b) Al-2M-5A-10S (c) Al-10A-5S (d) Al-2M-10A-5S

Fig. 4.2 shows optical microstructures of Al-MMC reinforced with varying amount of SiC and Al_2O_3 particles and Mg content. By comparing microstructures of Al-5A-10S and Al-10A-5S as shown in Fig. 4.2 (a) and 4.2 (c) along with Al-2M-5A-10S and Al-2M-10A-5S as shown in Fig. 4.2 (b) and 4.2 (d), it was observed that Al-2M-5A-10S and Al-2M-10A-5S showed better homogeneous distribution of reinforcing particles in

Al matrix and lower porosity content compared to Al-5A-10S and Al-10A-5S. This is believed due to 2 wt. % Mg addition to Al-2M-5A-10S and Al-2M-10A-5S which improved the wettability of SiC and Al_2O_3 particles in molten Al during casting as discussed in section 2.3.2.

Among four optical micrographs of Al-MMC, maximum amount of particle clustering and porosity content were observed in Al-5A-10S as shown in Fig. 4.2 (a). This might be due to poor wettability of SiC and Al_2O_3 particles in molten Al that resulted in clustering of particles and settling down by gravity during Al-MMC fabrication.

Mg has significant effect on particle distribution and porosity content observed in microstructures. A reduction in porosity and a better distribution of SiC and Al_2O_3 particles in Al matrix were observed after 2 wt. % Mg addition to Al-MMC which is in agreement with previous works [54, 61]. This was due to the increase in wettability of SiC and Al_2O_3 particles caused by Mg addition [61].

4.1.2 SEM microstructure

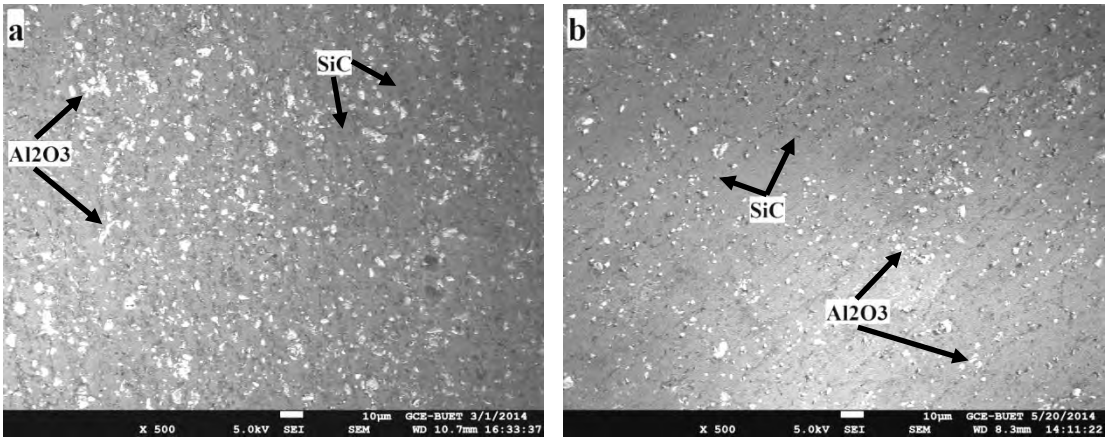

Fig. 4.3: SEM Microstructure of Al-MMC (a) as-cast Al-5A-10S
(b) heat treated Al-2M-5A-10S

Fig. 4.3 shows the SEM microstructure images of as-cast Al-5A-10S and heat treated Al-2M-5A-10S. It was observed from SEM microstructures reinforcing particles were distributed in Al matrix uniformly. Dispersed black particles were identified as SiC and white particles were identified as Al_2O_3 by Energy Dispersive X-Ray (EDX) spot analysis of particles as shown in Fig. 4.4 and Fig. 4.5 respectively. It is evident from Fig. 4.3 that both SiC and Al_2O_3 particles are distributed homogeneously in Al matrix.

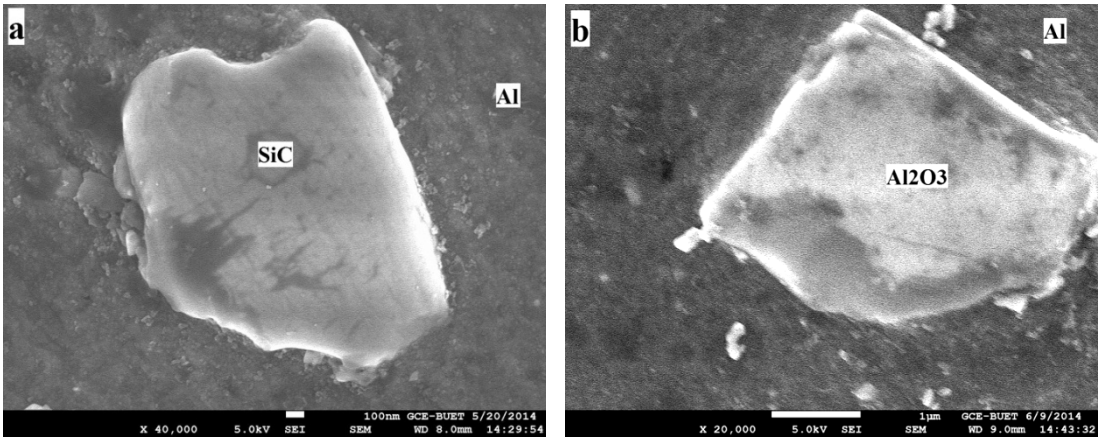

Fig. 4.4: SEM micrograph showing (a) SiC (b) Al_2O_3 particles in Al matrix

Fig. 4.4 (a) and 4.4 (b) show SiC and Al_2O_3 particles in Al matrix respectively. Good adhesion is seen between reinforcing particles and Al matrix in both cases.

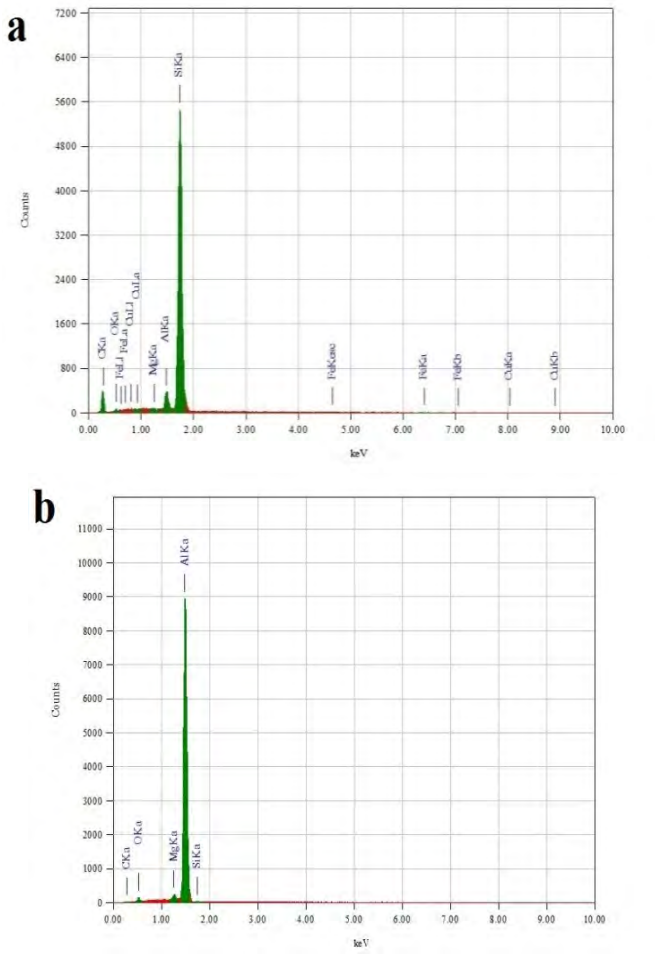

Fig. 4.5: EDX spectra of reinforcing particles (a) SiC (b) Al_2O_3

Fig. 4.5 (a) and 4.5 (b) show the EDX spectra of SiC and Al_2O_3 particles as shown in Fig. 4.4 (a) and 4.4 (b) respectively. The Presence of Si and C in the EDX spectra of

Fig. 4.5 (a) indicated that the particle shown in Fig. 4.4 (a) was SiC. Similarly, particle as shown in Fig. 4.4 (b) was identified as Al_2O_3.

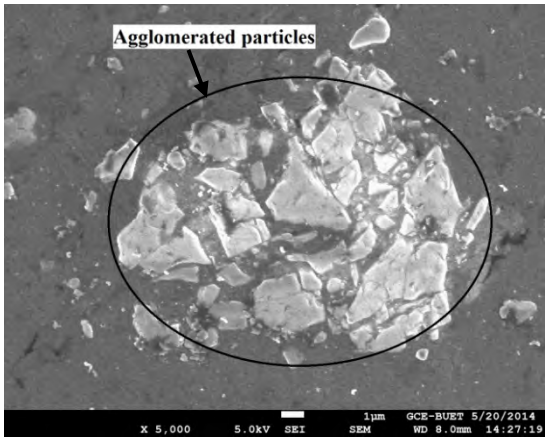

Fig. 4.6: SEM micrograph showing agglomerated particles in Al-5A-10S

Fig. 4.6 shows agglomeration of reinforcing particles in Al-5A-10S. Wettability of SiC and Al_2O_3 particles is poor in liquid Al that can be improved by adding a more wettable metal as discussed in section 2.3. As reactive element Mg content was not added to Al-5A-10S, this led to agglomeration of particles. Mg addition caused an interface layer formation between reinforcing particle and Al matrix which was supposed to observed at particle-metal interface in the microstructure of Al-MMC [54, 62].

During composite processing, SiC particles were preheated at 800 °C for 2 hours to increase the surface reactivity of the particles. Moisture, gas and other contaminants were removed from the surface during preheating; simultaneously a thin layer of SiO_2 was formed by oxidation on the surface of SiC. This SiO_2 layer reacts with Mg and forms nanoscale MgO initially. Then nanoscale MgO transforms into $MgAl_2O_4$ crystal due to the subsequent reaction with Al and SiO_2 [62].

$2\ Mg + SiO_2 \rightarrow 2MgO + Si$

$2\ MgO + 4Al + 3\ SiO_2 \rightarrow 2\ MgAl_2O_4 + 3\ Si$

Preheating of Al_2O_3 particles causes de-hydroxylation and increase of surface energy resulted in increased wettability. It has been reported that preheating of Al_2O_3 improves wettability by the formation of oxygen deficient surface containing some AlO in a spinel-type structure on the particle. Mg reacts with Al_2O_3 particles by follows [37]:

$3\ Mg + Al_2O_3 \rightarrow 3\ MgO + 2\ Al$

$3\ Mg + 4\ Al_2O_3 \rightarrow 3\ MgAl_2O_4 + 2\ Al$

4.1.3 Image Analysis

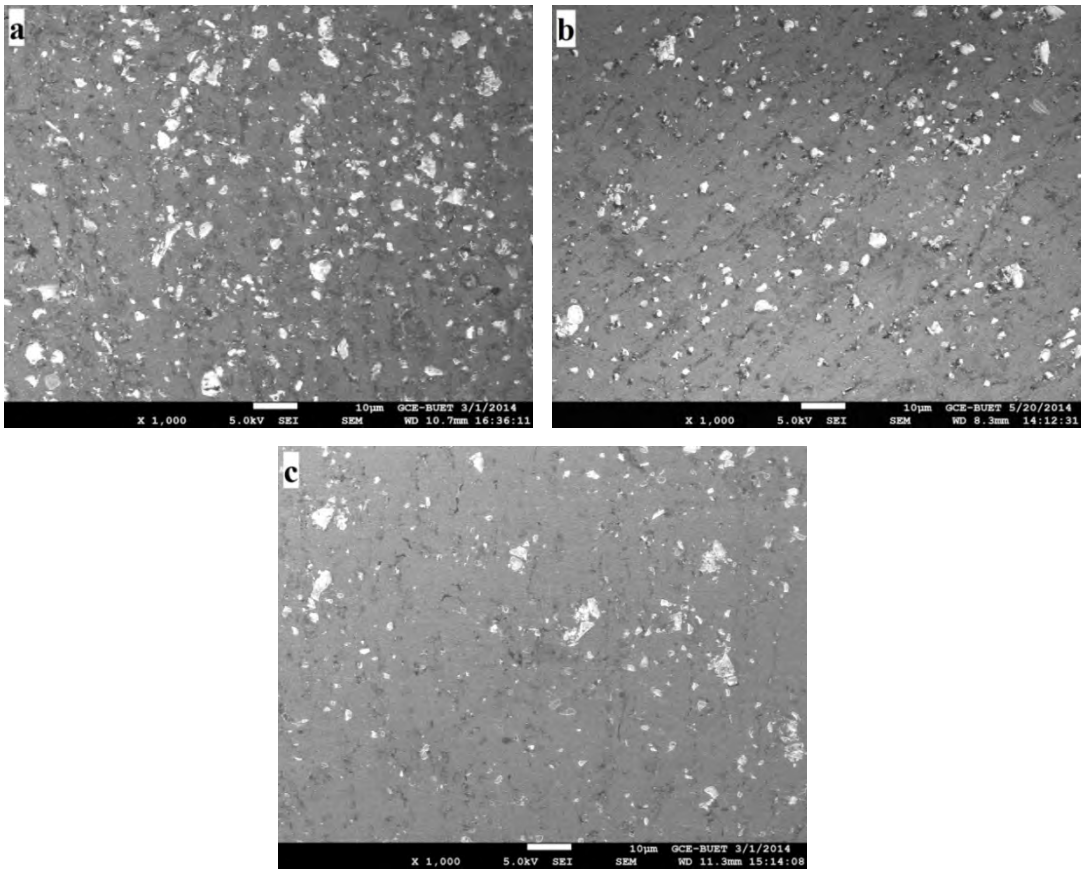

Fig. 4.7: Particle distribution in (a) Al-5A-10S (b) Al-2M-5A-10S (c) Al-2M-10A-5S

Fig. 4.7 shows SEM micrographs of Al-5A-10S, Al-2M-5A-10S and Al-2M-10A-5S. The distribution of SiC and Al_2O_3 particles in Al matrix was identified and analyzed to estimate area percentage of reinforcing particles in Al matrix.

Table 4.1: Area percentage of reinforcing particles in Al matrix

Al-MMC	**Area percentage of reinforcing particles**
Al-5A-10S	13.04
Al-2M-5A-10S	9.73
Al-2M-10A-5S	7.23

Table 4.1 shows area percentage of reinforcing particles in Al matrix of Al-MMC. It is seen from Table 4.1 that Al-5A-10S showed higher area percentage of reinforcing particles in Al matrix compared to Al-2M-5A-10S and Al-2M-10A-5S. Mg was added to Al-2M-5A-10S and Al-2M-10A-5S that promote uniform distribution of reinforcing

particles in Al matrix. As Mg was not added to Al-5A-10S, poor wettability of SiC and Al_2O_3 led to higher amount of particle agglomeration to the analyzed microstructure that resulted in higher area percentage of reinforcing particles in Al matrix [54, 63].

4.1.4 Effect of heat treatment

In order to homogenize the microstructure, Al alloy and Al-MMC were heated at 500 °C temperature for 4 hours and then quenched in water followed by age hardening at 150 °C for 1.5 hours. Such treatment causes a change in microstructure as well as mechanical properties.

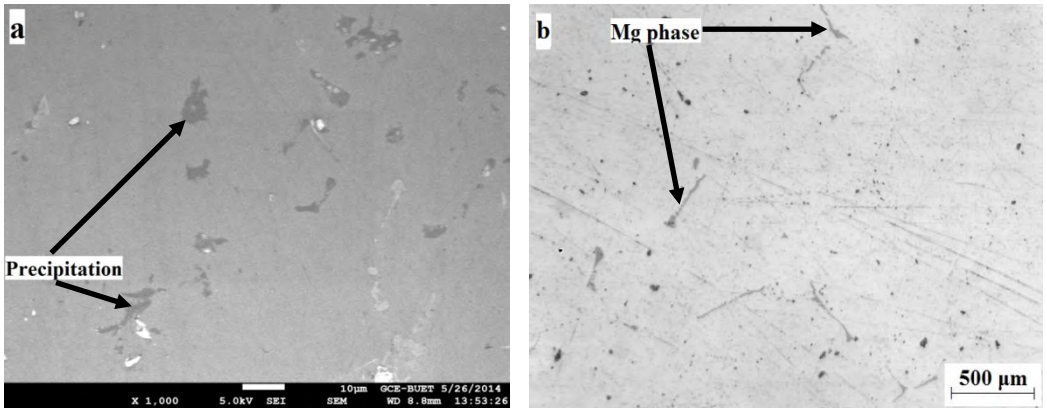

Fig. 4.8: (a) SEM micrograph showing precipitation in Al-2M after heat treatment (b) optical micrograph of Al-2M alloy after heat treatment

Prepared Al-2M alloy was subjected to heat treatment. Heat treated Al-2M showed fine precipitation in Al matrix as shown in Fig. 4.8 (a). From EDX analysis as shown in Fig. 4.9, precipitated compound was identified as $MgAl_2$. The formation of precipitated $MgAl_2$ can be attributed due to the fact that on quenching in water after solution treatment, the rate of cooling during quenching process was very high which enhanced the age hardening kinetics.

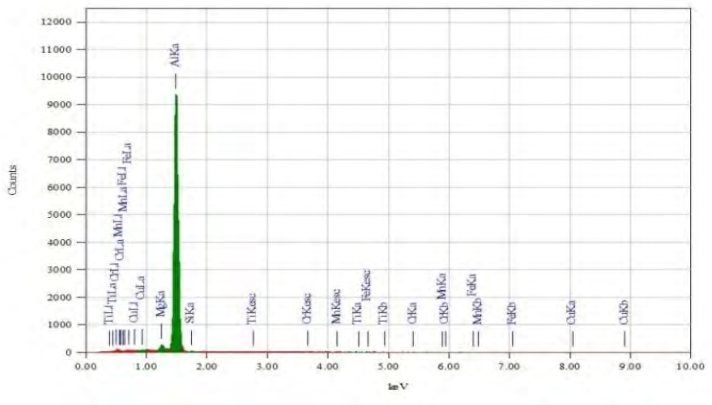

Fig. 4.9: EDX spectra showing the elements present in precipitated $MgAl_2$

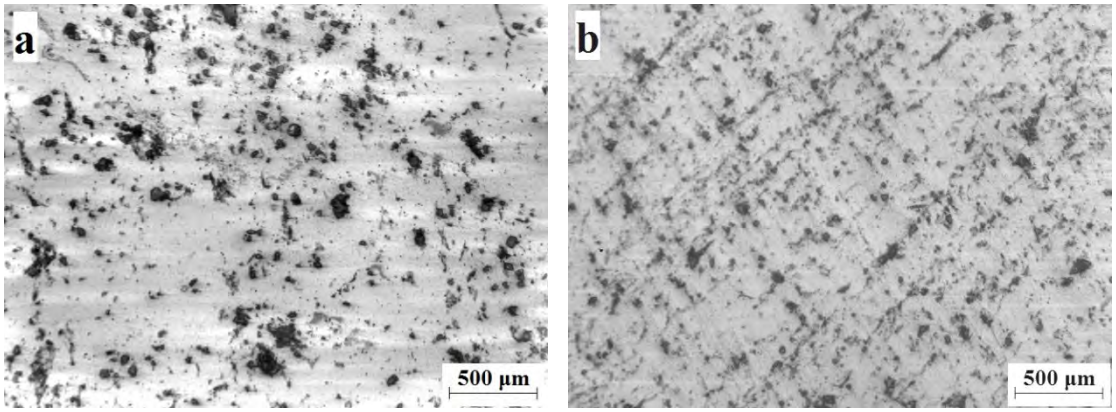

Fig. 4.10: Optical microstructure of Al-2M-10A-5S (a) as-cast (b) heat treated

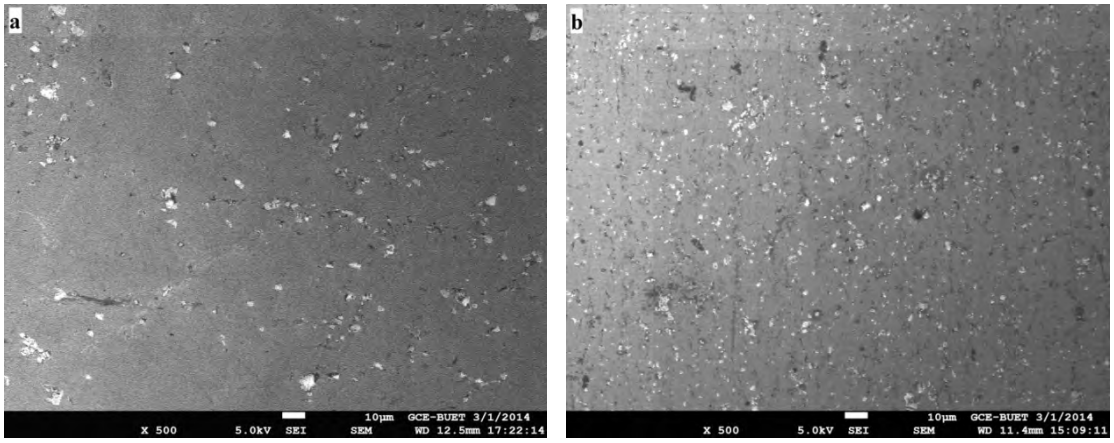

Fig.4.11: SEM microstructures of Al-2M-10A-5S (a) as-cast (b) heat treated

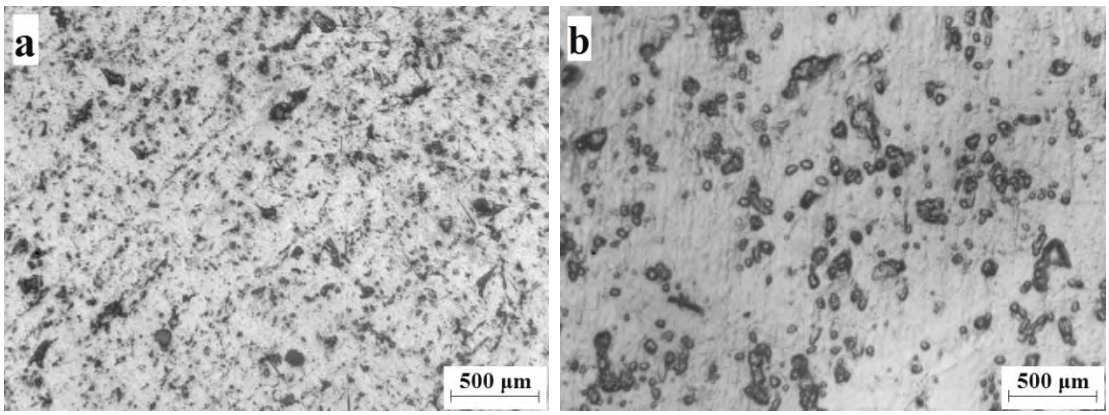

Fig. 4.12: Optical microstructure of heat treated Al-5A-10S (a) unetched (b) etched

Fig. 4.10 and 4.11 show optical and SEM micrographs of Al-2M-10A-5S respectively in as-cast and heat treated condition. Fig. 4.12 shows optical microstructure of heat treated Al-5A-10S in unetched and etched conditions. During etching phases present in Al matrix reacted with etching solution.

4.2 Hardness

Addition of alloying elements and change in reinforcement content to the Al-MMC affect the mechanical properties of Al-MMC. In this present study, effects of Mg addition, heat treatment and amount of reinforcements on the hardness of Al-MMC were observed. Following sections explain how these factors affect hardness.

4.2.1 Effect of Mg

The micro hardness is a direct, simple and easy method of measuring the interface bonding strength between the matrix and reinforcements. Fig. 4.13 shows the effect of Mg on the hardness of unreinforced Al and Al-MMC. It is seen that Al and Al-MMC with 2 wt. % Mg content showed higher hardness values compared to without Mg content. Hence, Mg addition increased the hardness values of both Al and Al-MMC.

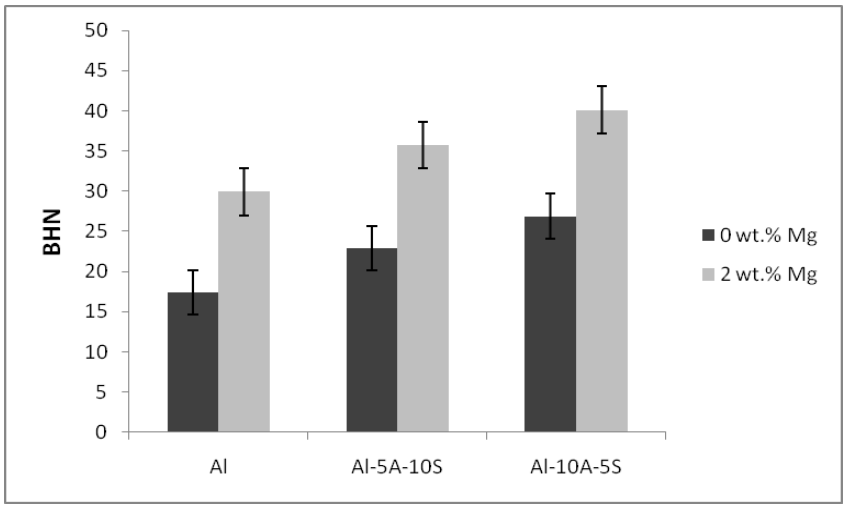

Fig. 4.13: Effect of Mg on hardness of Al-MMC

Al-2M-5A-10S showed higher hardness value than Al-5A-10S although both contained equal amount of reinforcements. 2 wt. % Mg addition to Al-2M-5A-10S improved interfacial bond strength by increasing wettability as described in section 2.3. 2. Improved interface bonding resulted in enhanced hardness of Al-2M-5A-10S by allowing applied load transfer from Al matrix to hard reinforcing particles which carried most of the applied load and restricting plastic deformation of ductile Al matrix. Besides, increased hardness of Al matrix caused by 2 wt. % Mg addition due to solid solution strengthening mechanism also contributed to enhance the hardness value of Al-2M-5A-10S [61]. For the same reason, Al-2M-10A-5S showed higher hardness value than Al-10A-5S.

4.2.2 Effect of heat treatment

Fig. 4.14 shows effect of heat treatment on hardness of Al-MMC. From the plot it is seen that heat treated Al-2M-5A-10S and Al-2M-10A-5S showed higher hardness values than as cast condition. Heat treatment caused precipitation hardening that conferred higher hardness values to the heat treated Al-2M-5A-10S and Al-2M-10A-5S [64].

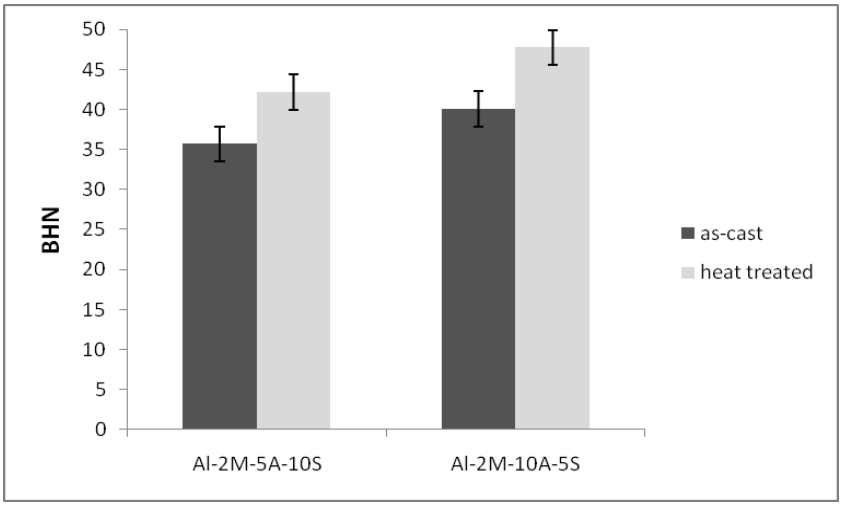

Fig. 4.14: Effect of heat treatment on hardness of Al-MMC

4.2.3 Effect of wt. % of reinforcement

Fig. 4.15 shows the effect of SiC content on the hardness of Al-MMC. It is seen from the plot that SiC reinforced Al-MMC showed higher hardness values than unreinforced Al and hardness value increased with increasing SiC content reached maximum for Al-1M-20S.

SiC particles are harder and stronger than Al matrix in which they are embedded. The presence of SiC particles in Al matrix impedes the movement of dislocations. The degree of strengthening depends on the size and distances between reinforcing particles, interfacial bond strength between matrix and reinforcements. Since that the particles are stronger than the matrix, the dislocation cannot pass through them, but if the stress is high enough, the dislocation can by-pass them leaving a dislocation loop around each particle. This will make the passage of a second dislocation much more difficult, particularly since dislocations have greater difficulty in passing between particles which are near to each other [65].

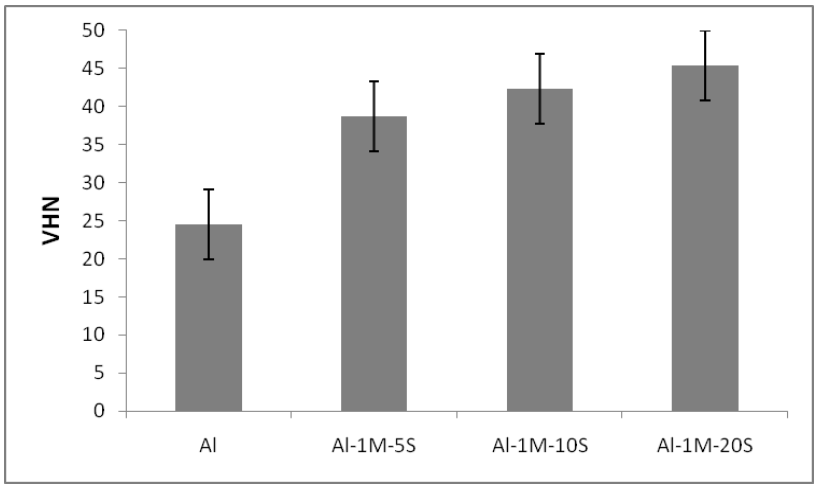

Fig. 4.15: Variation of hardness with SiC content in Al-MMC

Fig. 4.15 shows that an increase in wt. % of SiC particles in Al matrix enhanced the hardness of Al-MMC. Increased hardness with increase in wt. % of SiC particles in Al matrix can be attributed due to following reasons [64]:

a) High hardness value of SiC particles. Homogeneous dispersion of hard SiC particles in soft and ductile Al matrix increased the hardness values of Al-MMC
b) Interfacial bond formation between reinforcing particles and Al matrix that allowed transfer of external load from matrix to reinforcements
c) Increased wt. % of SiC in Al matrix led to increased dislocation densities during solidification due to large thermal mismatch between Al and SiC particles leading to retardation in plastic deformation
d) During hardness test, indentation pressure was partially accommodated by plastic flow of material and largely by localized increase in concentration of SiC particles

4.3 Tensile Test

Fig. 4.16 shows tensile strength of unreinforced Al and SiC reinforced Al-MMC. It is seen from the plots that tensile strength of SiC reinforced Al-MMC is higher than unreinforced Al.

Tensile strength unreinforced Al was found 28.5 MPa. SiC reinforced Al-MMC showed superior tensile strength than unreinforced Al. Tensile strength increased to 59.4 MPa for 5 wt. % SiC reinforced Al-MMC and 20 wt. % SiC reinforced Al-MMC

showed maximum tensile strength of 77.6 MPa. Tensile strength decreased to 50.2 MPa for 10 wt. % SiC reinforced Al-MMC. This was might be due to non-homogeneous distribution of SiC particles in Al matrix as shown in Fig. 4.1 (c). In SiC reinforced Al-MMC, a crack has to propagate across both strong interface and SiC particles which results in enhanced tensile strength of Al-MMC compared to unreinforced Al [37]. Non-homogeneous distribution of SiC particles was observed in the microstructure of 10 wt. % SiC reinforced Al-MMC which led crack across relatively soft Al matrix. This resulted in decrease of tensile strength of 10 wt. % SiC reinforced Al-MMC.

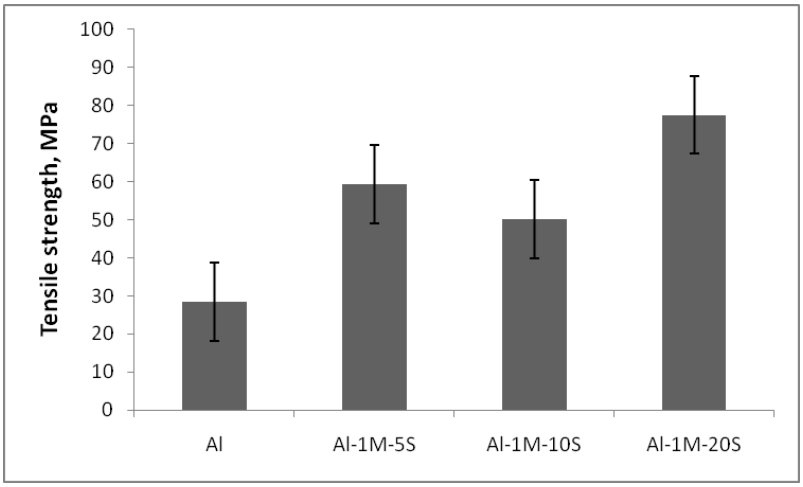

Fig. 4.16: Tensile strength of SiC reinforced Al-MMC

As shown in Fig. 4.16, SiC reinforced Al-MMC showed superior tensile strength than unreinforced Al. In general, the strengthening attributes to [66]:

a) Strength improvement due to grain refinement
b) Higher dislocation density due to the increased stress concentration near matrix-reinforcement interface
c) Higher hardness of SiC particles which increases load bearing capacity and hence results in improvement of tensile strength
d) The increase of dislocation density due to the thermal residual stress caused by the mismatch in the coefficient of thermal expansion between matrix and the reinforcements which improved the yield strength
e) The increase of strength might also be a result of closer packing of reinforcement within the soft Al matrix
f) A good interfacial bonding between reinforcing particles and soft Al matrix favored an enhancement of strength of the Al-MMC

4.4 Wear Test

4.4.1 Effect of Mg

Fig. 4.17 shows the effect of Mg on the wear rate of Al and Al-MMC. It is seen that Al-MMC showed lower wear rate than unreinforced Al and Mg addition reduced the wear rate of both unreinforced Al and Al-MMC.

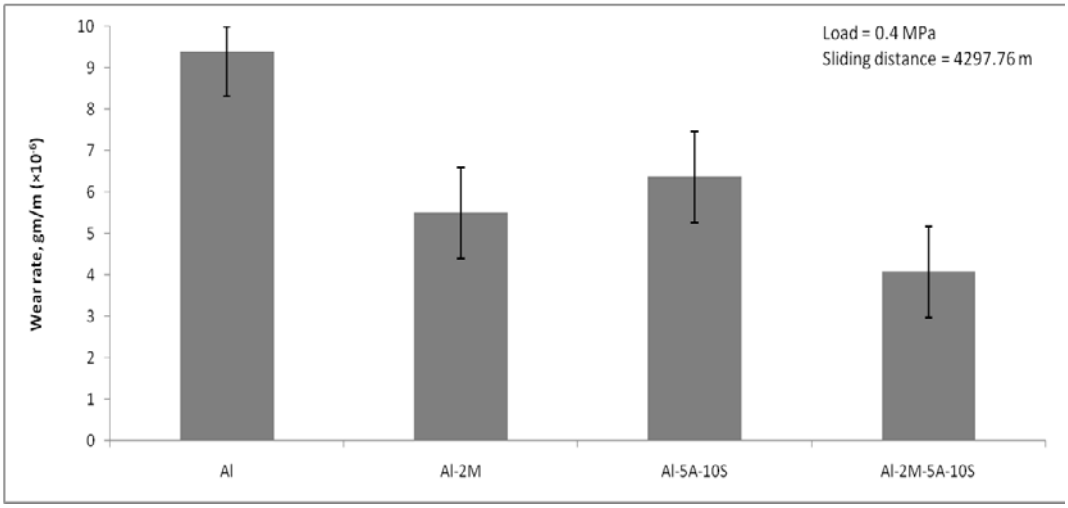

(a)

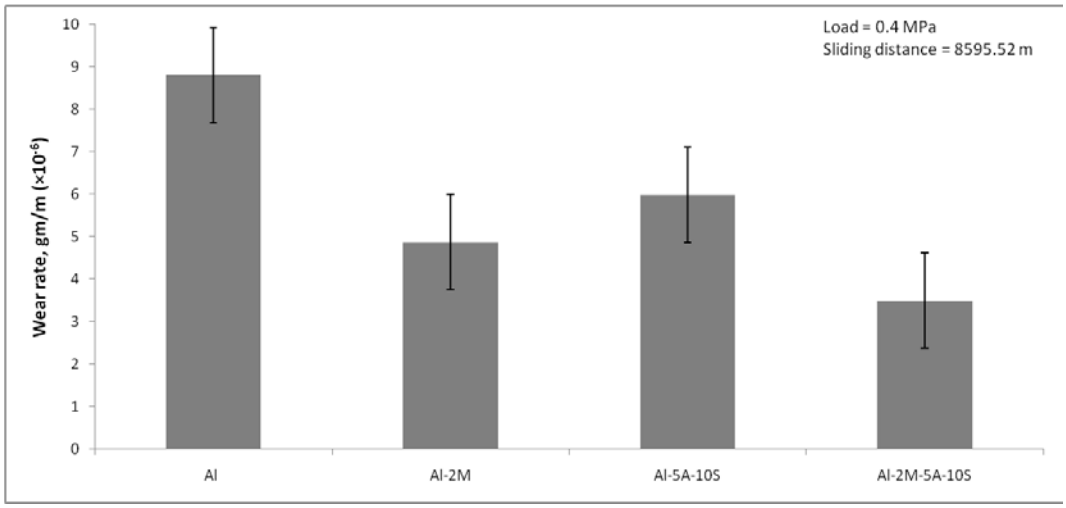

(b)

Fig. 4.17: Effect of Mg on wear rate of Al and Al-MMC at sliding distance of - (a) 4297.76 m (b) 8595.52 m

Wear rate of Al and Al-2M were found (9.4×10^{-6} g/m) and (5.5×10^{-6} g/m) for 4297.76 m sliding distance and (8.8×10^{-6} g/m) and (4.9×10^{-6} g/m) for 8595.52m

sliding distance respectively indicating a reduction in wear rate of Al-2M of around 41.5% and 44.3%. Al-2M showed higher hardness than Al due to solid solution strengthening mechanism as shown in Fig. 4.13. Due to high hardness value, Al-2M alloy showed better wear resistance compared to Al. It is also believed that higher amount of tribolayer observed on the worn surface of Al-2M contributed to reduce wear rate of Al-2M as described in section 2.5.1.5.

Al-2M-5A-10S exhibited lower wear rate compared to Al-5A-10S. Wear rate of Al-5A-10S and Al-2M-5A-10S were found (6.4×10^{-6} g/m) and (4.1×10^{-6} g/m) for 4297.76 m sliding distance and (6×10^{-6} g/m) and (3.5×10^{-6} g/m) for 8595.52m sliding distance respectively. Both Al-5A-10S and Al-2M-5A-10S contain equal amount of SiC and Al_2O_3 as reinforcements. But 2 wt. % Mg addition to Al-2M-5A-10S improved interfacial bond strength and reduced its wear rate which was found 35.9 % and 41.7 % for sliding distance of 4297.76 m and 8595.52 m respectively.

The wear behavior of hard particle reinforced Al-MMC depends primarily on the type of interfacial bonding between the Al-matrix and the reinforcement. Strong interfacial bond which plays a critical role in transferring loads from the matrix to the hard particles which results in less wear of the material. In case of poor interfacial bonding, the interface offers site for crack nucleation and tends to pull out the particle from the wear surface tending to higher mass loss [39]. Mg addition enhances strong interfacial bond formation between reinforcing particles and Al matrix that reduced the rate of material removal from worn surface. Besides, increased hardness of matrix caused by Mg addition contributed to reduce wear rate of Al-2M-5A-10S.

By comparing the wear rate of Al-2M and Al-5A-10S, it is observed that Al-2M showed lower wear rate than Al-5A-10S which was about 14.1 % and 18.3% for 4297.76 m and 8595.52 m sliding distances respectively. Hardness value of Al-2M is higher than Al-5A-10S as shown in Fig. 4.13. The rate of subsurface work hardening is higher for Al-2M alloy than Al-5A-10S. On worn surface observation, maximum amount of tribolayer was observed for Al-2M alloy that acted as a protective layer and solid lubricant. As the wear rate decreased with increasing tribolayer thickness [39], so Al-2M showed improved wear resistance than Al-5A-10S due to this increased amount of tribolayer.

4.4.2 Effect of heat treatment

Fig. 4.18 shows the effect of heat treatment on wear rate of Al-MMC. It is seen from Fig. 4.18 that heat treated Al-2M-10A-5S showed lower wear rate than as-cast Al-2M-10A-5S. As a consequence, wear resistance increased after heat treatment.

As-cast Al-2M-10A-5S and heat treated Al-2M-10A-5S showed wear rate of (6.8×10^{-6} g/m) and (5×10^{-6} g/m) for 4297.76 m sliding distance and (5.9×10^{-6} g/m) and (4.5×10^{-6} g/m) for 8595.52 m sliding distance that indicates 26.5 % and 23.7 % wear rate reduction for heat treated Al-2M-10A-5S caused by heat treatment.

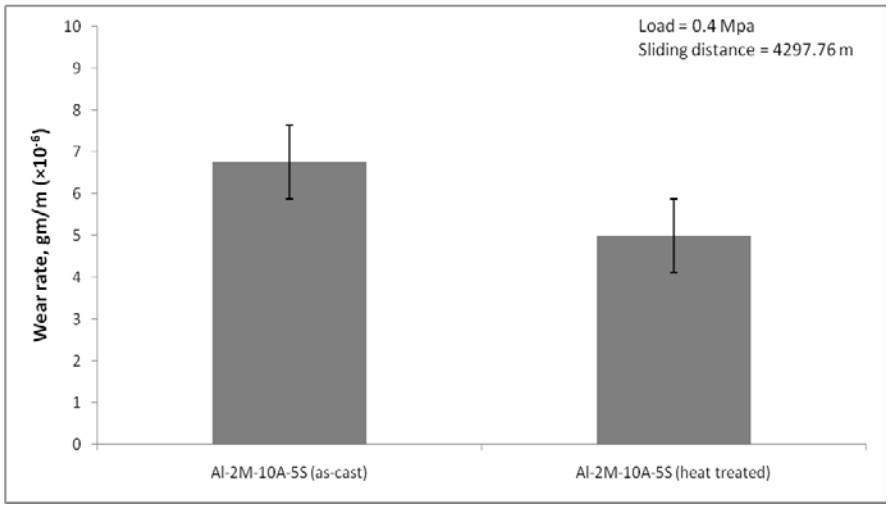

(a)

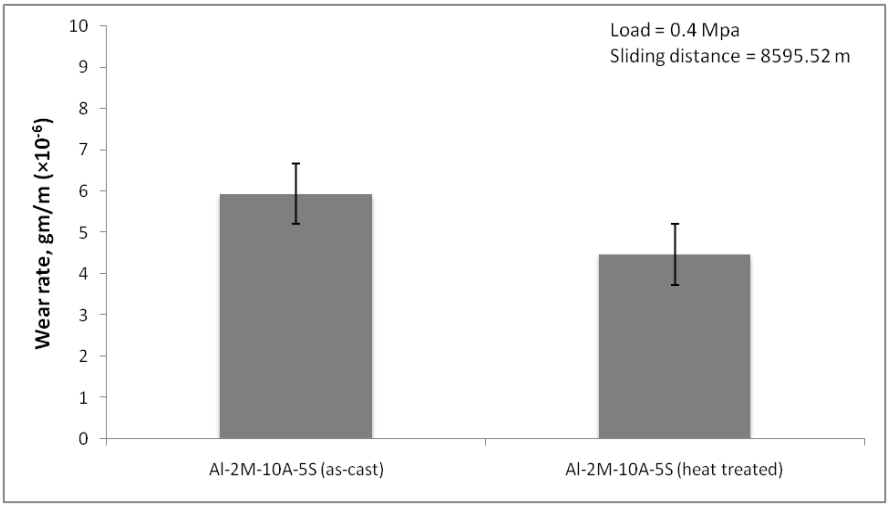

(b)

Fig. 4.18: Effect of heat treatment on wear rate of Al-MMC at sliding distance of - (a) 4297.76 m (b) 8595.52 m

Al alloy and Al-MMC exhibit lower wear rate after heat treatment due to improved hardness. During the wear process, the cracks are mainly nucleated at the matrix and reinforcement interfaces. Heat treated Al alloy and Al-MMC show better strength and hardness that result in fewer tendencies for crack nucleation. This enhances the wear resistance of heat treated Al-MMC as described in section 2.5.1.6.

Heat treatment caused hardening of the Al matrix by precipitation hardening which led to higher hardness and strength of the heat treated Al-2M-10A-5S. Hardness value of heat treated Al-2M-10A-5S was found higher than as-cast Al-2M-10A-5S as shown in Fig. 4.14. For heat-treated Al-2M-10A-5S, the effective stress applied on the composite surface during wear process is less due to higher strength and ductility of the Al matrix. This resulted in less cracking tendency of the heat treated Al-2M-10A-5S surface as compared to the as cast Al-2M-10A-5S [39].

4.4.3 Comparison of SiC and Al_2O_3 as reinforcement

Fig. 4.19 compares the wear rate of Al-2M-10A-5S and Al-2M-5A-10S at sliding distance of 4297.76 m and 8595.52 m. It is clear from Fig. 4.19 that Al-2M-5A-10S shows lower wear rate than Al-2M-10A-5S.

Al-2M-10A-5S and Al-2M-5A-10S showed wear rate of (6.8×10^{-6} g/m) and (4.1×10^{-6} g/m) for 4297.76 m sliding distance and (5.9×10^{-6} g/m) and (3.5×10^{-6} g/m) for 8595.52 m sliding distance respectively during wear test. Both Al-2M-10A-5S and Al-2M-5A-10S reinforced with total 15 wt. % of reinforcements. Al-2M-10A-5S contained 10 wt. % Al_2O_3 and 5 wt. % of SiC while Al-2M-5A-10S contained 5 wt. % Al_2O_3 and 10 wt. % SiC. The higher amount of SiC in Al-2M-5A-10S made it more wear resistant.

The SiC reinforcement in the Al-MMC is more fracture resistant compared to Al_2O_3. The reduction in wear rate for Al-2M-5A-10S was observed due to the increase of SiC content in the reinforcement mixture. Hardness of SiC particle is 2800 Kg/mm^2 when Al_2O_3 has hardness of only 1400 kg/mm^2 [67]. The SiC particles are harder than other reinforcements and provide a more effective barrier to subsurface shear by the motion of the adjacent cast iron counter-face.

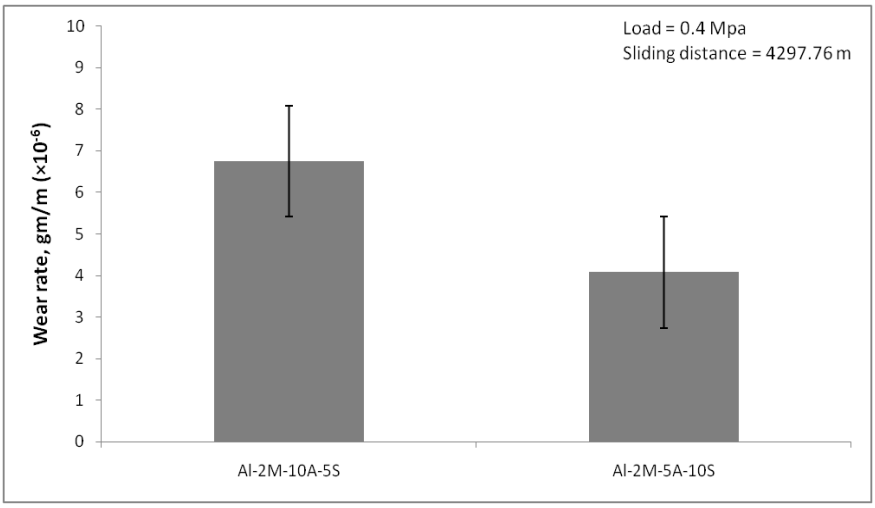

(a)

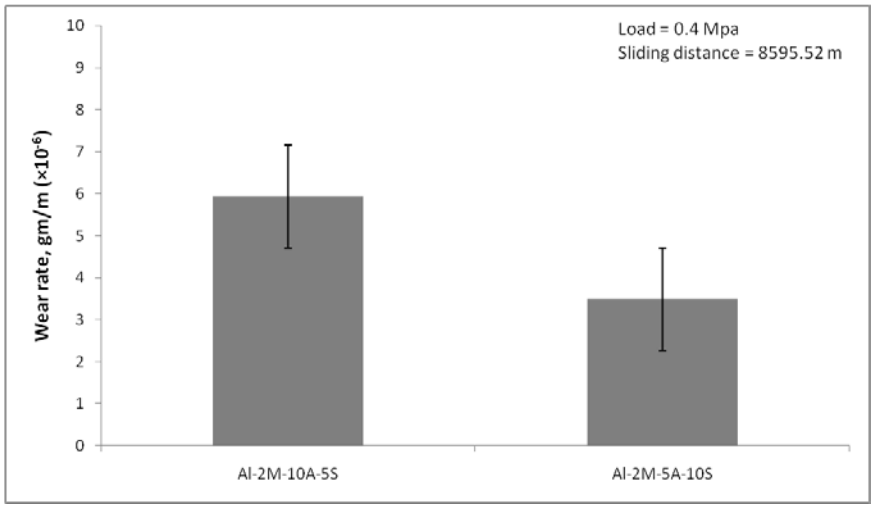

(b)

Fig. 4.19: Wear rate of Al-2M-10A-5S and Al-2M-5A-10S at sliding distance of - (a) 4297.76 m (b) 8595.52 m

Comparing Fig. 4.19 (a) and 4.19 (b), it is also observed that wear rate decreased with sliding distance indicating improved wear resistance for longer distance [59]. This can be attributed due to work hardening of subsurface regions with increasing wear induced plastic deformation. Subsurface hardening enhanced the hardness of subsurface region as compared to the unaffected bulk and this reduced wear rate subsequently. Besides, increased thickness of tribolayer with sliding distance on worn surface also contributes to reduce wear rate [39].

4.4.4 Effect of wt. % of reinforcement

Fig. 4.20 shows the effect of wt. % of SiC particles on the wear rate of Al-MMC. It is seen from Fig. 4.20 that SiC reinforced Al-MMC showed lower wear rate than unreinforced Al and wear resistance increased with increasing wt. % of SiC particles in Al-MMC. As shown in Fig. 4.20, unreinforced Al showed maximum wear rate and subsequently wear rate decreased with the increase of SiC content. Increasing hard SiC content in Al matrix, enhanced hardness as shown in Fig. 4.15, improved load bearing properties during sliding and restricted the flow or deformation of the matrix material with respect to load. This resulted in minimum wear rate for Al-1M-20S.

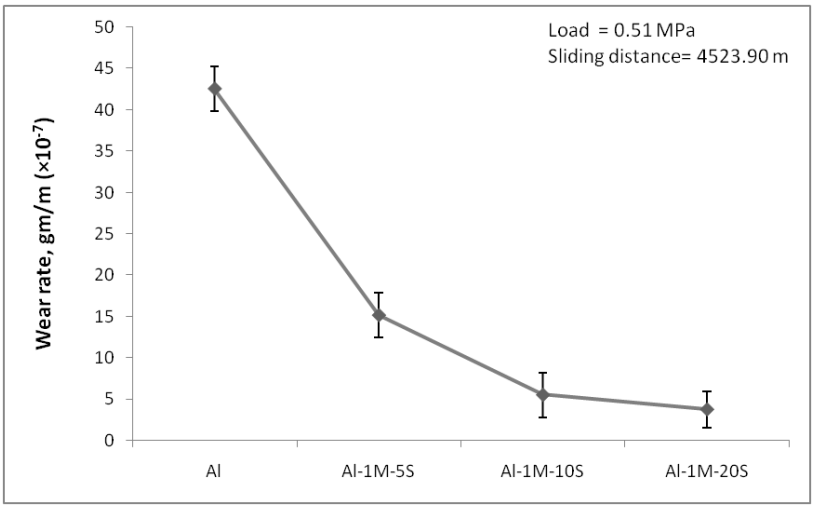

(a)

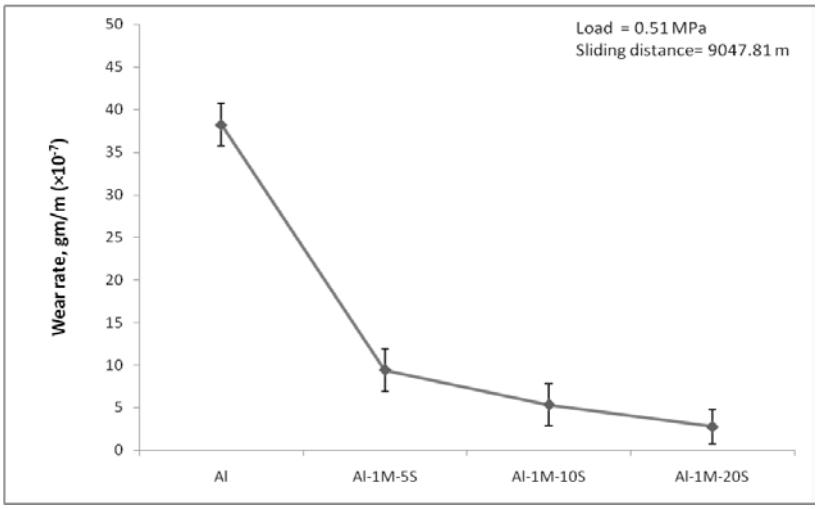

(b)

Fig. 4.20: Effect of wt. % of SiC reinforcements on the wear rate of Al-MMC at sliding distance of - (a) 4523.90 m (b) 9047.81 m

During wear test, softer metal matrix material is usually worn away first, leaving the protrusions of the hard reinforcing particles on worn surface which protect the metal matrix from further wear [68]. As the wt. % of reinforcements in Al-MMC is increased, exposed SiC particles on worn surface are also increased that reduce the plastic deformation in the layer below the worn surface. For a certain critical volume fraction of the reinforcement, the metal matrix will be completely protected.

4.5 Worn Surface Analysis

Fig. 4.21 shows the image of worn surfaces of Al alloy and Al-MMC observed with stereo microscope. On worn surfaces, tribolayer layer of compacted wear debris was observed. During wear, this layer reached to critical thickness before detached from worn surface and produce wear debris [59]. Besides, fine scratches along with larger grooves were also observed in worn surface.

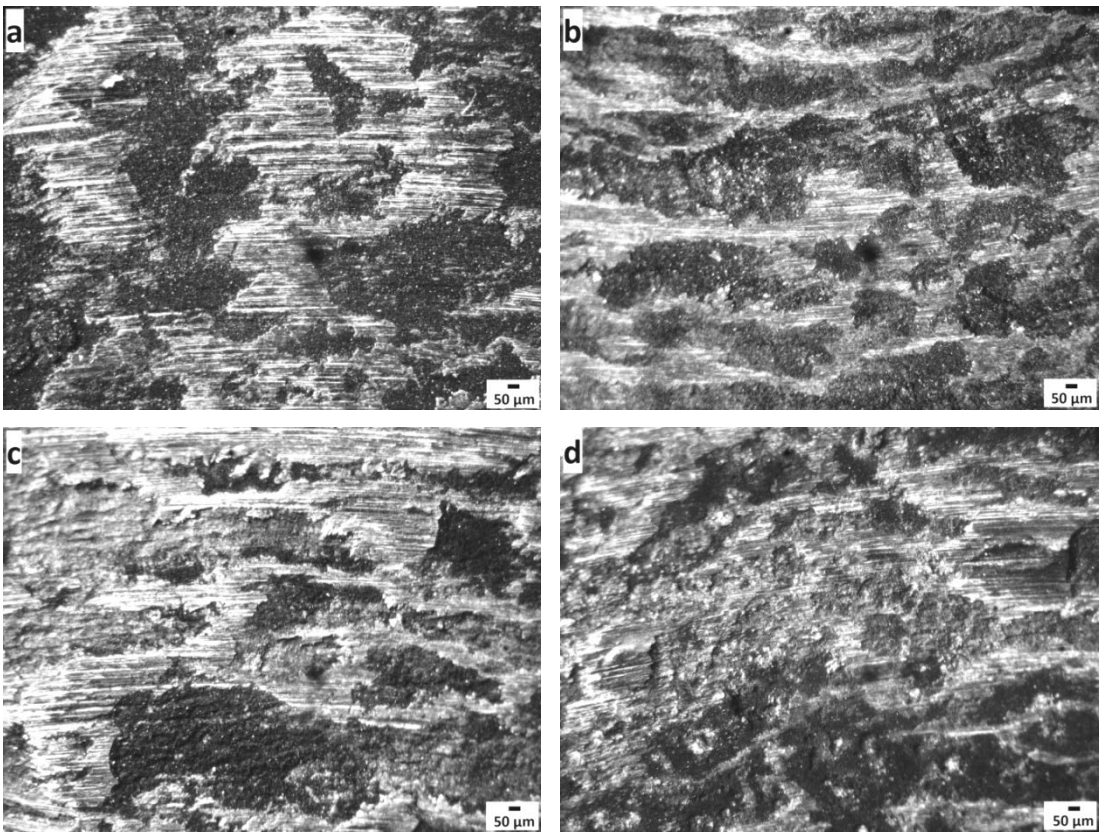

Fig. 4.21: Worn surfaces of (a) Al-2M (b) Al-5A–10S (c) Al–2M–10A–5S (d) Al–2M–5A–10S observed with stereo microscope

By comparing four worn surfaces of Al alloy and Al-MMC as shown in Fig. 4.21, it was evident that maximum amount of tribolayer was observed on the worn surface of Al-2M as shown in Fig. 4.21 (a). The presence of parallel grooves was visible on all

worn surfaces and maximum number of parallel grooves was observed on the worn surface of Al-2M. Worn surface of Al-2M was relatively smooth than the worn surfaces of Al-MMC. Worn surface of Al–2M–5A–10S was the most roughest among four worn surfaces with clear indication of fractures and plastic deformation as shown in Fig. 4.21(d).

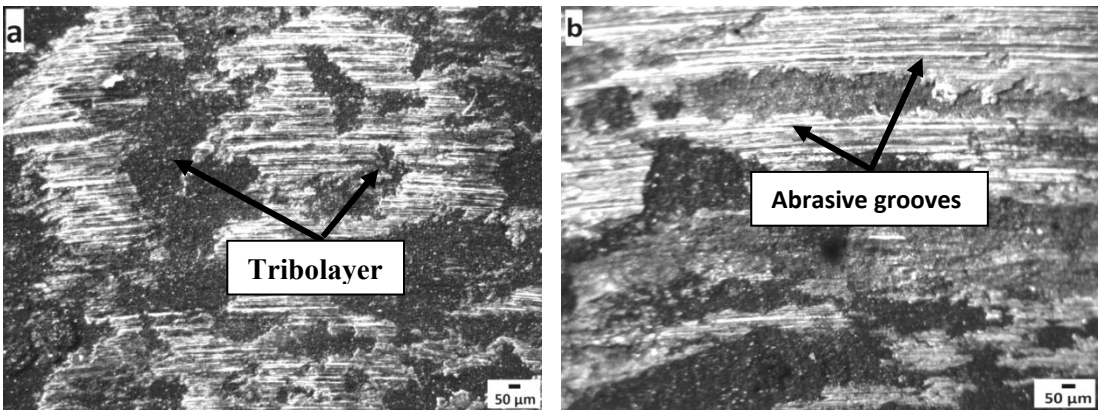

Fig. 4.22: (a) Tribolayer of wear debris (b) abrasive grooves on worn surfaces

Fig. 4.22 shows tribolayer of wear debris and abrasive grooves observed on the worn surfaces of Al-2M and Al-MMC. Formation of tribolayer on worn surface further enhanced the wear resistance of Al-MMC which has been discussed in section 2.2.2. Parallel abrasive grooves observed on worn surface are shown in Fig. 4.22 (b).

Fig. 4.23 shows optical photographs of worn surfaces of unreinforced Al and Al-MMC. As shown in Fig. 4.23, there are some patches on worn surfaces which indicated the removal of material from worn surfaces by wear mechanism. The parallel grooves suggest that abrasive wear was involved in wear process. The grooves might be formed due to deposition of wear-hardened deposits on disc track. As shown in Fig. 4.23(b), maximum amount of tribolayer was observed on the worn the worn surface Al-2M.

Abrasive wear took place with unreinforced Al where parallel grooves continuously dominated the wear process as shown in Fig. 4.23(a). But in case of SiC and Al_2O_3 reinforced Al-MMC, major mechanism was delamination wear which caused excessive fracture and plastic deformation of the reinforcements and the matrix [67]. Hence, plastic deformation occurred on worn surface layer and cracks were nucleated in the deformed layer at the second phase particles. Growth and joining of cracks resulted in wear debris formation. Here crack propagation control wear rate [50].

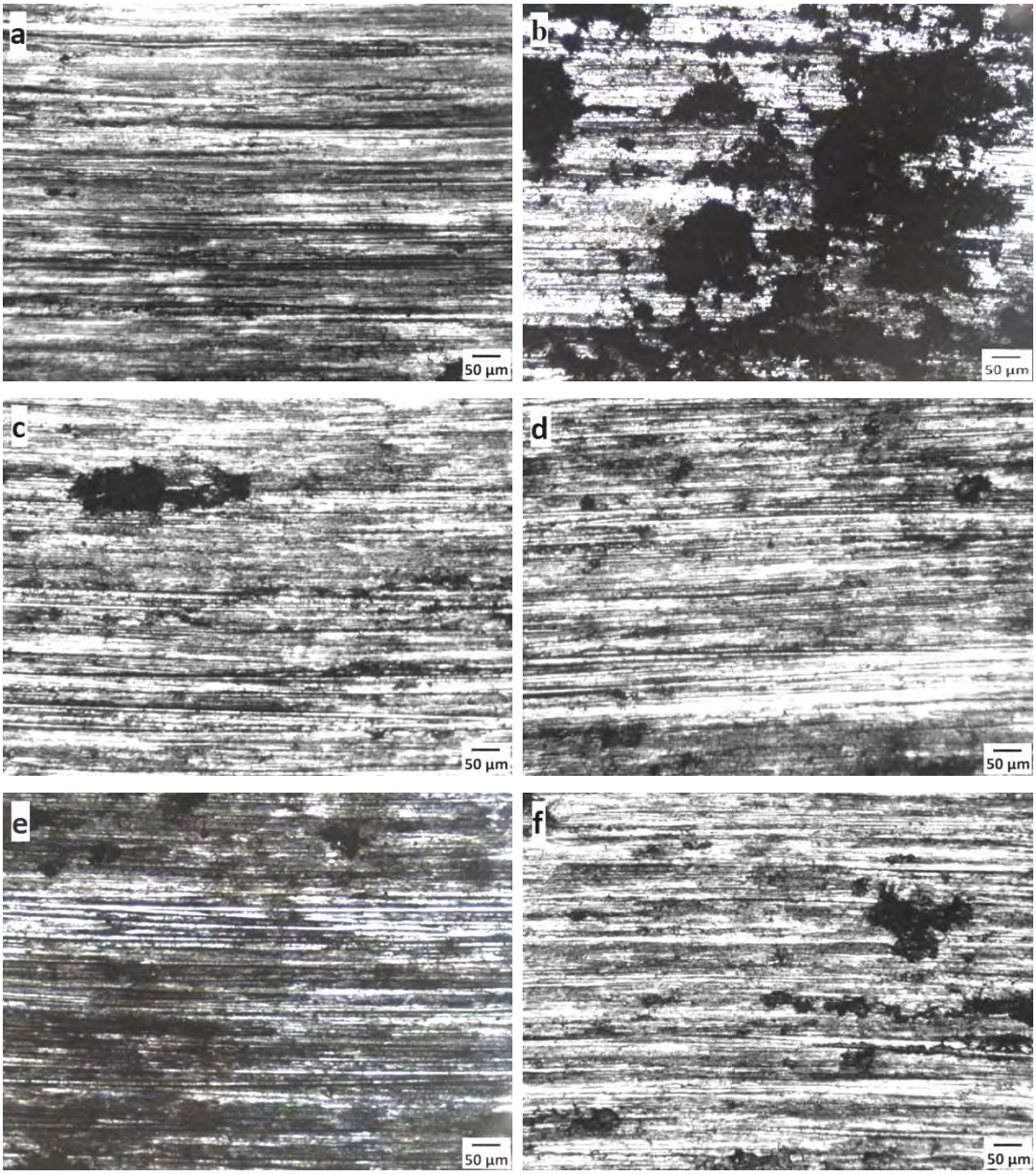

Fig. 4.23: Worn surfaces of (a) Al (b) Al–2M (c) Al–5A–10S (d) Al–2M–5A–10S (e) Al–2M–10A–5S [as-cast] (f) Al–2M–10A–5S [heat treated] observed with optical microscope

In dry sliding wear of SiC and Al_2O_3 particles reinforced Al-MMC, delamination wear theory is a major wear mechanism where hardness plays a major role in the overall wear process. Delamination wear of Al-MMC can be explained in terms of Suh's delamination wear theory as described in section 2.5.2.7.

Thus it was observed that abrasive wear took place with unreinforced Al metal and alloy indicated by continuous parallel grooves. But as the amount of reinforcing particles increased in Al-MMC, It was seemed that delamination wear process replaced ploughing and thus subsurface fracture dominated in the wear mechanism of Al-MMC.

Table 4.4 shows the groove width measured on worn surfaces of Al and Al-MMC. It is evident from the table that groove width is maximum for unreinforced Al, minimum for Al-2M-5A-10S and higher in heat treated Al-MMC than as-cast Al-MMC.

Table 4.2: Groove width of Al-MMC

No.	Al-MMC designation	Groove width (μm)
1	Al	16.11 ± 3.71
2	Al-2M	7.61 ± 2.20
3	Al-5A-10S	7.06 ± 2.83
4	Al-2M-5A-10S	5.02 ± 2.28
5	Al-2M-10A-5S (as-cast)	9.81 ± 3.15
6	Al-2M-10A-5S (heat treated)	12.62 ± 2.62

Material was removed from the worn surface of Al by ploughing action of asperities in course of abrasive wear mechanism. This Continuous ploughing action on the worn surface of relatively soft Al resulted in maximum groove width. But delamination process replaced ploughing and thus subsurface fracture dominated in Al-MMC. Exposed SiC than Al_2O_3 particles on worn surface could resist ploughing action of asperities on conterface. This resulted in lower groove width of Al-MMC than unreinforced Al.

SiC particles are more fracture resistant and harder than Al_2O_3 due to which Al-2M-5A-10S showed lower wear rate compared to Al-2M-10A-5S as discussed in section 4.4.3. Higher amount of SiC content along with increased load bearing cap ability resulted in minimum groove width for Al-2M-5A-10S.

CHAPTER 5
CONCLUSIONS

The objective of this work was to investigate the effects of Mg on wear characteristics of SiC and Al_2O_3 reinforced Al-MMC. Results obtained from this work can be summarized as follows:

[1] Microstructural observation revealed random and homogeneous distribution of reinforcing particles in Al matrix. Cluster of particles and porosities were found in microstructures.

[2] Mg addition to Al-MMC improved homogeneous distribution of reinforcing particles in Al matrix, promoted interface formation between reinforcing particle and Al matrix, and reduced porosity due to enhanced wettability. Also, Mg addition increased the hardness values of unreinforced Al and Al-MMC by solid solution strengthening and strong interfacial bond formation respectively.

[3] Heat treatment caused precipitation in the Al matrix that resulted in enhanced hardness values of Al-MMC.

[4] Hardness values of SiC reinforced Al-MMC was found larger than unreinforced Al and increased with increasing SiC content. Also, prepared SiC reinforced Al-MMC showed superior tensile strength compared to unreinforced Al due to the presence of strongly bonded SiC particles in Al matrix which caused grain refinement. Tensile strength decreased for 10 wt. % SiC reinforced Al-MMC due to non-homogeneous distribution of SiC particles in Al matrix.

[5] Mg addition improved wear resistance of both unreinforced Al and Al-MMC by increasing hardness and wettability.

[6] Heat treated Al-MMC showed lower wear rate than as-cast condition due to improved hardness in heat treated condition.

[7] The SiC reinforcement in Al-MMC was found more fracture resistant compared to Al_2O_3 reinforcement due to high hardness value of SiC particles.

[8] The wear rate of SiC reinforced Al-MMC decreased with the increase of SiC content.

[9] Tribolayer of compacted wear debris was observed on worn surfaces and was maximum for Al-2M.

Abrasive grooves were observed on worn surfaces and unreinforced Al showed maximum groove width. Also, there was clear indication of excessive fracture and plastic deformation on the worn surfaces of Al-MMC.

From worn surface analysis, it was seemed that abrasive wear mechanism was involved in the wear process of unreinforced Al and delamination wear mechanism was involved in the wear process of Al-MMC.

REFERENCES

[1] M. K. Surappa, (2003) " Aluminium Matrix Composites: Challenges and Opportunities", Sadhana, Vol. 28, pp. 319-334.

[2] K. M. Shorowordi, T. Laoui, A. S. M. A. Haseeb, J. P. Celis and L. Froyen, (2003) " Microstructure and Interface Characteristics of B_4C, SiC and Al_2O_3 Reinforced Al Matrix Composites: A Comparative Study", Journal of materials processing technology, Vol. 142, pp. 738-743.

[3] C. N. Devi, N. Selvaraj and V. Mahesh, (2012) "Micro Structural Aspects of Aluminium Silicon Carbide Metal Matrix Composite", International Journal of Applied Sciences and Engineering Research, Vol. 1, pp. 250-254.

[4] T. P. D. Rajan, R. M. Pillai and B. C. Pai, (1998) " Review: Reinforcement Coatings and Interfaces in Aluminium Metal Matrix Composites", Journal of Materials Science, Vol. 33, pp. 3491–3503.

[5] F. Delannay, L. Froyen and A. Deruyttere, (1987) " Review: The Wetting of Solids by Molten Metals and Its Relation to the Preparation of Metal–Matrix Composites", Journal of Materials Science, Vol. 22, pp. 1–16.

[6] P. K. Jayashree, M. C. G. Shankar, A. Kini, S. S. Sharma and R. Shetty, (2013) "Review on Effect of Silicon Carbide (SiC) on Stir Cast Aluminium Metal Matrix Composites", International Journal of Current Engineering and Technology, Vol. 3, pp. 1061-1071.

[7] W. D. Callister, Jr. (2007) *Materials science and engineering An introduction*. John Wiley & Sons, Inc., New York.

[8] A. Kisasoz, K. A. Guler and A. Karaaslan, (2012) " Infiltration of A6063 Aluminium Alloy into SiC−B_4C Hybrid Preforms Using Vacuum Assisted Block Mould Investment Casting Technique", Transactions of Non Ferrous Metals Society of China, Vol. 22, pp. 1569-1567.

[9] Composites, http://www.essentialchemicalindustry.org/materials-and-applications/composites.html, Date accessed: 18-08-2014.

[10] Metals and Metal Matrix Composites, http://www.ae.iitkgp.ernet.in/ebooks/chapter2.html, Date accessed: 06-04-2014.

[11] Aluminum Matrix Composites: Processing and Properties, cimewww.epfl.ch/people/cayron/Fichiers/thesebook-chap2.pdf, Date accessed : 12-08-2014.

[12] Y. C. M. Kumar and U. Shankar, (2012) "Evaluation of Mechanical Properties of Aluminum Alloy 6061 -Glass Particulates Reinforced Metal Matrix Composites", International Journal of Modern Engineering Research, Vol. 2, pp. 3207-3209.

[13] T. W. Clyne and P. J. Withers (1993) *An introduction to metal matrix composite*. Cambridge University Press, Cambridge.

[14] Solid state fabrication of Metal Matrix Composites, http://www.substech.com/dokuwiki/doku.php?id=solid_state_fabrication_of_metal_matrix_composites, Date accessed: 13-04-2014.

[15] Science Dictionary, http://thesciencedictionary.org/physical-vapour-deposition/, Date accessed: 13-04-2014.

[16] K. U. Kainer (2006) *Metal matrix composite. Custom-made materials for automotive and aerospace engineering*. Wiley-vch Verlag Gmbh and Co.

[17] Liquid state fabrication of Metal Matrix Composites, http://www.substech.com/dokuwiki/doku.php?id=liquid_state_fabrication_of_metal_matrix_composites, Date accessed: 13-04-2014.

[18] Introduction to Manufacturing Processes, http://www.sharepdf.com/115e20552c7c4676a32bb90873b8c794/TA%20201%28Home%20Assgn%202%29%20Solution.html, Date accessed: 12-08-2014.

[19] K.K. Chawla and N. Chawla *Metal-Matrix Composites.*

[20] In-situ fabrication of Metal Matrix Composites, http://www.substech.com/dokuwiki/doku.php?id=insitu_fabrication_of_metal_matrix_composites, Date accessed: 13-04-2014.

[21] Silicon Carbide (Black) Grit Abrasives, 25 lbs or More, All Grades to Choose From, http://sandblastingabrasives.com/black-silicon-carbide-abrasive.html, Date accessed: 13-04-2014.

[22] Silicon Carbide, http://www.britannica.com/EBchecked/topic/544369/silicon-carbide, Date accessed: 13-04-2014.

[23] Pulkit Bajaj, *Mechanical behavior of aluminum based metal matrix composites reinforced with SiC and alumina*, M. Engg. Thesis, Department of Mechanical Engineering, Thapar University, India.

[24] Patnaik, P. (2002) *Handbook of inorganic chemicals*. McGraw-Hill.

[25] Silicon Carbide, http://www.ioffe.ru/SVA/NSM/Semicond/SiC/, Date accessed: 13-08-2014.

[26] Alumina (AL2O3) I ndustry G rade, http://www.southstarchina.com/html_ products/Alumina-%28AL2O3%29-Industry-Grade-228.html, D ate a ccessed: 13-08-2014.

[27] Alumina, http://www.makeitfrom.com/material-data/?for=Alumina-Aluminum-Oxide-Al2O3, Date accessed: 13-08-2014.

[28] R. Raymond (2009) *Handbook of Pharmaceutical Excipients.*

[29] Alumina, http://www.britannica.com/EBchecked/topic/17897/alumina, Date accessed: 13-04-2014.

[30] Elemental f ame, P ublish w ith Glogster, http://www.glogster.com/doegirl/elemenal-fame/g-6l8o34ubsl4nel8pd6m68a0, Date accessed: 13-08-2014.

[31] Boron C arbide (B_4C)-Properties a nd I nformation a bout B oron C arbide, http://www.azom.com/article.aspx?ArticleID=75, Date accesses: 01-05-2014.

[32] Properties, A pplications a nd Product I nformation of B oron C arbide, http://www.7-stars-international.com/b4c.html, Date accessed: 13-08-2014.

[33] Titanium C arbide P owder–303, http://tttmetalpowder.com/titanium-carbide-powder-303/, Date accesses: 01-05-2014.

[34] Titanium C arbide, http://cdn.worldheritage.org/articles/Titanium_carbide, Date accessed: 13-08-2014.

[35] L. Pauling, "Molecular S ructure of Ti8C12 a nd R elated C omplexes", in 1992 *Proceeding of National Academy of Science*, USA.

[36] Guo, B c, K erns, K p, Castleman, A w, J r., (1992) " Ti8C12+-Metallo-Carbohedrenes: A New Class of Molecular Clusters?" Science, Vol. 255.

[37] S. V aucher and O . B effort (2001) *Bonding and interface formation in metal matrix composites*. MMC- Assess Thematic Network, Switzerland.

[38] B. C. Pai, G. Ramani, R. M. P illai and K. G. Satyanarayana, (1995) "Role of magnesium in ca st aluminium al loy m atrix co mposites," J ournal o f M aterials Science, Vol. 30, pp. 1903-1911.

[39] G. B. V. Kumar, C. S. P. Rao and N. Selvaraj, (2011) "Mechanical and Tribological Behavior of Particulate Reinforced Aluminum Metal Matrix Composites - A Review," Journal of Minerals & Materials Characterization & Engineering, Vol. 10, pp. 59-91.

[40] A. H. Clauer and N. Hansen, (1984), Acta Metallic Materials, Vol. 32, pp. 269-278.

[41] P. Barai, G. J. Weng, (2008) "Mechanics of Creep Resistance in Nanocrystalline Solids", Acta Mechanical, Vol. 195, pp. 327–348.

[42] R. S. Rana. R. Purohit and S. Das, (2012) "Review of recent studies in Al matrix composites", International Journal of Scientific and Engineering Research, Vol. 3, pp. 1-16.

[43] B. Bhushan (2002) *Introduction to tribology*. John Wiley & Sons, Inc. New York.

[44] Mechanisms of Wear, http://www.substech.com/dokuwiki/doku.php?id=mechanisms_of_wear# corrosive_wear, Date accessed: 07-04-2014.

[45] Wear: The Inside Story, http://www.ssab.com/Products--Services/Service--support/Technical-support/Knowledge-Service-Center/Wear-TechnologyGroup-TM/Wear-The-Inside-Story/, Date accessed: 07-04-2014.

[46] Waterjetting 10c- Abrasive waterjet cutting, http://bittooth.blogspot.com/ 2013/ 06/ waterjetting-10c-abrasive-waterjet.html, Date accessed: 07-04-2014.

[47] Basic of Wear, http://www.stle.org/resources/lubelearn/wear/, Date accessed: 13-04-2014.

[48] N.P. Suh, (1977) "The delamination theory of wear", Wear, Vol. 25, pp. 111-124.

[49] S. Jahanmir and N. P. Suh, (1977) "Mechanics of subsurface void nucleation in delamination wear", Wear, Vol. 44, pp. 17-38.

[50] R. L. Deuis, C. Subramanian and J. M. Yellup, (1997) "Dry Sliding Wear of Aluminium Composites - A Review", Composites Science and Technology, Vol. 57, pp. 415-435.

[51] M. Nagaral, V. Bharath and V. Auradi, (2013) "Effect of Al_2O_3 Particles on Mechanical and Wear Properties of 6061 Al Alloy Metal Matrix Composites", Journal of Materials Science and Engineering, Vol. 2, pp. 1-4.

[52] V. Jadiwarad, R. Shadakshari, M. H. Annaiah, Dr. K. Mahesha and H. V. H. Kumar, (2013) "The Effect of Heat Treatment on Microstructure, Mechanical

Properties and Damping Behavior of Hybrid Composite of A 356.0", International Journal of Innovative Research in Science, Engineering and Technology, Vol. 2, pp. 1026-1032.

[53] V. C. Uvaraja and N. Natarajan, (2012) "Tribological Characterization of Stir Cast Hybrid Composite Aluminum 6061 Reinforced with SiC and B_4C Particulates", European Journal of Scientific Research, Vol. 76, pp. 539-552.

[54] G. Lin, Z. Hong-Wei, L. Hao-ze, G. Li-na and H. Lu-jun, (2010) "Effects of Mg Content on Microstructure and Mechanical Properties of SiCp/Al-Mg Composites Fabricated by Semi-solid Stirring Technique", Transactions of non ferrous metals society of China, Vol. 20, pp. 1851-1855.

[55] R. S. Rana and R. Purohit, (2012) "Effect of magnesium enhancement on mechanical property and wear behavior of LM6 aluminum alloy", International Journal of Scientific and Engineering Research, Vol. 3, +pp. 1-4, 2012.

[56] A. K. Israa, (2012) "Studying the Effect of Reinforcing by SiC_p on the Dry Sliding Wear Behavior and Mechanical Properties of Al- 4% Cumatrix Alloy", Diyala Journal of Engineering Sciences, Vol. 6, pp. 139-153.

[57] S. Das, R. Behera, S. Koyal, G. Majumdar, B. Oraona and G. Sutradhar, (2013) "Study on the Effect of Heat Treatment on the Mechanical Properties and Forgeability of AMMCs", International Journal of Emerging Trends in Engineering and Development, Vol. 2, pp. 62-72.

[58] S. Kayal, R. Behera and G. Sutradhar, (2012) "Mechanical Properties of the As-Cast Silicon Carbide Particulate Reinforced Aluminium Alloy Metal Matrix Composites", International Journal of Current Engineering and Technology, Vol. 2, pp. 318-322.

[59] H. N. Reddappa, K. R. Suresh, H. B. Niranjan and K. G. Satyanarayana, (2011) "Dry Sliding Friction and Wear Behavior of Aluminum/beryl Composites", International Journal of Applied Engineering Research, Vol. 2, pp.502-511.

[60] A. Vencl, A. Rac, I. Bobić and Z. Mišković, (2008) "Tribological properties of A356 Al-Si alloy with Al_2O_3 particles", Tribology in Industry, Vol. 28, pp. 27-31.

[61] H. Ahlatci, T. Koc¸er, E. Candan and H. C¸imenog˘lu, (2006) "Wear behaviour of Al/(Al_2O_{3p}+SiC_p) hybrid composites," Tribology International, Vol. 39, pp. 213–220.

[62] S. Zhongliang, G. Mingyuan, L. Junyou, L. Guoquan, L. Jae-chul, Z. Di and W. Renjie, (2001) "Interfacial Reaction Between the Oxidized SiC Particles and Al-Mg Alloys", Chinese Science Bulletin, Vol. 46, pp. 1948-1952.

[63] D. A. Saheb, (2011) "Aluminum Silicon Carbide and Aluminum Graphite Particulate Composites", ARPN Journal of Engineering and Applied Sciences, Vol. 6, pp. 41-46.

[64] T. P. Bharathesh, C. S. Ramesh, S. M. Verma and R. Keshavamurthy, "Influence of Heat Treatment on Tribological Properties of Hot Forged Al6061-TiO_2 Composites", International Journal of Emerging Technology and Advanced Engineering, Vol. 3, pp. 103-111.

[65] R. A. Higgins (2006) Materials for engineering and technicians, Butterworth-Heinemann.

[66] R. Karthigeyan, G. Ranganath and S. Sankaranarayanan, (2012) "Mechanical Properties and Microstructure Studies of Aluminium (7075) Alloy Matrix Composite Reinforced with Short Basalt Fibre", European Journal of Scientific Research, Vol.68, pp. 606-615.

[67] K. M. H. Badhon and M. A. I. Mehedi, *Tribological Characteristics of Aluminium Matrix Hybrid Composited Reinforced with SiC and Al_2O_3,* B. Sc. Engg. Thesis, Department of Materials and Metallurgical Engineering, Bangladesh University of Engineering and Technology, Bangladesh, 2012.

[68] A. Vencl, A. Rac and I. Bobić, (2004) "Tribological behaviour of Al-based MMCs and their application in automotive industry", Tribology in industry, Vol. 26, pp. 31-38.

[69] Y. Abdullah, A. R. Daud, R. Shamsudin and M. B. Harun, (2009) "Flexural Strength and Fracture Studies of Al-Si/SiC_p Composites", International Journal of Mechanical and Materials Engineering, Vol. 4, pp. 109-114.

[70] A. Mazahery and M. O. Shabani, (2012) "Characterization of Cast A356 Alloy Reinforced with Nano SiC Composites", Transactions of nonferrous metals society of China, vol. 22, pp. 275-280.

[71] A. Vencl and I. Bobić, "Tribological properties of A356 Al-Si alloy composite reinforced with Al_2O_3 particles (MMC)", in 2008 V^{th} Congress of Metallurgists of Macedonia-5.

[72] R. S. Rana, R. Purohit and S. Das, (2012) "Reviews on the Influences of Alloying Elements on the Microstructure and Mechanical Properties of

Aluminum Alloys and Aluminum Alloy Composites", International Journal of Scientific and research publications, Vol. 2, pp. 1-7.

[73] K. R. Gopi, K. N. Mohandas, H. N. Reddappa and M. R. Ramesh, (2013) "Characterization of As Cast and Heat Treated Aluminium 6061/Zircon Sand/Graphite Particulate Hybrid Composites", International Journal of Engineering and Advanced Technology, Vol. 2, pp. 340-344.

[74] K. F. Rahman, M. M. Benal, (2012) "Effect of Heat Treatment on the Coefficient of Thermal Expansion of Aluminium 7075 Alloy- SiC_p (5 wt. %) Composites", IOSR Journal of Mechanical and Civil Engineering, Vol. 1, pp. 17-20.

[75] A. Włodarczyk-Fligier, L. A. Dobrzański, M. Adamiak, (2007) "Influence of Heat Treatment on Properties and Corrosion Resistance of Al-composites", Journal of Achievements in Materials and Manufacturing Engineering, Vol. 21, pp. 55-58.

[76] H. Singh, Sarabjit, N. Jit, A. K. Tyagi, (2011) "An Overview of Metal Matrix Composite: Processing and SiC Based Mechanical Properties", Journal of Engineering Research and Studies, Vol. 2, pp. 72-78.

[77] K. B. Girisha and Dr. H. C. Chittappa, (2013) "Preparation, Characterization and Mechanical Properties of Al356.1 Aluminium Alloy Matrix Composites Reinforced with MgO Nanoparticles", International Journal of Innovative Research in Science, Engineering and Technology, Vol. 2, pp. 5593-5600.

[78] M. Marimuthu and L. J. Berchmans, (2013) "Preparation and Characterization of B_4C Particulate Reinforced Al-Mg Alloy Matrix Composites", International Journal of Modern Engineering Research, Vol. 3, pp. 3723-3729.